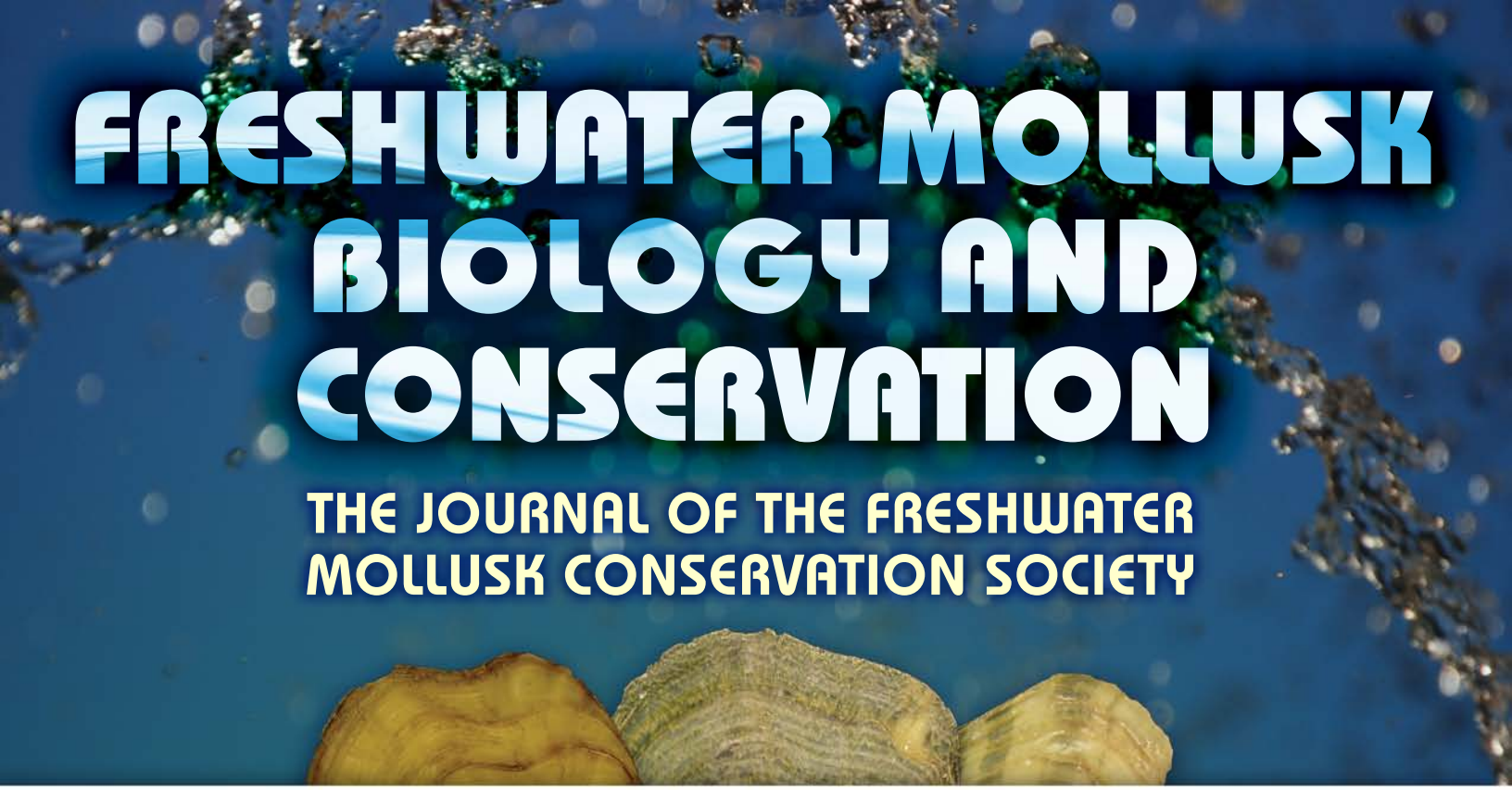

FRESHWATER MOLLUSK BIOLOGY AND CONSERVATION

THE JOURNAL OF THE FRESHWATER MOLLUSK CONSERVATION SOCIETY

VOLUME 25 NUMBER 1 MARCH 2022

Freshwater Mollusk Biology and Conservation 25:1–6, 2022

DOI:10.31931/fmbc-d-21-00002

REGULAR ARTICLE

DEVELOPMENT AND CHARACTERIZATION OF MICROSATELLITE LOCI IN THE ENDANGERED CATSPAW, *EPIOBLASMA OBLIQUATA* (BIVALVIA:UNIONIDAE)

Katlyn Ortiz[1], Jess W. Jones[1,2]*, and Eric M. Hallerman[1]

[1] *Department of Fish and Wildlife Conservation, Virginia Polytechnic Institute and State University, Blacksburg, VA 24061 USA*

[2] *U.S. Fish and Wildlife Service, Department of Fish and Wildlife Conservation, Virginia Polytechnic Institute and State University, Blacksburg, VA 24061 USA*

ABSTRACT

The endangered Catspaw, *Epioblasma obliquata*, is restricted to one known reproducing population in Killbuck Creek, Coshocton County, Ohio. Little is known about the genetic diversity of this small population, and such information is needed to help inform recovery planning. We nonlethally sampled 44 individuals of *E. obliquata* using buccal swabs, from which we developed and characterized 14 polymorphic microsatellite loci. Significant deviations from Hardy–Weinberg Equilibrium (HWE), showing deficiencies in heterozygotes, were observed at 6 of the 14 loci, and linkage disequilibrium (LD) was observed at 9 (∼10%) of 91 possible pairwise comparisons among loci. Allelic diversity ranged from 2 to 15 alleles per locus and averaged 7.6 alleles per locus. Observed heterozygosity per locus ranged from 0.091 to 1.000 and averaged 0.674. Possible explanations for deviations from HWE and LD could be from loci located close together on the same chromosome, segregation of null alleles, family structure within the small population, population bottlenecks, inbreeding, hermaphroditic reproduction, or some combination of these factors. Managers can use these microsatellite markers to assess and monitor genetic diversity in the remaining wild population in Killbuck Creek, prospective broodstock, hatchery-reared progeny, and reintroduced populations founded to promote recovery of the species.

KEY WORDS: Catspaw, *Epioblasma obliquata*, freshwater mussel, DNA microsatellite loci, primers, genetic diversity

INTRODUCTION

The Catspaw, *Epioblasma obliquata*, was listed as endangered under the U.S. Endangered Species Act in 1990; at that time, two isolated nonreproducing populations were known, one in the Green River in Kentucky and the other in the Cumberland River in Tennessee (USFWS 1990). These two populations now are considered extirpated. However, in 1994, a population of reproducing *E. obliquata* was discovered in a short reach of Killbuck Creek, a tributary of the Walhonding River in the Muskingum River watershed in Coshocton County, Ohio (Hoggarth et al. 1995). State and federal agencies are using this population as a source of broodstock for captive propagation in an attempt to recover the species.

Given the single-source population, genetic variation in hatchery progeny is a concern. Potential genetic threats to survival of the species include loss of within-population genetic variation from nonrepresentative sampling or low numbers of broodstock and family-size variation in the hatchery (Jones et al. 2006; Cooper et al. 2009). Microsatellites, or simple sequence repeats, are tandemly repeated motifs of multiple bases of nuclear DNA found in all eukaryotic genomes (Zane et al. 2002). Microsatellites are highly

*Corresponding Author: Jess_Jones@fws.gov

polymorphic loci that are ideally suited for genetic monitoring of wild and captive populations. The goal of this study was to develop and evaluate a set of microsatellite DNA PCR primers to analyze the genetic variation of the small source population in Killbuck Creek and any progeny produced in hatcheries.

METHODS

We obtained DNA samples from 44 adult *Epioblasma obliquata* that originally were collected from Killbuck Creek, Coshocton County, Ohio. These adults represented all individuals found at multiple sites and during multiple visits to the creek to collect broodstock in 2016–17. Adults were transported to and held at the Kentucky Department of Fish and Wildlife Resources' Minor E. Clark Fish Hatchery as part of the recovery program for the species. We nonlethally sampled these 44 individuals from the hatchery in the fall of 2018 by gently opening each mussel and vigorously swabbing the foot with a buccal swab (Kit DDK-50, Isohelix, Harrietsham, UK). From the buccal swab, DNA was isolated and extracted using an Isohelix DNA isolation kit, and its concentration and purity were assessed by using a μLite PC spectrophotometer (Biodrop, Cambridge, UK). In addition to morphological identification, the identification of all individuals as *E. obliquata* was confirmed using the mitochondrial DNA sequence from the first subunit of NADH dehydrogenase (*ND1*), a protein-encoding gene amplified by PCR using primers and conditions reported by Serb et al. (2003).

The Savannah River Ecology Laboratory at the University of Georgia developed a microsatellite library. Genomic DNA used to isolate the microsatellite loci was extracted from two individuals collected from the wild in 2016, utilizing a DNEasy Blood and Tissue Kit (Qiagen, Germantown, MD, USA). A genomic library was prepared with inserts size-selected to range from 300 to 600 bp. Paired-end reads were sequenced on an Illumina HiSeq sequencer. Using the program MSATCOMMANDER (Faircloth 2008), 463,713 reads containing 3–6 bp repeat motifs were identified. Primer3 (Untergasser et al. 2012) was used for PCR primer design. Initially, we screened 60 primer pairs on a panel of eight *E. obliquata* individuals and narrowed our evaluation to a set of 14 microsatellite polymorphic primer pairs. The criteria used to select these primer pairs were polymorphism of the loci amplified (i.e., observation of more than one allele), tri- or tetranucleotide repeat motif, and annealing temperature close to 59°C for use in subsequent multiplexing. Forward primers were labelled with fluorescent markers as noted in Table 1. Four sets of loci were coamplified in multiplex PCR—*Eoo11* and *Eoo20*; *Eoo16* and *Eoo19*; *Eoo22* and *Eoo24*; *Eoo8*, *Eoo9*, and *Eoo10*; other loci were amplified individually. PCR conditions consisted of H_2O, 5× PCR buffer (Promega, Madison, WI, USA), 2.5 mM $MgCl_2$ (Promega), 2.5 mM deoxynucleotide triphosphate (dNTPs) (ThermoFisher Scientific, Waltham, MA, USA), 1 mg/mL bovine serum albumin (BSA) (ThermoFisher Scientific), 5 μM of each primer, 0.1 μL Go*Taq* Polymerase (New England Biolabs, Ipswich, MA, USA), and 1 μL of genomic DNA at 50 ng/μL, in a total reaction volume of 22 μL. PCR thermal cycling conditions were as follows: 94°C for 3 min, followed by 35 cycles of 94°C for 40 s, 59°C for 40 s, and 72°C for 1 min; a final extension at 72°C for 5 min; and a hold at 4°C. Amplification of PCR products was verified by visualization under ultraviolet light in an ethidium bromide-stained agarose gel. PCR products were sent to the Institute of Biotechnology at Cornell University, Ithaca, New York, for DNA fragment-size analysis. Microsatellites were scored for length using Genemarker (SoftGenetics, State College, PA, USA). Arlequin v3.0 (Excoffier et al. 2005) was used to assess heterozygosity, number of observed alleles per locus, conformance to Hardy–Weinberg equilibrium (HWE), and linkage disequilibrium (LD). Testing for HWE and LD used Arlequin and a critical type I error rate = 0.05. Evidence for a bottleneck at each locus was tested using the Garza–Williamson index (*M*-ratio, the ratio of the number of alleles observed to the number of alleles possible within the observed range in allele sizes) using Arlequin; values of *M* below 0.7 suggest the occurrence of a bottleneck (Garza and Williamson 2001). MICROCHECKER 2.2.3 (Van Oosterhout et al. 2004) was used to assess the possibility of segregation of null alleles.

RESULTS AND DISCUSSION

Allelic diversity ranged from 2 to 15 alleles per locus and averaged 7.6 alleles per locus, while observed heterozygosity per locus ranged from 0.091 to 1.000 and averaged 0.674 (Table 1). Significant deviations from HWE, showing deficiencies in heterozygotes, were observed at 6 of the 14 loci, and LD was observed at 9 (∼10%) of the 91 pairwise comparisons among loci and involved 12 of the 14 total loci sampled (*Eoo9* and *Eoo19*; *Eoo11* and *Eoo19*; *Eoo9* and *Eoo22*; *Eoo20* and *Eoo22*; *Eoo16* and *Eoo24*; *Eoo11* and *Eoo31*; *Eoo8* and *Eoo44*; *Eoo31* and *Eoo38*; *Eoo11* and *Eoo60*). The *M*-ratios for six loci were below 0.70, suggesting recent loss of allelic diversity at these loci. Possible segregation of null alleles was detected at loci *Eoo16*, *Eoo20*, *Eoo22*, and *Eoo38*. Because of the small size of the population sampled, deviations from HWE and LD could result from loci being closely located on the same chromosome, segregation of null alleles, family structure, population bottlenecks, inbreeding, hermaphroditic reproduction (van der Schalie 1970), or some combination of these factors. Appendix A1 lists individual genotypes at the 14 loci.

These primer pairs are the third set of microsatellite primers developed for the genus *Epioblasma*. The first set of primers was developed for *Epioblasma capsaeformis* (Jones et al. 2004) and the second for *Epioblasma rangiana* (Zanatta and Murphy 2006). We did not test primers developed for *E. capsaeformis* and *E. rangiana* on *E. obliquata*, but allelic diversity of *E. obliquata* was lower than in those two species. For the 10 loci developed for *E. capsaeformis* ($n = 20$ individuals assessed/locus), allelic diversity ranged from 5 to 17 alleles/locus and averaged 9.7 alleles/locus. For the six loci

Table 1. Characteristics of 14 microsatellite loci developed using DNA obtained in 2016 and 2017 from 44 individuals of the Catspaw (*Epioblasma obliquata*) from Killbuck Creek, Coshocton County, Ohio. H_O and H_E are observed and expected heterozygosity, respectively. Statistically significant deviations from Hardy–Weinberg Equilibrium (HWE) are denoted by an asterisk (*). *M*-ratio is the Garza–Williamson index. Individual genotypes at the 14 loci are reported in Appendix A1.

Locus	Primer Sequence (5′–3′) and Fluorescent Label	Melting Temperature (°C)	Repeat Motif	Allele Size Range (bp)	No. of Alleles/ Locus	H_o	H_E	HWE *P* Value	*M*-Ratio
*Eoo8**	F:TATCCCTCCGCTGCTGTAAG – PET	59.7	$ACT_{(16)}$	125–173	5	1.000	0.586	0.000*	0.714
	R:CCCTGGCCTGTAACAATCTTG	59.7							
Eoo9	F:CTCTCCGTGATGTTTGCTCC – VIC	59.3	$AAT_{(29)}$	110–197	4	0.477	0.512	0.081	1.000
	R:TTCCATTCCAAGCACGTACG	59.7							
*Eoo10**	F:CTGGTTGTTCGGTCTTGTGG – NED	59.4	$ATC_{(8)}$	137–161	13	0.864	0.815	0.019*	0.867
	R:ACTTTACATCCTGTCCAACTGC	59.8							
Eoo11	F:GCCGCCATGAATAGCCTATC – 6FAM	59.4	$AAC_{(10)}$	197–227	2	0.455	0.505	0.556	0.667
	R:TCTCCCATCAACCAACATTGTC	59.4							
*Eoo16**	F:TGGGTAGTCTCTGTCGTATGC – NED	59.7	$ACAT_{(11)}$	132–176	8	0.477	0.597	0.021*	0.363
	R:AATGGCGCTAATCCCACAAC	59.7							
Eoo19	F:CCTAGGCAGCAAACAGTTCG – 6FAM	59.8	$AGAT_{(10)}$	109–149	13	0.977	0.900	0.137	0.541
	R:GCGGCCAGTATTAATGGTGG	59.9							
Eoo20	F:ACTACAGTACACGACCAGGC – PET	59.6	$ACAT_{(19)}$	74–150	15	0.786	0.921	0.050	0.789
	R:ACCCATGACCTTCCGTATCC	59.9							
*Eoo22**	F:CAGTCCAAGTCATCTCTCAGG – VIC	58.4	$AGAT_{(15)}$	91–151	12	0.750	0.894	0.003*	0.923
	R:GCATACGTGTAGCTTTATCGTG	58.2							
Eoo24	F:TCACAAGTCCTACACCCTCTC – PET	59.0	$AATC_{(6)}$	169–193	2	0.500	0.471	0.748	1.000
	R:TCTTATCAGTTGGGTTTGGTGG	59.2							
Eoo31	F:CAGTCGGGCGTCATCATTCCCTAGCAA – PET	59.7	$ATC_{(9)}$	205–232	6	0.591	0.651	0.314	0.500
	R:GTTTGGTGTAGTGCTCGGAAAC	58.9							
*Eoo38**	F:CAGTCGGGCGTCATCAGCTAACTCCA – 6FAM	59.4	$AAG_{(11)}$	101–134	13	0.659	0.882	0.000*	0.722
	R:GTTTCGCCACCTGAACAGCATATG	60.1							
*Eoo44**	F:CAGTCGGGCGTCATCACCATTAATACT - VIC	59.8	$AAC_{(8)}$	84–108	2	1.000	0.506	0.000*	0.667
	R:GTTTGGGCATCAACGACTTTCATTC	58.6							
Eoo46	F:CAGTCGGGCGTCATCACTGTAACGAG – NED	58.9	$ATCC_{(6)}$	223–247	2	0.091	0.088	1.000	0.500
	R:GTTTGTTAGTTGGGCGGATGGTTG	59.9							
Eoo60	F:GTTTGCTTGCGGTATGTGCTG – VIC	60.5	$AATC_{(10)}$	167–207	10	0.818	0.845	0.814	0.714
	R:CAGTCGGGCGTCATCACCATCTTCAAG	59.0							
Mean					7.6	0.675	0.655		0.712

developed for *E. rangiana* (n = 73–86 individuals/locus), allelic diversity ranged from 12 to 28 alleles/locus and averaged 19.3 alleles/locus. After careful screening for null alleles, HWE, and LD, some of our microsatellite loci developed for *E. obliquata* may prove useful for cross-species amplification in other species, especially other *Epioblasma*. Likewise, future studies could screen the microsatellite loci developed by Jones et al. (2004) and Zanatta and Murphy (2006) to determine whether additional loci are suitable for cross-species amplification in *E. obliquata*.

Sampling more individuals of *E. obliquata* for further population genetic analysis would benefit conservation management. The screening of more wild individuals and any other populations that may be found could provide insight into the population genetic diversity and natural history of this species. Given the isolation and small size of the remaining known population of *E. obliquata*, these microsatellite loci and other genetic markers will be valuable for monitoring the effects of propagation and management practices seeking to maintain or increase genetic diversity in hatchery stocks and wild populations receiving stocked individuals. For example, if hatchery technology improves to allow for the long-term holding, spawning, and fertilization of broodstock in captivity, the loci developed in this study will be useful for monitoring genetic diversity and inbreeding in parental stocks and progeny, which will be critical for maintaining healthy captive and wild populations of *E. obliquata* (Jones et al. 2020).

ACKNOWLEDGMENTS

The U.S. Fish and Wildlife Service (USFWS), Frankfort, Kentucky, provided support for this project. We thank Dr.

Monte McGregor, Kentucky Department of Fish and Wildlife Resources, and Leroy Koch, USFWS, for their assistance in collecting mussel tissue samples from Killbuck Creek, Ohio, and Minor Clark Fish Hatchery, Kentucky. The participation of E. M. Hallerman was supported in part by the U.S. Department of Agriculture through the National Institute of Food and Agriculture. The findings and conclusions in this article are those of the authors and do not necessarily represent the views of the U.S. Fish and Wildlife Service.

LITERATURE CITED

Cooper, A. M., L. M. Miller, and A. R. Kapuscinski. 2009. Conservation of population structure and genetic diversity under captive breeding of remnant coaster brook trout, *Salvelinus fontinalis*, populations. Conservation Genetics 11:1087–1093.

Excoffier, L., G. Laval, and S. Schneider. 2005. Arlequin ver. 3.0: An integrated software package for population genetics data analysis. Evolutionary Bioinformatics Online 1:47–50.

Faircloth, B. C. 2008. MSATCOMMANDER: Detection of microsatellite repeat arrays and automated, locus-specific primer design. Molecular Ecology Resources 8:92–94.

Garza, J. C., and E. G. Williamson. 2001. Detection of reduction in population size using data from microsatellite loci. Molecular Ecology 10:305–318.

Hoggarth, M. A., D. L. Rice, and D. M. Lee. 1995. Discovery of the federally endangered freshwater mussel, *Epioblasma obliquata obliquata* (Rafinesque, 1820) (Unionidae), in Ohio. The Ohio Journal of Science 4:298–299.

Jones, J. W., M. Culver, V. David, J. Struthers, N. A. Johnson, R. J. Neves, S. J. O'Brien, and E. M. Hallerman. 2004. Development and characterization of microsatellite loci in the endangered oyster mussel *Epioblasma capsaeformis* (Bivalvia:Unionidae). Molecular Ecology Notes 4:649–652.

Jones, J. W., E. M. Hallerman, and R. J. Neves. 2006. Genetic management guidelines for captive propagation of freshwater mussels (Unionoidea). Journal of Shellfish Research 25:527–535.

Jones, J. W., W. F. Henley, A. J. Timpano, E. Frimpong, and E. M. Hallerman. 2020. Spawning and gravidity of the endangered freshwater mussel *Epioblasma capsaeformis* (Bivalvia: Unionidae) in captivity for production of glochidia. Invertebrate Development and Reproduction 64:312–325.

Serb, J. M., J. E. Buhay, and C. Lydeard. 2003. Molecular systematics of the North American freshwater bivalve genus *Quadrula* (Unionidae: Ambleminae) based on mitochondrial *ND1* sequences. Molecular Phylogenetics and Evolution 28:1–11.

Untergasser, A., I. Cutcutache, T. Koressaar, J. Ye, B. C. Faircloth, M. Remm, and S.G. Rozen. 2012. Primer3–New capabilities and interfaces. Nucleic Acids Research 40(15):e115.

USFWS (U.S. Fish and Wildlife Service). 1990. Purple cat's paw pearlymussel determined to be an endangered species. Federal Register 55:28209–28213.

van der Schalie, H. 1970. Hermaphroditism among North American freshwater mussels. Malacologia 10:93–112.

Van Oosterhout, C., W. F. Hutchinson, D. P. Wills, and P. Shipley. 2004. MICROCHECKER: software for identifying and correcting genotyping errors in microsatellite data. Molecular Ecology Notes 4:535–538.

Zanatta, D. T., and R. W. Murphy. 2006. Development and characterization of microsatellite markers for the endangered northern riffleshell mussel *Epioblasma torulosa rangiana* (Bivalvia: Unionidae). Molecular Ecology Notes 6:850–852.

Zane, L., L. Bargelloni, and T. Patarnello. 2002. Strategies for microsatellite isolation: a review. Molecular Ecology 11:1–16.

Appendix A1. Scored microsatellite genotypes of 44 individuals of the Catspaw (*Epioblasma obliquata*) from Killbuck Creek, Coshocton County, Ohio, at 14 loci. Microsatellite amplicons were scored for length using Genemarker software (SoftGenetics, State College, PA, USA). Individuals and loci without a scored allele (—) indicate that no allele product was observed at that locus. Columns with either 1 or 2 designate alleles per locus.

Loci	*Eoo8* ACT(16)		*Eoo9* AAT(29)		*Eoo10* ATC(8)		*Eoo11* AAC(10)		*Eoo16* ACAT(11)		*Eoo19* AGAT(10)		*Eoo20* ACAT(19)		*Eoo22* AGAT(15)		*Eoo24* AATC(6)		*Eoo31* ATC(9)		*Eoo38* AAG(11)		*Eoo44* AAC(8)		*Eoo46* ATCC(6)		*Eoo60* AATC(10)	
Individual	1	2	1	2	1	2	1	2	1	2	1	2	1	2	1	2	1	2	1	2	1	2	1	2	1	2	1	2
Wildstock1	169	184	182	188	199	211	260	266	224	236	189	201	—	—	205	217	—	—	199	199	289	289	253	259	124	124	242	246
Wildstock2	169	184	182	185	211	217	260	266	240	240	197	213	—	—	209	221	171	175	199	199	253	259	253	259	124	136	234	254
Wildstock3	169	184	179	179	211	220	266	266	240	240	193	197	294	294	185	193	175	175	211	211	256	292	253	259	124	124	242	246
Wildstock4	169	184	182	185	205	205	266	266	228	228	185	201	282	298	213	221	171	175	199	217	253	289	253	259	124	124	234	246
Wildstock5	169	184	182	182	199	199	260	266	240	240	193	201	254	326	221	221	175	175	199	211	241	256	253	259	124	124	242	246
Wildstock6	169	184	182	182	199	211	266	266	240	240	193	197	282	298	185	201	171	175	199	217	253	253	253	259	124	124	246	246
Wildstock7	169	184	182	182	199	220	260	266	240	240	177	205	282	298	213	213	175	175	217	223	250	271	253	259	124	136	242	242
Wildstock8	169	184	179	182	190	211	266	266	240	244	185	225	302	326	201	201	171	175	199	217	277	292	253	259	124	124	202	242
Wildstock9	169	184	185	185	190	199	266	266	240	240	201	217	282	302	201	201	171	171	199	217	286	286	253	259	124	124	218	230
Wildstock10	169	184	182	185	190	199	260	266	240	240	197	205	306	326	209	209	171	175	199	223	271	289	253	259	124	124	246	246
Wildstock11	169	184	182	188	202	211	266	266	228	240	185	189	254	294	173	185	171	171	199	199	289	289	253	259	124	124	234	234
Wildstock12	169	184	182	182	190	208	260	260	240	240	193	205	278	278	193	201	171	175	223	223	256	256	253	259	124	124	242	246
Wildstock13	169	184	182	182	190	199	266	266	228	240	185	201	298	314	201	209	175	175	199	199	265	289	253	259	124	124	218	246
Wildstock14	169	184	182	185	199	199	260	260	240	240	185	205	282	314	185	213	175	175	199	199	259	259	253	259	124	124	230	246
Wildstock15	169	181	182	182	193	211	266	266	232	240	177	205	278	298	205	221	171	175	199	217	250	256	253	259	124	124	234	242
Wildstock16	169	184	182	182	187	208	260	266	240	240	193	201	310	326	185	193	171	175	217	217	241	277	253	259	124	124	242	242
Wildstock17	169	184	179	185	190	202	260	260	232	232	193	213	254	314	213	213	175	175	199	199	256	289	253	259	124	124	218	226
Wildstock18	169	181	182	182	199	220	260	266	240	240	133	189	262	286	205	205	171	175	199	226	259	292	253	259	124	124	218	234
Wildstock19	169	184	182	188	199	199	260	260	240	240	193	213	286	326	173	221	175	175	199	211	256	256	253	259	124	124	242	242
Wildstock20	169	184	182	185	202	211	260	266	240	240	185	201	282	306	213	221	171	175	199	199	256	265	253	259	124	124	218	234
Wildstock21	169	184	182	182	190	190	260	266	232	240	177	181	282	318	181	213	175	175	211	211	256	292	253	259	124	124	218	242
Wildstock22	169	187	179	179	199	211	260	266	240	240	197	201	254	294	205	205	171	175	199	211	256	256	253	259	124	124	234	242
Wildstock23	169	184	182	185	190	199	260	266	228	228	133	201	314	314	185	197	171	171	211	211	241	253	253	259	124	124	202	246
Wildstock24	169	184	182	185	196	220	260	260	232	236	181	205	298	310	213	217	—	—	211	217	250	262	253	259	124	124	242	246
Wildstock25	169	184	182	185	190	199	260	266	232	240	133	201	278	314	201	209	171	175	199	199	259	259	253	259	124	124	218	246
Wildstock26	169	184	182	185	190	199	260	260	240	240	181	205	302	322	193	201	171	175	211	211	256	265	253	259	124	124	206	226
Wildstock27	169	184	182	185	190	199	260	260	240	240	189	197	254	254	193	201	171	175	199	211	256	265	253	259	124	124	226	246
Wildstock28	169	181	179	185	190	199	266	266	240	240	209	209	314	322	201	213	175	175	199	211	256	289	253	259	124	124	218	218
Wildstock29	169	184	182	188	199	211	260	266	228	240	185	189	254	314	173	185	171	171	199	217	289	289	253	259	124	124	234	242
Wildstock30	169	184	182	182	190	199	266	266	168	240	197	201	306	306	221	221	171	175	199	199	256	289	253	259	124	124	234	246
Wildstock31	169	181	179	182	208	217	260	266	232	240	189	201	278	290	193	213	175	175	199	211	253	253	253	259	124	124	226	254
Wildstock32	169	184	182	188	196	220	260	260	240	240	133	193	282	290	209	217	175	175	199	217	259	259	253	259	124	124	218	242
Wildstock33	169	184	182	182	190	208	260	266	168	240	133	197	282	302	209	209	171	175	211	217	292	292	253	259	124	124	202	234
Wildstock34	169	184	182	182	199	211	260	266	168	240	133	197	282	294	201	209	175	175	199	217	241	259	253	259	124	124	206	238
Wildstock35	169	184	182	182	211	220	260	260	168	240	185	193	278	298	181	193	175	175	199	211	262	262	253	259	124	124	218	246

Appendix A1. Scored microsatellite genotypes of 44 individuals of the Catspaw (*Epioblasma obliquata*) from Killbuck Creek, Coshocton County, Ohio, at 14 loci. Microsatellite amplicons were scored for length using Genemarker software (SoftGenetics, State College, PA, USA). Individuals and loci without a scored allele (—) indicate that no allele product was observed at that locus. Columns with either 1 or 2 designate alleles per locus.

Loci	*Eoo8* ACT(16)		*Eoo9* AAT(29)		*Eoo10* ATC(8)		*Eoo11* AAC(10)		*Eoo16* ACAT(11)		*Eoo19* AGAT(10)		*Eoo20* ACAT(19)		*Eoo22* AGAT(15)		*Eoo24* AATC(6)		*Eoo31* ATC(9)		*Eoo38* AAG(11)		*Eoo44* AAC(8)		*Eoo46* ATCC(6)		*Eoo60* AATC(10)	
Wildstock36	169	184	182	185	199	205	260	266	168	168	197	217	302	302	185	201	171	175	199	232	256	289	253	259	124	136	202	218
Wildstock37	169	178	182	182	199	214	260	266	168	240	133	193	310	310	185	221	175	175	199	217	253	292	253	259	124	124	246	254
Wildstock38	169	178	182	182	199	211	260	266	232	240	133	193	282	282	189	193	175	175	199	199	259	265	253	259	124	136	234	246
Wildstock39	169	178	182	182	199	199	266	266	240	240	185	201	302	314	185	201	171	175	199	217	277	289	253	259	124	124	202	218
Wildstock40	169	184	182	185	202	214	260	266	236	240	133	185	294	302	185	205	171	175	199	211	256	289	253	259	124	124	218	234
Wildstock41	169	184	182	182	199	211	266	266	160	232	189	201	278	306	209	221	175	175	199	199	241	259	253	259	124	124	234	234
Wildstock42	169	184	182	182	199	211	260	260	168	232	193	205	310	310	189	193	171	171	199	211	256	256	253	259	124	124	218	238
Wildstock43	169	184	182	182	193	199	260	260	168	240	197	205	294	302	201	201	171	175	211	232	265	280	253	259	124	124	218	226
Wildstock44	169	184	182	182	178	199	266	266	160	228	133	197	254	298	205	217	171	175	199	199	262	289	253	259	124	124	234	246

Freshwater Mollusk Biology and Conservation 25:7–14, 2022

DOI:10.31931/fmbc-d-21-00009

REGULAR ARTICLE

POTENTIAL RECOVERY OF THE MUSSEL FAUNA OF THE CLARION RIVER, PENNSYLVANIA

Charles E. Williams[1]*

[1] *Williams Ecological, LLC, 103 Hillcrest Lane, Shippenville, PA 16254 USA*

ABSTRACT

The Clarion River, a tributary of the Allegheny River in northwestern Pennsylvania, underwent heavy industrialization during the late 19th and early 20th centuries. In the early 1900s, eight tanneries, 11 wood chemical plants, and a large paper mill operated on the Clarion River, releasing a cumulative 98 million liters of industrial effluent daily, in addition to the discharge of coal-mining wastes. By 1911, aquatic life was considered eliminated from the river, but **its original mussel fauna was never recorded. In 1993, four living individuals of *Strophitus undulatus*, the Creeper, were discovered by chance near Clarington, Forest County, which constituted the first documented collection of mussels from the river. I conducted qualitative shell surveys from 2007 to 2019 at 157 sites to document past and present mussel distribution along a 55-km reach of the river. Recently dead shells, weathered shells, or living individuals of *S. undulatus* were encountered at 146 sites within the study reach. Relic shells of *Actinonaias ligamentina* were found at 12 sites, recently dead shells and one living individual of *Lampsilis fasciola* were found at five sites, and a single recently dead shell of *Lampsilis ovata* was collected. Ages of a subsample of 60 recently dead *S. undulatus* ranged from 2 to 16 yr (mean = 8.0 yr) and length ranged from 26.8 to 81.7 mm (mean = 29.8 mm), suggesting that natural recruitment may be occurring in the river. Source populations for recolonization of the river are unknown, but tributaries of the Clarion River are a possibility. My results suggest that the Clarion River now supports a substantial mussel population, but additional surveys are needed to provide a baseline for monitoring future recovery.**

KEY WORDS: Clarion River, industrial pollution, mine waste, Pennsylvania, river recovery

INTRODUCTION

Unregulated pollution by coal mine drainage and industrial effluents decimated the aquatic biota of many streams in western Pennsylvania by the early 1900s (Ortmann 1909). Ortmann (1909) singled out the Clarion River in northwestern Pennsylvania as "possibly one of the worst streams in the state" with regard to water pollution. Eight tanneries, 11 wood chemical plants, and a large paper mill operated on the river, chiefly in Elk County, releasing a cumulative 98 million liters of industrial effluent daily in addition to mine wastes entering the river from tributaries (Department of Health of the Commonwealth of Pennsylvania 1915). Ortmann's description of the condition of the Clarion River at the time was stark: "The water of [the] Clarion River. . .is black like ink, and retains its peculiar color all the way down to where it empties into the Allegheny [River]." He later concluded that the aquatic fauna of the Clarion River was "entirely destroyed" (Ortmann 1913) but acknowledged that no historical mussel records were known from the stream (Ortmann 1919).

Mussels remained unknown from the Clarion River until 1993, when biologists conducting an odonate survey made a chance discovery of four living individuals of *Strophitus undulatus*, the Creeper, near Clarington, Forest County (Carnegie Museum and Western Pennsylvania Conservancy 1993). The authors suggested that *S. undulatus* might be slowly recolonizing formerly degraded habitat but doubted that the river could support substantial mussel populations; however, they gave no specific reasons for their doubt.

I conducted qualitative shell surveys from 2007 to 2019 to document past and present mussel distribution along a 55-km reach of the Clarion River. I measured and aged a representative sample of recently dead *S. undulatus* shells to

*Corresponding Author: chuckwilliams2019@outlook.com

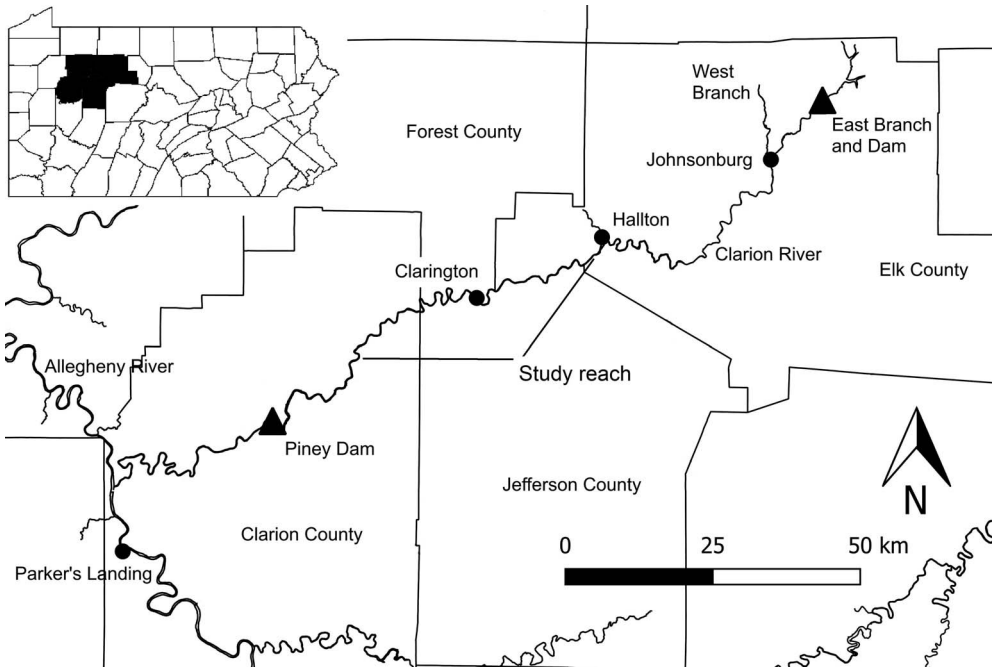

Figure 1. Map of the Clarion River, Pennsylvania, with study reach and key locales. Insert map shows the four-county region drained by the river.

provide demographic information about the population. I discuss my findings with regard to the potential recovery of the mussel fauna of the Clarion River.

STUDY AREA

The Clarion River is a tributary of the Allegheny River in northwestern Pennsylvania. The Clarion River watershed encompasses 2,850 km^2 located in two sections of the nonglaciated Appalachian Plateau physiographic province: the Allegheny High Plateau in the north and the Pittsburgh Low Plateau to the south (Commonwealth of Pennsylvania 2018). Landscapes of the High Plateau include broadly rounded uplands of moderate to high relief with deep, angular valleys; those of the Low Plateau consist of irregular to smooth, undulating uplands of low to moderate relief with relatively shallow valleys. Drainage patterns in both sections are dendritic with sandstone, siltstone, and shale as the predominant bedrock types (Commonwealth of Pennsylvania 2018). Forestry and oil and natural gas extraction are dominant land uses on the High Plateau. On the Low Plateau, agriculture and strip mining for bituminous coal are common (Williams 1995).

The Clarion River proper forms at Johnsonburg, Elk County, at the confluence of the East Branch and West Branch and flows 164 km southwest to meet the Allegheny River upstream of Parker's Landing, Armstrong County (Fig. 1). The watershed has two major dams, Piney Dam, completed in 1924 on the mainstem in Clarion County for flood control and hydropower generation (Williams 1995), and East Branch Dam, completed in 1952 on the East Branch Clarion River for flood control and summer flow enhancement (USACOE 2021). Piney Dam both isolates the upper Clarion River from the rich aquatic fauna of the Allegheny River and creates irregular flows downstream that can affect aquatic biota (Bardarik 1965).

Efforts to abate industrial pollution of the Clarion River began in the 1940s with improved waste treatment technologies and effluent retention facilities, particularly at the paper mill in Johnsonburg (Anonymous 1949; Camp, Dresser, and McKee, Consulting Engineers 1949). Water quality improved significantly from the 1960s to the 1980s as additional point source pollution and abandoned mine drainage issues were addressed (Williams 1995). These efforts were largely successful: in 1996, an 83-km reach of the Clarion River upstream of Piney Dam was given National Wild and Scenic River status. Presently, the Clarion River is an important recreational resource for the region and was named Pennsylvania River of the Year in 2019 (POWR 2019).

METHODS

I conducted qualitative shell surveys from 2007 to 2019 at 157 sites along a 55-km reach of the Clarion River between river kilometer (rkm, measured from the mouth of the river) 64, just above the slack water of Piney Reservoir in Clarion County, to rkm 119 at the mouth of Spring Creek in Hallton, Elk County (Fig. 1). I chose this reach because it contained ample access points, and it included the 1993 collection site for *S. undulatus* at about rkm 97 (Carnegie Museum and Western Pennsylvania Conservancy 1993). I searched for shells by walking gravel point bars, wading the river, and kayaking. I classified shells as either recently dead, having intact periostracum and lustrous nacre; weathered shells,

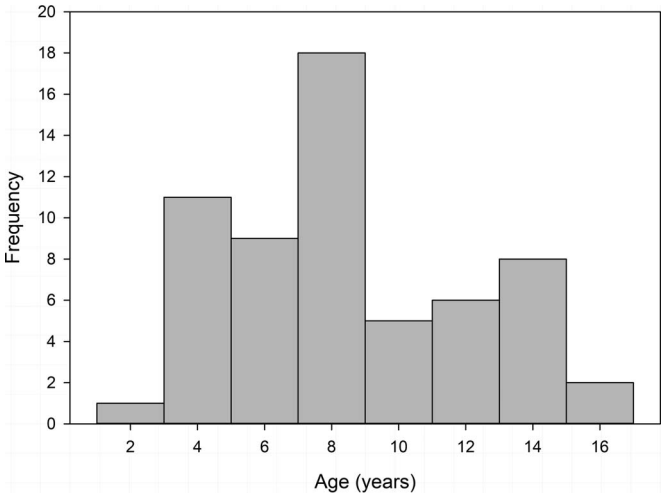

Figure 2. Age-frequency distribution for recently dead shells ($n = 60$) of *Strophitus undulatus* collected from the Clarion River.

having weathered periostracum and nacre; or relic shells, having heavy wear and little periostracum, indicative of having been dead for an extended time (Blodgett and Sparks 1987; Sietman et al. 2001). Because this was an initial survey of mussel occurrence in the river, I made no consistent efforts to find live mussels, but I report incidental occurrences of live mussels encountered during shell surveys. Live mussels were returned to the area of collection after identification.

I measured and aged a random sample ($n = 60$) of recently dead shells of *S. undulatus* to provide demographic information on the species in the Clarion River. I measured the anterior-to-posterior shell length (nearest 0.1 mm) with digital caliper prior to sectioning. I selected one valve from each specimen and cut the valve radially from the umbo into two halves using a fine jeweler's saw. Instead of cutting thin sections from the valve (e.g., Neves and Moyer 1988), I lightly sanded the cut edge of the valve with 400-grit sandpaper and examined the wetted, cut edge under a dissecting microscope; wetting the shell accentuated shell rings. I identified annuli and distinguished them from nonannual rings as rings that could be traced from the umbo to the shell margin (Neves and Moyer 1988). Aging mussel species with slow growth and closely spaced annuli requires thin-sectioning techniques (Neves and Moyer 1988), but rapidly growing species such as *S. undulatus* can be aged effectively without thin sectioning (Neves and Moyer 1988; Haag and Commens-Carsons 2008; Harriger et al. 2009)). I examined the relationship between age and shell length with linear regression using QED Statistics version 1.5.1.456 (Pisces Conservation Ltd. 2015).

RESULTS

A total of 321 shells and living individuals of four mussel species were collected; at least one shell or mussel was collected from each of the 157 sites (Table 1). Two hundred forty-one recently dead shells, 58 weathered shells, and four live individuals of *S. undulatus* were collected from 146 sites (93% of total shells collected across sites; mean = 2.1 shells or live mussels/site at sites with *S. undulatus*). Twelve relic shells of *Actinonaias ligamentina* were found at 12 sites (3.7% of total shells collected across sites), five recently dead shells and one live *Lampsilis fasciola* were found at five sites (3.2% of total shells collected across sites), and one recently dead shell of *Lampsilis ovata* was found at one site (0.6% of total shells collected across sites). The few living individuals of *S. undulatus* and *L. fasciola* were found in slow-moving reaches of the river with substrates of fine sand and gravel.

Ages of 60 recently dead *S. undulatus* shells ranged from 2 to 16 yr, with a mean age of 8.0 yr (±1.0 SE; Fig. 2). Length of sampled shells ranged from 26.8 to 81.7 mm with a mean length of 29.8 mm (±0.5 SE). Shell length was positively associated with age ($r^2 = 0.86$, $P = 0.005$, shell length = 3.8[age] + 23.8).

DISCUSSION

Contrary to previous ideas that the Clarion River is unsuitable for mussels (Carnegie Museum and Western Pennsylvania Conservancy 1993), my results show that mussels, particularly *S. undulatus*, are of widespread occurrence, at least in my 55-km study reach. Species richness was low, and I have no information about the abundance of live mussels in the river. Nevertheless, the frequent occurrence of recently dead shells suggests that the study reach supports a substantial mussel population. Suitability of the river for mussels is further supported by a recent mussel relocation project; survival of several mussel species translocated from the Allegheny River to the upper Clarion River was 98% after 1 yr (Western Pennsylvania Conservancy 2015).

Strophitus undulatus possesses several life history traits that may allow it to readily recolonize streams recovering from severe pollution. First, *S. undulatus* is a host generalist whose glochidia can parasitize many different fish species (Cliff et al. 2001; Van Snik Gray et al. 2002; Ford and Oliver 2015). Second, *S. undulatus* is a widespread species and occurs across a range of environmental conditions (Ortmann 1919; Strayer and Jirka 1997), but it is predominantly found in smaller rivers and streams (Haag 2012). Finally, *S. undulatus* is classified as having a periodic life-history strategy, intermediate in position on the *r–K* continuum, with moderate life span, low to moderate age at maturity, and moderate to high growth rate, traits that can allow rapid population growth in some situations (Haag 2012). My results support a low–moderate life span of at least 16 yr. The wide range of ages represented in the population, including individuals as young as 2 yr old, suggests that natural recruitment is occurring in the river.

The other three species found in the Clarion River were rare. *Lampsilis fasciola* and *L. ovata* both were represented by live individuals or recently dead shells, suggesting that at least small populations currently exist in the river. *Actinonaias ligamentina* was represented only by relic shells. These shells may indicate occurrence of the species in the river prior to

Table 1. Sites on the Clarion River sampled for mussel shells from 2007 to 2019.

Site	Date	Coordinates	Findings
1	September 7, 2007	41.39583, 79.27611	2 RD *Strophitus undulatus*
2	September 10, 2007	41.55028, 79.39000	1 RD *S. undulatus*
3	September 20, 2007	41.36361, 79.35139	1 RD *S. undulatus*
4	September 20, 2007	41.32667, 79.46917	1 RD *S. undulatus*
5	September 25, 2007	41.45222, 79.15389	2 RD, 1 W *S. undulatus*
6	September 25, 2007	41.34250, 79.16250	1 RD *S. undulatus*
7	September 25, 2007	41.35111, 79.07750	1 RD *S. undulatus*
8	September 26, 2007	41.42889, 79.37278	1 RD *S. undulatus*
9	September 26, 2007	41.38528, 79.41472	1 RD *S. undulatus*
10	September 26, 2007	41.39056, 79.38306	1 RD *S. undulatus*
11	April 15, 2008	41.38778, 79.26361	1 RD, 2 W *S. undulatus*
12	April 29, 2008	41.39778, 79.49333	2 RD *S. undulatus*
13	April 29, 2008	41.39667, 79.38028	2 RD *S. undulatus*
14	April 30, 2008	41.39306, 79.38217	1 RD *S. undulatus*
15	April 30, 2008	41.40361, 79.33972	2 RD *S. undulatus*
16	April 30, 2008	41.29694, 79.27278	1 RD *S. undulatus*
17	April 30, 2008	41.43833, 79.27194	2 RD *S. undulatus*
18	April 30, 2008	41.40972, 79.33556	2 RD *S. undulatus*
19	May 5, 2008	41.39417, 79.37972	1 RD *S. undulatus*
20	May 6, 2008	41.38389, 79.25111	2 RD *S. undulatus*
21	May 6, 2008	41.37306, 79.49944	1 RD *S. undulatus*
22	May 6, 2008	41.37667, 79.47194	1 RD *S. undulatus*
23	May 6, 2008	41.37944, 79.25611	1 RD *S. undulatus*
24	May 12, 2008	41.39361, 79.38000	1 RD *S. undulatus*
25	May 15, 2008	41.37917, 79.46778	2 RD, 1 W *S. undulatus*
26	May 15, 2008	41.37306, 79.49611	1 RD *S. undulatus*
27	June 6, 2008	41.49111, 79.36833	2 RD *S. undulatus*
28	June 6, 2008	41.42250, 79.40222	1 R *Actinonaias ligamentina*; 1 RD *S. undulatus*
29	June 13, 2008	41.39250, 79.42667	1 RD *S. undulatus*
30	July 2, 2008	41.39306, 79.39222	1 RD *S. undulatus*
31	September 21, 2008	41.33167, 79.43694	1 RD *S. undulatus*
32	September 21, 2008	41.33639, 79.43972	1 RD *S. undulatus*
33	October 6, 2008	41.38278, 79.26056	1 RD, 1 W *S. undulatus*
34	October 6, 2008	41.37750, 79.51083	1 RD *S. undulatus*
35	October 8, 2008	41.47639, 79.30972	1 RD *S. undulatus*
36	October 8, 2008	41.46083, 79.28889	1 RD *S. undulatus*
37	October 8, 2008	41.36361, 79.30861	2 RD *S. undulatus*
38	October 8, 2008	41.37861, 79.18083	1 RD, 1 W *S. undulatus*
39	October 8, 2008	41.38528, 79.31306	1 RD *S. undulatus*
40	October 9, 2008	41.33444, 79.21778	1 RD *S. undulatus*
41	October 10, 2008	41.38528, 79.31306	1 R *A. ligamentina*
42	October 10, 2008	41.43917, 79.39361	1 RD *S. undulatus*
43	October 10, 2008	41.34250, 79.37306	1 RD, 1 W *S. undulatus*
44	October 10, 2008	41.42444, 79.37306	1 RD *S. undulatus*
45	October 10, 2008	41.42167, 79.36917	1 RD *S. undulatus*
46	October 10, 2008	41.41556, 79.36361	1 RD, 3 W *S. undulatus*
47	October 10, 2008	41.41056, 79.35861	1 RD *S. undulatus*
48	October 10, 2008	41.40806, 79.35500	2 RD *S. undulatus*
49	October 10, 2008	41.41028, 79.36056	1 L *S. undulatus*
50	October 13, 2008	41.51389, 79.03500	1 R *A. ligamentina*
51	April 27, 2009	41.30083, 79.25944	1 RD *S. undulatus*
52	April 27, 2009	41.38222, 79.25778	1 RD *S. undulatus*
53	April 27, 2009	41.38167, 79.25083	1 RD *S. undulatus*

Table 1, continued.

Site	Date	Coordinates	Findings
54	April 27, 2009	41.37278, 79.49778	1 RD *S. undulatus*
55	April 27, 2009	41.37306, 79.49806	1 RD *S. undulatus*
56	April 28, 2009	41.44417, 79.33000	1 RD *S. undulatus*
57	April 28, 2009	41.44667, 79.33139	1 RD *S. undulatus*
58	April 28, 2009	41.44250, 79.33583	1 RD *S. undulatus*
59	April 28, 2009	41.44222, 79.33917	2 RD, 1 W *S. undulatus*
60	April 28, 2009	41.44194, 79.34000	1 RD *S. undulatus*
61	April 28, 2009	41.44139, 79.35056	1 RD *S. undulatus*
62	April 28, 2009	41.44111, 79.35611	1 RD *S. undulatus*
63	April 28, 2009	41.44139, 79.35861	1 RD *S. undulatus*
64	April 28, 2009	41.44250, 79.36972	1 RD *S. undulatus*
65	April 28, 2009	41.32917, 79.37167	1 RD *S. undulatus*
66	April 28, 2009	41.32972, 79.20333	1 RD *S. undulatus*
67	April 28, 2009	41.44861, 79.38917	1 W *S. undulatus*
68	April 28, 2009	41.44806, 79.31861	1 RD *S. undulatus*
69	June 5, 2009	41.44528, 79.17417	1 RD *S. undulatus*
70	August 8, 2009	41.37250, 79.49917	1 RD *S. undulatus*
71	April 6, 2010	41.39861, 79.28111	1 RD *S. undulatus*
72	April 6, 2010	41.44778, 79.37917	1 RD *S. undulatus*
73	June 15, 2010	41.37638, 79.46139	1 RD *S. undulatus*
74	June 25, 2010	41.39389, 79.37972	1 RD *S. undulatus*
75	June 25, 2010	41.39000, 79.42611	1 RD *S. undulatus*
76	August 31, 2010	41.38333, 79.26278	1 RD *S. undulatus*
77	August 31, 2010	41.38028, 79.25583	1 RD *S. undulatus*
78	September 5, 2010	41.36083, 79.31750	1 RD *S. undulatus*
79	September 5, 2010	41.35528, 79.31083	1 RD *S. undulatus*
80	April 21, 2011	41.37333, 79.50083	1 R *A. ligamentina*; 27 RD, 12 W *S. undulatus*
81	June 1, 2011	41.40583, 79.42306	1 R *A. ligamentina*
82	June 15, 2011	41.38667, 79.43222	1 RD *S. undulatus*
83	June 15, 2011	41.36222, 79.31444	1 RD *S. undulatus*
84	September 2, 2011	41.40056, 79.26444	2 RD *S. undulatus*
85	September 2, 2011	41.37278, 79.48556	2 RD *S. undulatus*
86	September 2, 2011	41.37444, 79.49750	1 RD *S. undulatus*
87	September 2, 2011	41.38444, 79.26417	1 RD *S. undulatus*
88	September 2, 2011	41.39028, 79.27111	1 RD *S. undulatus*
89	September 2, 2011	41.39556, 79.27861	1 R *A. ligamentina*; 1 RD *S. undulatus*
90	March 5, 2012	41.38472, 79.26167	2 RD *S. undulatus*
91	March 5, 2012	41.37333, 79.50028	1 RD *S. undulatus*
92	March 5, 2012	41.37472, 79.50250	1 RD *S. undulatus*
93	May 20, 2012	41.47556, 79.14028	1 R *A. ligamentina*
94	May 20, 2012	41.47861, 79.11972	1 RD, 1 W *S. undulatus*
95	August 24, 2012	41.38056, 79.25639	1 RD *S. undulatus*
96	August 24, 2012	41.37444, 79.50222	1 RD *S. undulatus*
97	August 24, 2012	41.40306, 79.29250	1 RD *S. undulatus*
98	April 15, 2013	41.32361, 79.24139	1 RD *S. undulatus*
99	May 27, 2013	41.47528, 79.13222	1 R *A. ligamentina*; 1 RD *S. undulatus*
100	May 27, 2013	41.46972, 79.16361	3 RD, 2 W *S. undulatus*
101	May 27, 2013	41.60722, 79.33944	1 R *A. ligamentina*
102	June 15, 2013	41.36667, 79.33861	1 RD *S. undulatus*
103	July 21, 2013	41.37889, 79.37972	1 R *A. ligamentina*
104	May 26, 2014	41.31806, 79.30333	23 RD, 11 W *S. undulatus*
105	May 26, 2014	41.56500, 79.32750	1 L *S. undulatus*
106	June 8, 2014	41.46611, 79.16611	1 R *A. ligamentina*

Table 1, continued.

Site	Date	Coordinates	Findings
107	June 8, 2014	41.46861, 79.16694	5 RD, 4 W *S. undulatus*
108	July 23, 2014	41.39306, 79.27500	2 RD *S. undulatus*
109	July 23, 2014	41.38806, 79.26806	1 RD *S. undulatus*
110	July 23, 2014	41.38944, 79.26972	1 RD *S. undulatus*
111	September 1, 2014	41.32194, 79.28972	2 RD, 1 W *S. undulatus*
112	October 17, 2014	41.44306, 79.36917	1 RD *S. undulatus*
113	April 18, 2015	41.36500, 79.33833	2 RD *S. undulatus*
114	April 18, 2015	41.36583, 79. 33611	1 RD *S. undulatus*
115	May 3, 2015	41.39528, 79.26139	2 RD *S. undulatus*
116	May 3, 2015	41.60472, 79.33750	1 L, 1 RD *Lampsilis fasciola*
117	May 4, 2015	41.46056, 79.17000	1 RD *L. fasciola*; 1 L, 1 RD, 2 W *S. undulatus*
118	May 4, 2015	41.47667, 79.20528	7 RD *S. undulatus*
119	May 21, 2015	41.44583, 79.32139	2 RD, 2 W *S. undulatus*
120	May 21, 2015	41.50444, 79.24167	2 RD *S. undulatus*
121	May 21, 2015	41.44361, 79.35139	1 RD *S. undulatus*
122	May 21, 2015	41.44417, 79.37833	1 RD *S. undulatus*
123	May 21, 2015	41.45000, 79.39278	1 RD *S. undulatus*
124	May 21, 2015	41.45278, 79.39917	1 RD *S. undulatus*
125	June 6, 2015	41.35722, 79.18611	1 RD *S. undulatus*
126	June 6, 2015	41.46444, 79.16222	1 RD *S. undulatus*
127	June 11, 2015	41.32806, 79.21917	1 W *S. undulatus*
128	June 11, 2015	41.36417, 79.33778	1 RD *S. undulatus*
129	August 13, 2015	41.46333, 79.17389	1 RD *S. undulatus*
130	September 13, 2015	41.36556, 79.33722	1 RD *S. undulatus*
131	September 23, 2015	41.34528, 79.31361	1 RD *L. fasciola*
132	September 23, 2015	41.35028, 79.31000	1 L *S. undulatus*
133	September 23, 2015	41.59417, 79.31944	1 RD *S. undulatus*
134	September 24, 2015	41.57778, 79.32472	1 W *S. undulatus*
135	September 24, 2015	41.55111, 79.32583	1 RD *S. undulatus*
136	September 24, 2015	41.53500, 79.32611	1 RD *S. undulatus*
137	September 24, 2015	41.50306, 79.32111	1 RD *S. undulatus*
138	September 24, 2015	41.50972, 79.32278	1 RD *S. undulatus*
139	September 24, 2015	41.50944, 79.32278	1 RD *S. undulatus*
140	September 24, 2015	41.51889, 79.32333	1 RD, 1 W *S. undulatus*
141	September 24, 2015	41.52694, 79.32528	1 RD *S. undulatus*
142	September 24, 2015	41.54194, 79.32667	1 RD *S. undulatus*
143	September 24, 2015	41.56778, 79.32611	1 RD *S. undulatus*
144	October 21, 2015	41.32000, 79.28972	3 RD *S. undulatus*
145	November 3, 2015	41.45167, 79.17333	2 RD, 1 W *S. undulatus*
146	March 30, 2016	41.46861, 79.30111	2 RD *S. undulatus*
147	April 19, 2017	41.31833, 79.29639	1 RD *L. fasciola*
148	May 16, 2017	41.43750, 79.22556	1 RD, 1 W *S. undulatus*
149	July 29, 2017	41.32028, 79.29306	1 R *A. ligamentina*; 1 RD *S. undulatus*
150	August 15, 2017	41.46750, 79.28611	1 RD *S. undulatus*
151	August 5, 2018	41.55472, 79.16778	1 RD *S. undulatus*
152	October 7, 2018	41.46056, 79.28917	14 RD, 6 W *S. undulatus*
153	June 28, 2019	41.36333, 79.20222	1 RD *L. fasciola*; 3 RD *S. undulatus*
154	June 29, 2019	41.33956, 79.14048	1 RD *S. undulatus*
155	July 14, 2019	41.29887, 79.26907	1 RD *S. undulatus*
156	September 11, 2019	41.32536, 79.17357	1 RD *S. undulatus*
157	September 11, 2019	41.32536, 79.35700	1 RD *Lampsilis ovata*

RD = recently dead shells; W = weathered shells; R = relic shells; L = live mussels.

severe water pollution, but the time of death of the specimens is unknown, and it is unknown if the river currently supports a natural population of the *A. ligamentina*.

The absence of any historical mussel records prior to severe pollution in the early 1900s or any contemporary mussel surveys prior to this study make it impossible to reconstruct the Clarion River's original mussel fauna and difficult to assess the extent to which the fauna may be recovering. Possibly, the river never supported a substantial mussel fauna, but this seems unlikely in a region characterized by diverse mussel faunas in most streams (e.g., Ortmann 1919). More likely, the Clarion River supported a diverse fauna similar to other tributaries of the Allegheny River. If so, the widespread occurrence of mussels in the river today may represent recovery of the river and recolonization by the mussel fauna.

Potential source populations and dispersal routes for recolonization of the Clarion River likely differ among mussel species. *Actinonaias ligamentina* and *L. ovata* are generally restricted to larger streams such as the Allegheny River, where *A. ligamentina* is a dominant species (Anderson 2000; Smith et al. 2001). The Allegheny River was likely the source population for both species prior to the completion of Piney Dam, but the dam is currently a barrier to recolonization. *Strophitus undulatus* and *L. fasciola* inhabit both small tributary streams and the mainstem Allegheny River (Ortmann 1919; Harriger et al. 2009). Populations of both species in the Clarion River could have originated from the Allegheny River, but they are uncommon in the latter river (Anderson 2000; Smith et al. 2001). The apparently substantial population of *S. undulatus* in the Clarion River suggests the presence of a nearby source population in a tributary stream. Many tributaries within the Clarion Basin escaped pollution in the early 1900s (Department of Health of the Commonwealth of Pennsylvania 1915), but it is unknown if they support mussel faunas that serve as source populations for recolonization of the Clarion River. Tributaries are proposed as source populations for recolonization of the historically polluted upper Illinois River by mussels (Seitman et al. 2001) and for recolonization of fishes in the Clarion River (Bardarik 1965).

Another possible source for recovery of the mussel fauna is the Clarion River itself—if some species survived severe pollution. This seems unlikely given the severity and duration of pollution. However, the conclusion that the aquatic fauna was eliminated (Ortmann 1913) was not based on a comprehensive survey, and the lack of subsequent mussel surveys makes it impossible to determine whether any species survived. A third possible source of mussel fauna is the release of fishes infected with glochidia from other populations (Hayes 2000), but to my knowledge, this possibility has not been examined.

The decimation of the aquatic fauna of the Clarion River by pollution is a great tragedy, but so is the fact that no record of the historical fauna exists. The shell collections made during this study provide a glimpse of what the mussel fauna of the Clarion River may have looked like. All four species I found are characteristic members of mussel assemblages in small to midsized streams in the Ohio River basin of western Pennsylvania (Walsh et al. 2007). Other characteristic species of these assemblages, such as *Lasmigona costata*, *Alasmidonta marginata*, *Lampsilis cardium*, and *Ptychobranchus fasciolaris,* were not collected during this study. However, in 2015, I found a relic shell of *Lasmigona costata* in the Clarion River below Piney Dam just above the mouth of Deer Creek (C. Williams, personal observation). My results show that the Clarion River is now capable of supporting mussel populations, but additional surveys are needed to document mussel abundance and provide a baseline for monitoring future natural recovery. Conservation actions meant to hasten mussel recovery, such as translocation from other populations or release of hatchery-propagated individuals, face the challenge of determining appropriate species for reintroduction or augmentation, and these decisions will need to be made based on assumptions about the original fauna of the river.

ACKNOWLEDGMENTS

I thank Pat and Peggy Kearney, Nancy Pyle, and Kim, Kelsey, and Tara Williams for assisting in shell surveys. Charles Bier and Beth Meyer verified species identifications. Serena Ciparis, Wendell Haag, Kim Williams, and an anonymous reviewer provided helpful comments on the manuscript.

LITERATURE CITED

Anderson, R. M. 2000. Assessment of freshwater mussels in the Allegheny River at Foxburg, Pennsylvania, 1998. U.S. Geological Survey Water-Resources Investigations Report 00-4058. Available at: https://pubs.usgs.gov/wri/2000/4058/wri20004058.pdf (accessed November 5, 2021).

Anonymous. 1949. Paper mill abates pollution. Pennsylvania Angler 18(10):24.

Bardarik, D. G. 1965. Distribution and composition of fish communities in a polluted and unpolluted stream in the Upper Ohio River basin. Pages 79–94 *in* C. A. Tryon, Jr., R. T. Hartmann, and K. S. Cummins, editors. Studies of the Aquatic Ecology of the Upper Ohio River System. Special Publication No. 3, Pymatuning Laboratory of Ecology, University of Pittsburgh, Pittsburgh, Pennsylvania.

Blodgett, K. D., and R. E. Sparks. 1987. Analysis of a mussel die-off in pools 14 and 15 of the Upper Mississippi River. Aquatic Biology Technical Report 87/15. Illinois Natural History Survey River Research Laboratory, Havana.

Camp, Dresser, and McKee, Consulting Engineers. 1949. Report on Clarion River pollution abatement. Commonwealth of Pennsylvania, Department of Health, Sanitary Water Board, Harrisburg. Available at: https://archive.org/details/reportonclarionr00camp (accessed 12 June 2021).

Carnegie Museum and Western Pennsylvania Conservancy. 1993. A survey of the dragonflies and damselflies of the Clarion River and its tributaries near the Allegheny National Forest, Pennsylvania. Carnegie Museum and Western Pennsylvania Conservancy, Pittsburgh, Pennsylvania.

Cliff, M., M. Hove, and M. Haas. 2001. Creeper glochidia appear to be host generalists. Ellipsaria 3:18–19.

Commonwealth of Pennsylvania. 2018. Physiographic provinces of Pennsylvania. Department of Conservation and Natural Resources, Bureau of Topographic and Geologic Survey, Harrisburg, Pennsylvania. Available at: http://elibrary.

dcnr.pa.gov/PDFProvider.ashx?action=PDFStream&docID=1752507&chksum=&revision=0&docName=Map13_PhysProvs_Pa&nativeExt=pdf&PromptToSave=False&Size=810216&ViewerMode=2&overlay=0 (accessed May 21, 2021).

Department of Health of the Commonwealth of Pennsylvania. 1915. Report on the sanitary survey of the Allegheny River Basin. Harrisburg, Pennsylvania. Available at: https://archive.org/details/reportonsanitary00penn (accessed 10 November 2021).

Ford, D. F., and A. M. Oliver. 2015. The known and potential hosts of Texas mussels: Implications for future research and conservation. Freshwater Mollusk Biology and Conservation 18:1–14.

Haag, W. R. 2012. North American Freshwater Mussels: Natural History, Ecology, and Conservation. Cambridge University Press, New York.

Haag, W. R., and A. M. Commens-Carsons. 2008. Testing the assumption of annual ring shell deposition in freshwater mussels. Canadian Journal of Fisheries and Aquatic Sciences 65:493–508.

Harriger, K., A. Moerke, and P. Badra. 2009. Freshwater mussel (Unionidae) distribution and demographics in relation to microhabitat in a first-order Michigan stream. Michigan Academician 39:149–162.

Hayes, T. 2000. Our native mussels. American Currents 26(4):21–22. Available at: http://www.nanfa.org/ac/our-native-freshwater-mussels.pdf (accessed 15 May 2021).

Neves, R. J., and S. N. Moyer 1988. Evaluation of techniques for age determination of freshwater mussels (Unionidae). American Malacological Bulletin 6:179–188.

Ortmann, A. E. 1909. The destruction of the fresh-water fauna in western Pennsylvania. Proceedings of the American Philosophical Society 48:90–110.

Ortmann, A. E. 1913. The Alleghenian Divide, and its influence upon the freshwater fauna. Proceedings of the American Philosophical Society 52:287–390.

Ortmann, A. E. 1919. A monograph of the naiades of Pennsylvania. Part III. Systematic account of the genera and species. Memoirs of the Carnegie Museum 8:1–385.

Pisces Conservation Ltd., 2015. QED Statistics. Available at: http://qedstatistics.com/ (accessed 7 July 2020).

POWR (Pennsylvania Organization for Watersheds and Rivers). 2019. 2019 River of the year, the Clarion River. Available at: http://pariveroftheyear.org/2019-river-of-the-year-2/ (accessed 12 June 2021).

Sietman, B. E. S. D. Whitney, D. E. Kelner, K. D. Blodgett, and H. L. Dunn. 2001. Post-extirpation recovery of the freshwater mussel (Bivalvia: Unionidae) fauna in the upper Illinois River. Journal of Freshwater Ecology 16:273–281.

Smith, D. R., R. F. Villella, and D. P. Lemarie. 2001. Survey protocol for assessment of endangered freshwater mussels in the Allegheny River, Pennsylvania. Journal of the North American Benthological Society 20:118–132.

Strayer, D. L., and K. J. Jirka. 1997. The Pearly Mussels of New York State. New York State Museum Memoir 26, Albany.

USACOE (U.S. Army Corps of Engineers, Pittsburgh District). 2021. East Branch Clarion River Lake. Available at: https://www.lrp.usace.army.mil/Missions/Recreation/Lakes/East-Branch-Clarion-River-Lake/ (accessed 12 June 2021).

Van Snik Gray, E., W. A. Lellis, J. C. Cole, and C. S. Johnson. 2002. Host identification for *Strophitus undulatus* (Bivalvia: Unionidae), the creeper, in the Upper Susquehanna River Basin, Pennsylvania. American Midland Naturalist 147:153–161.

Walsh, M. C., J. Deeds, and B. Nightingale. 2007. User's Manual and Data Guide to the Pennsylvania Aquatic Community Classification. Pennsylvania Natural Heritage Program and Western Pennsylvania Conservancy, Pittsburgh. Available at: http://www.naturalheritage.state.pa.us/aquaticsUserMan.aspx (accessed 11 June 2021).

Western Pennsylvania Conservancy. 2015. Mussels have new homes in the Clarion, other rivers. Conserve 61(4):6–7. Available at: https://waterlandlife.org/publications/e-conserve/winter_15/ (accessed 10 November 2021).

Williams, C. E. 1995. A clean slate for the Clarion. Pennsylvania Wildlife 16(1):27–29. Available at: https://www.academia.edu/4004029/A_clean_slate_for_the_Clarion (accessed 11 June 2021).

Freshwater Mollusk Biology and Conservation 25:15–26, 2022

DOI:10.31931/fmbc-d-21-00004

REGULAR ARTICLE

ASSESSMENT OF A HABITAT EQUIVALENCY ANALYSIS FOR FRESHWATER MUSSELS IN THE UPPER MISSISSIPPI RIVER

Teresa J. Newton[1]*, Patricia R. Schrank[1†], Steven J. Zigler[1], Scott Gritters[2], Aleshia Kenney[3], and Kristin Skrabis[4]

[1] *U.S. Geological Survey, Upper Midwest Environmental Sciences Center, La Crosse, WI 54603 USA*
[2] *Iowa Department of Natural Resources, Bellevue, IA 52031 USA*
[3] *U.S. Fish and Wildlife Service, Moline, IL 61265 USA*
[4] *U.S. Department of the Interior, Office of Policy Analysis, Washington, DC 20240 USA*

ABSTRACT

The upper Mississippi River (UMR) contains diverse, dense, and reproducing assemblages of native freshwater mussels. In the case of an injury to mussels and their habitats, such as a hazardous material spill, train derailment, or barge grounding, resource managers have few restoration strategies. Resource managers need a means to document, quantify, and mitigate adverse effects on mussels resulting from injury. Habitat equivalency analysis (HEA), developed for use with a wide variety of habitat types, is a restoration scaling technique that compares ecological services lost from injury to ecological services gained through restoration actions. The U.S. Fish and Wildlife Service and Iowa Department of Natural Resources modified the HEA for use with native mussels. The mussel HEA has been applied within the UMR to estimate the quantity of restoration needed to compensate the public for injuries to mussels due to contaminant spills and construction projects. Our objective was to describe the UMR HEA for a general audience and assess if the four biological input variables used in the mussel HEA were reasonable based on literature values. We also evaluated the performance of HEA under a range of input scenarios. Although the input estimates used in HEA were within ranges reported in the peer-reviewed literature or were supported by professional judgment in the absence of peer-reviewed literature, outcomes of the mussel HEA were highly variable and would benefit from additional research to reduce uncertainty in the biological inputs. The application of HEA to mussels provides resource managers with a tool to quantify mussel-related ecological services lost from injury and to guide restoration efforts in the UMR.

KEY WORDS: freshwater mussels, habitat equivalency analysis, natural resource damage assessment, injury, sensitivity analysis

INTRODUCTION TO DAMAGE ASSESSMENTS

Resource managers in federal and state agencies must document, quantify, and mitigate ecological disturbances resulting from human activity (Bouska et al. 2018). In the event of a construction project, hazardous material spill, or other injury to a natural resource, environmental protection laws (e.g., Comprehensive Environmental Response, Compensation, and Liability Act) hold responsible parties accountable through recovery of monetary compensation (called damages) necessary to fund projects to offset environmental injuries. Through the Natural Resource Damage Assessment and Restoration Program (NRDAR), natural resource trustees (certain federal, state, or tribal government agencies) are authorized to assess and recover damages from potentially responsible parties to compensate the public for losses due to injury to natural resources (Table 1). Damage assessments typically have three components: (1) determine and quantify the extent of the injury, destruction, or loss (injury

*Corresponding Author: tnewton@usgs.gov
†Present address: University of Minnesota, Department of Integrative Biology and Physiology, Minneapolis, MN 55455 USA

Table 1. Glossary of terms associated with natural resource damage assessments (definitions from NOAA 1997, except where otherwise indicated).

Term	Definition
Baseline	The condition of natural resources and services that would have existed had the incident not occurred.
Compensatory restoration	Any action taken to compensate for interim losses of natural resources and services that occur from the date of the incident until recovery of natural resources and services to baseline.
Damages	The amount of money sought by trustees as compensation for injury, destruction, or loss of natural resources (43 CFR[a] § 11.14).
Discount rate	The rate at which dollars or other valued items or services being provided in different time periods are converted into current time period equivalents. A discount rate is used to compensate for delayed provision of services.
Ecological services	The physical and biological functions performed by the resource including the human use of those functions (43 CFR[a] § 11.14).
Equivalency analysis	Process to determine the amount of ecological restoration required to mitigate or compensate for environmental injury or habitat loss (Strange et al. 2002).
Injury	A measurable adverse change in a resource such that the resource does not provide the same services as it would have in the absence of the unpermitted release of oil or a hazardous substance (Barnthouse and Stahl 2002).
Interim losses	The reduction in resources and the services they provide, relative to baseline levels, that occur from the onset of an incident until complete recovery of the injured resources.
Natural resources	Land, fish, wildlife, biota, air, water, ground water, drinking water supplies, and other such resources belonging to, managed by, held in trust by, appertaining to, or otherwise controlled by the United States, any State or local government or Indian tribe, or any foreign government.
Primary restoration	Any action, including natural recovery, that returns injured natural resources and services to baseline.
Restoration	Any action, or combination of actions, to restore, rehabilitate, replace, or acquire the equivalent of injured natural resources and services.
Scaling	The process of determining, for identified restoration actions, the size or scale of the actions that would be required to expedite recovery of injured resources to baseline and compensate the public for interim lost resources and services.
Service flows	Cumulative provision of services over time (Fonseca et al. 2000).
Service loss	The lost or reduced opportunity such as for fishing, nature viewing, hunting, or natural water treatment due to the injury to the resource, or basic life support (Barnthouse and Stahl 2002).

[a]Code of Federal Regulations.

quantification); (2) calculate and recover the damages needed to compensate for the injury (scaling and damages determination); and (3) use the recovered damages to restore, replace, or acquire the equivalent of the injured natural resources (restoration implementation; Baker et al. 2020). This paper addresses components 1 and 2.

Once the injury has been quantified, trustees determine the type and quantity of restoration (scaling) that will adequately compensate the public for injuries to natural resources. Several tools have been developed to help NRDAR practitioners estimate the amount of restoration required. Habitat equivalency analysis (HEA; Unsworth and Bishop 1994) and resource equivalency analysis (REA; Sperduto et al. 2003) quantify compensation by equating ecological services (HEA) or species (REA) lost due to injury with those gained through restoration, without directly estimating economic values. The more recent habitat-based resource equivalency method (HaBREM) is a biomass-based REA with habitat scaling (Baker et al. 2020).

The principal concept underlying HEA is that the public can be compensated for past losses of habitat resources through habitat enhancement or replacement projects that provide additional resources of the same type as those injured. Habitat equivalency analysis has been used extensively in NRDAR (e.g., Ando et al. 2004; Roach and Wade 2006; Israel 2019). For example, a pipeline ruptured and released ~3 million L of tar sands oil into a tributary of the Kalamazoo River, Michigan, injuring numerous species, including freshwater mussels (USFWS et al. 2015). Natural resource trustees conducted an HEA that indicated that 5,790 discounted service acre years (i.e., the value of all ecological services provided by 1 acre [0.4047 ha] of the habitat in 1 yr) were lost due to the injury. Other examples include assessing environmental losses after forest fires (Hanson et al. 2013) and assessing the effects of the invasive lionfish (*Pterois volitans*) on Bahamian reef fish populations (Johnston et al. 2015).

In NRDAR, ecological services are defined as the physical and biological functions performed by the natural resource, including the human uses of those functions (Dunford et al. 2004). Restoration actions seek to fully recover the ecological services provided by a resource before injury. In other words, it is not the resource itself, but the services it would have

provided in the absence of injury, that form the basis for damage assessments. To fully recover these services, trustees must estimate the services lost from a natural resource injury and develop restoration alternatives that will provide the same level of services to the public. The underlying assumption is that the public will accept a one-to-one trade-off between a unit of lost services and a unit of restored services. Because most ecological services have no market value, damage assessments use indicators of ecological services rather than measuring services directly (Ruiz-Jaen and Aide 2005). Furthermore, because it is not feasible to measure and quantify each of the individual services provided by mussel habitats, such as production, sediment stabilization, nutrient cycling, and improved water quality, a key consideration in HEA is identifying a sensitive indicator for the targeted ecological service (Dunford et al. 2004). Practitioners have several options for indicators depending on the type of ecosystem and the targeted services (Vaissière et al. 2013; Scemama and Levrel 2016). In salt marsh ecosystems, practitioners have used plant biomass as an indicator of primary production, vegetative canopy structure as an indicator of habitat, and organic matter content as an indicator of biogeochemical cycling (Strange et al. 2002). In marine systems, shellfish density has been used as an indicator of secondary production because it was correlated with the magnitude of ecological services provided by bivalves (McCay et al. 2003).

THE HEA MODEL APPLIED TO MUSSELS IN THE UMR

The upper Mississippi River (UMR, defined as the 1400-km reach from Minneapolis, Minnesota, to Cairo, Illinois) supports diverse and valuable natural resources, including federally endangered, threatened, and candidate species (USFWS 2006). However, the river is a major transportation artery, making natural resources vulnerable to toxic spills and other injury. More than 90 million metric tons (90 billion kg) of industrial and agricultural commodities are shipped annually by barge (UMRBA 2014), and many commodities, including hazardous materials, are shipped by railroads, which cross the UMR or run within 1.5 km of the river for at least 55% of its length (UMRBA 2014). In addition to spills of hazardous materials, natural resources in the UMR are at potential risk from construction (e.g., bridges, barge loading facilities), barge groundings, and many other human activities that affect shoreline and water resources.

The UMR supports a globally important native freshwater mussel resource (hereafter mussels; Newton et al. 2011; Haag 2012). Mussels reach their greatest diversity in North America but have among the highest extinction and imperilment rates of any group of organisms on the planet (Haag and Williams 2013). For example, about 60% of the 50 native species in the UMR are now extirpated or state or federally listed (Tucker and Thieling 1999). Long-lived mussels are keystone species with strong linkages to other ecosystem components and ecological processes (Vaughn 2018). Mussels provide important ecological services that benefit other aquatic species, such as nutrient cycling and storage, the creation and modification of riverine habitats, and biofiltration. However, research to quantify the ecological services performed by mussels is in its infancy, and the mechanisms by which short- and long-term losses of these services might affect ecosystems are largely undocumented (Vaughn and Hoellein 2018).

Because of their imperiled status and the ecological services that they provide, mussels are frequently the focus of restoration and mitigation efforts in the UMR. Resource managers from the Iowa Department of Natural Resources (IADNR) and the U.S. Fish and Wildlife Service (USFWS) have applied HEA to estimate the quantity of restoration needed to replace mussels lost from hazardous spills and construction activities in the UMR and to determine monetary damages. They used a three-step process to assess injury to mussel habitat. First, HEA was used to quantify the loss of habitat (component 1). Second, the amount of restoration required to offset the loss of habitat was estimated (scaling in component 2). Specifically, for every square meter of a mussel bed lost to injury, how many additional square meters (termed replacement habitat [RH]) are owed. Given that HEA is used to estimate the amount of habitat restoration needed to compensate for *ecological service losses over time*, HEA requires a proxy for ecological services. The mussel HEA uses the pre-injury density of mussels (in mussels/m^2) as an indicator of secondary production, assuming that production is correlated with the magnitude of ecological services provided by mussels (e.g., McCay et al. 2003). Third, resource managers use RH estimates from the HEA output and the pre-injury density of mussels to estimate how many mussels need to be replaced into the restored habitat to generate the same level of ecological services as the original habitat (damages in component 2). This is typically accomplished by estimating the propagation costs necessary to replace the quantity of mussels lost, while maintaining a similar species composition to the pre-injury bed. This aspect of the mussel HEA uses published propagation values (Southwick and Loftus 2017) and will not be discussed further.

The mussel HEA contains 11 input variables that influence estimates of the amount of RH needed to compensate for losses (i.e., square meters owed). The input variables were categorized into four site-specific variables, three standard variables, and four biological variables (Table 2). Our objectives were to assess (1) if the four biological input variables used by UMR resource managers in the mussel HEA were reasonable based on values in the literature and (2) the performance of HEA under a range of input scenarios.

PARAMETERIZATION OF THE HEA MODEL AND EVALUATION OF BIOLOGICAL INPUTS

A workshop was held with members of the IADNR, the USFWS, and the U.S. Geological Survey to evaluate how HEA was applied to mussels in the UMR, with an emphasis on the input variables used to generate estimates of RH owed. Seven input variables were not evaluated in our review. Three

Table 2. Habitat equivalency analysis input variables, description, category classification, and indication if a given input was assessed in this paper.

Input	Description	Category	Assessed?
Years to natural recovery	Length of time after recovery starts for the mussel bed to return to pre-injury condition	Biological	Yes
Relative productivity of created versus natural habitat	The fraction of natural productivity that the restored habitat will produce	Biological	Yes
Years to full-service flow after creation	Time lag for the new or reclaimed habitat to reach full service	Biological	Yes
Lifespan of the created habitat	The expected usable lifespan of the created or reclaimed habitat	Biological	Yes
Functional form of the recovery function	The form of the model used to compute the recovery function	Standard	No
Functional form of the maturity function	The form of the model used to compute the maturity function	Standard	No
Real discount rate (annual)	Discount or depreciable life in business is set at 3%	Standard	No
Year injury begins	The year in which the injury occurred	Site-specific	No
Area injured	The number of square meters injured	Site-specific	No
Percent of services lost	The percent of each mussel bed unit lost	Site-specific	No
Year restoration begins	The year that recovery could start	Site-specific	No

of these were categorized as standard HEA inputs: the real discount rate, the functional form of the recovery function, and the functional form of the maturity function (Table 2). The values of these inputs are relatively standard across most HEA applications and are consistent with a sensitivity analysis that found the shape of the recovery and maturity functions did not greatly affect model outcomes (Dunford et al. 2004). Four of the input variables were categorized as site-specific: the year injury began, area injured, percent of services lost, and the year restoration began (Table 2). These inputs have values that rely on site-specific information about an injury and would not benefit from a biological assessment.

The four biological inputs are years to natural recovery, relative productivity of created versus natural habitat, years to full-service flow after creation, and lifespan of the created habitat. These were identified as variables that are likely responsive and specific to the life history and ecology of mussels and would therefore benefit from scientific assessment (Table 2). At the workshop, IADNR and USFWS provided estimates they have used for each biological input based on their professional experience (Table 3). Our task was to assess if these estimates were reasonable based on values in the literature or on professional judgment in the absence of peer-reviewed data. For each of the four biological inputs, we completed a literature review, compiled a range of scientifically defensible estimates, and computed the minimum, maximum, and median values (Table 3). We consider each of the biological inputs in the subsequent sections.

Years to Natural Recovery

This input describes how long it takes an injured mussel bed to return to a pre-injury condition (used in component 1). This value depends largely on the severity of the injury. For example, if a chemical spill occurs directly over a mussel bed and kills most individuals, recovery may take considerable

Table 3. The four biologically based habitat equivalency analysis (HEA) input variables that we assessed. Range used by managers are the input values currently being used by resource managers in the mussel HEA for the upper Mississippi River. Also listed are the primary factors that influence the input values and the assessed range that was determined based on literature-derived data and professional judgment.

Input parameter	Range used by managers	Factors influencing input values	Assessed range
Years to natural recovery	10–30 yr	Severity of injury, lifespan	Range: 10–30 yr, median: 20 yr
Relative productivity of created versus natural habitat	33–100%	Density, species richness	Range: 33–100%, median: 67%
Years to full-service flow after creation	10–30 yr	Lifespan, age at sexual maturity, physiological condition	Range: 10–30 yr, median: 20 yr
Lifespan of the created habitat	30–100 yr	Species composition, habitat type (specifically, hydraulic conditions at the site)	Range: 30–100 yr, median: 65 yr

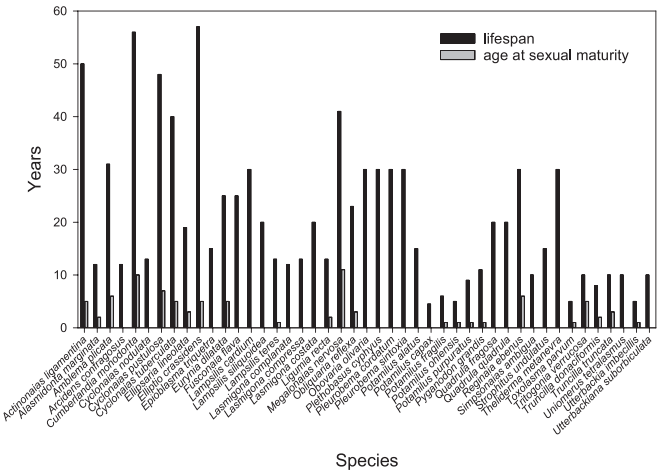

Figure 1. Estimates of maximum lifespans (Watters et al. 2009; Haag 2012) and age at sexual maturity (Payne and Miller 1989; Jirka and Neves 1992; Haag 2012) of select freshwater mussel species in the upper Mississippi River. Scientific names follow the 2021 Freshwater Mollusk Conservation Society checklist of freshwater mussels (FMCS 2021).

time because mussels will need to recolonize the area. In contrast, if a chemical spill occurs on the edge of a bed and kills only a fraction of the individuals, recovery should take less time. Larger affected areas also may take longer to recolonize, especially near the center of the area, because of limitations in the number of immigrants from nearby areas. The life-history traits of the resident species, specifically the lifespans of mussels in the original bed, may affect the years to natural recovery. For example, if a bed is dominated by longer-lived species, it will take longer to return to pre-injury conditions. In contrast, beds dominated by shorter-lived species may take less time to return to baseline. In the mussel HEA, UMR resource managers assigned values ranging from 10 yr (if >50% of the population is shorter-lived) to 30 yr (if >50% of the population is longer-lived) as the years to natural recovery.

To assess if the range of 10 to 30 yr was reasonable based on literature values, we compiled data on the lifespan of 45 species of mussels that reside in the UMR. The average lifespan was 21 yr but ranged from 5 to 57 yr (Fig. 1). This variation indicates that the number of years needed for a bed to return to its pre-injury condition could be highly variable depending on the lifespans of the individual species within the bed. Although the values used by resource managers are consistent with the literature, a more defensible estimate of this input can come only from population models or related approaches.

Relative Productivity of Created versus Natural Habitat

This input estimates the fraction of the natural productivity that the restored habitat will produce (used for scaling in component 2). For example, consider a wetland as the injured resource and primary productivity as the ecological service. If the restored wetland provides only 50% of the original productivity, twice as much restored wetland would be required to offset the losses, not accounting for any effects of time through discounting. Resource managers in the UMR assumed that productivity would vary as a function of mussel density. Using professional expertise, they assumed that if density in the original bed was low (~0–5 mussels/m^2), they might restore most (approaching 100%) of the original productivity; with moderate densities (~5–10 mussels/m^2) they might restore ~80%; and with high densities (>10 mussels/m^2), they might restore ~33% of the original productivity.

Because we know little about the productivity of natural mussel assemblages, this input was difficult to assess from either the literature or professional judgment. Although the ranges in density used by UMR resource managers are consistent with peer-reviewed data on mussels in the UMR (i.e., Newton et al. 2011; Dunn et al. 2020), we could find no data to support the level of productivity as a function of density. Because mussels in species-rich assemblages are often in better condition (Spooner and Vaughn 2009), productivity may be higher in diverse beds. Thus, species richness also may influence productivity of the restored bed. If restoration can capture the species richness of the original bed, its productivity should be comparable to the original assemblage (i.e., closer to 100% replacement). However, because propagation methods for many species are undeveloped, it may not be feasible to reintroduce some species into the restored bed. This would reduce the diversity of the restored bed and potentially reduce its productivity relative to the original bed. In the absence of peer-reviewed data, we were unable to assess this input. Thus, data to inform this input are a critical research need (see "Data Needed to Inform Mussel HEA Models").

Years to Full-Service Flow after Creation

This input addresses the time lag from establishment of a newly created or restored mussel bed to the time when it reaches its full ecological potential (used for scaling in component 2). It is influenced largely by the lifespan and age at maturity of the mussels in the original bed. For example, if a bed is dominated by a species that takes 5 yr to reach maturity and another 5 yr for their offspring to reach maturity, then the input value would be at least 10 yr. Because species in good condition contribute a greater magnitude of ecological services (Fridley 2001), the condition of species in the bed may also influence this input. Resource managers in the UMR assigned values ranging from 10 yr (if the original bed was dominated by shorter-lived species) to 30 yr (if the original bed was dominated by longer-lived species).

Literature-derived values of the lifespan (45 species) and age at sexual maturity (23 species) were used to estimate the years to full service after creation. The mean lifespan of mussels in the UMR was 21 yr and ranged from 5 to 57 yr, and the mean age at sexual maturity was 4 yr and ranged from 1 to 11 yr (Fig. 1). The longer it takes a mussel to reproduce, the longer the time lag from establishment of a restored bed to the time when it reaches its full ecological potential. Even if a

regional supply of glochidia and newly released juveniles result in rapid settlement into the restored bed, mature stages could take decades to recover, especially since adults have limited mobility (Newton et al. 2008). If mussel lifespan is largely driving this input, the literature value of 21 yr is consistent with the range of values used by managers (10–30 yr). For age at sexual maturity, resource managers assumed a mean age of 5 yr, and our literature review indicated a mean of 4 yr. If physiological condition of mussels influences this input, then the restored bed should contain a sufficient quantity and quality of food to maintain species in good physiological condition to maximize performance of the entire assemblage (Spooner and Vaughn 2009). Although the input values used by resource managers are consistent with the literature review, more defensible estimates are needed. For example, age at sexual maturity is known for only a fraction of mussel species, and the error around these estimates is largely unknown. Similarly, the lack of robust data on what constitutes "good" physiological condition in mussels—and how this varies over time and space—limits assessment of this input.

Lifespan of the Created Habitat

This input seeks to describe the expected useable lifespan of the created or restored habitat (used for scaling in component 2). Resource managers have used estimates that ranged from 30 to 100 yr for this input, acknowledging that it could be shorter or longer if a bed was dominated by shorter-lived or longer-lived species, respectively. Mussel assemblages in the UMR are often dominated by longer-lived equilibrium and periodic species, with shorter-lived opportunistic species comprising <25% of assemblages (Newton et al. 2011). A review of 24 mussel beds across the United States indicated they remained intact for ~62 yr (Sansom et al. 2018). In the UMR, some mussel beds have persisted for >70 yr (Scott Gritters, Iowa Department of Natural Resources, written communication, May 22, 2019). Thus, the range of input values used by managers is consistent with literature values. For reference, habitat restoration projects in the UMR are typically designed for a 50-yr project life (USACE 2012).

We propose that the lifespan of the restored habitat will depend on the hydraulic characteristics of the habitat to a much greater extent than the lifespan of mussels that inhabit it. If a bed is created in a dynamic habitat (e.g., shifting sand), the lifespan may be shorter than if the bed is created in a stable habitat. For example, in a hydraulically unstable area, beds can be ephemeral even if they are colonized by long-lived mussel species. Conversely, a hydraulically stable area could support a long-lived assemblage of short-lived mussel species (i.e., many generations). Some beds in the UMR are ephemeral (Ries et al. 2016), and extreme hydrologic events such as floods or droughts can influence persistence of beds in marginal areas (Zigler et al. 2008). For example, a 30- or 50-yr flood event could displace mussels in areas that have stable substrates during most years but experience high shear stress and mobile substrates at unusually high streamflow conditions. In the UMR, flow models indicated that high shear stress (resulting from high flows) negatively affects mussel abundance and can prevent juveniles from settling to the river bottom (Morales et al. 2006; Zigler et al. 2008). In contrast, empirical data reported no change in abundance or species richness of mussels after the 1993 flood in the UMR (Miller and Payne 1998).

SENSITIVITY ANALYSIS

We performed a sensitivity analysis on the four biological inputs to assess how uncertainties in the inputs contributed to uncertainty in HEA outputs. Managers from the IADNR and USFWS provided data from four locations in the UMR where they had previously applied the mussel HEA to address injuries to mussels (Table 4). In our sensitivity analysis, we created a baseline scenario for each dataset where each input was set to the median value from the literature. That is, the median values for the variable inputs were selected relative to the condition of the mussel beds absent the injury (also called relative productivity of restoration to baseline). First, the effect of each HEA input variable was assessed individually. Each input was modified, one at a time, to the minimum or the maximum value from the range to estimate the percent change in RH owed relative to the baseline condition (Dunford et al. 2004). Then the cumulative effect of simultaneously changing multiple input variables was evaluated by comparing the output (RH) of the baseline scenario to two bounding scenarios: the lowest possible RH estimate ("low scenario," least amount of restoration required) and the highest possible RH estimate ("high scenario," most amount of restoration required).

The individual and cumulative effects of changes in the input values resulted in substantial differences in loss estimates. Changing the values of inputs individually resulted in estimates that were –45% to 112% of the RH in the baseline scenario (Table 5). The loss estimates across the four UMR examples were most sensitive to the relative productivity of created versus natural habitat and the lifespan of the created habitat (Table 5).

All four HEA datasets reflected a similar sensitivity in RH between the bounded scenarios (greatest amount of RH, least amount of RH). Thus, we will discuss only one example in detail (Appendix A contains the results of the other three examples). Example 1 concerns a mussel bed that was affected by a train derailment in 2011 (Table 4). Seven cars of a train containing coal derailed into the UMR at Keokuk, Iowa, and resource managers estimated ~17,000–25,000 mussels were injured. The constant inputs used by resource managers were the injured area units (353 m^2), the percent of services lost initially (25%), and the real discount rate (3%). The percent of services lost initially was estimated by resource managers who assumed that 25% of the bed was injured by coal smothering the mussels. The variable inputs were years to natural recovery (10–30 yr), relative productivity of created versus natural habitat (33–100%), years to full-service flow after creation (10–30 yr), and lifespan of the created habitat (30–100 yr).

Table 4. Descriptions of habitat equivalency analyses that have been conducted in the upper Mississippi River and that were used in the assessment process.

Example	Description	Location	Year	Outcome
1	Seven cars of a coal train derailed into the upper Mississippi River; an estimated 17,000-25,000 mussels were affected	Keokuk, Iowa	2011	Settled in 2013 for $137,000
2	Train derailment that covered 301 m^2 of a mussel bed with ~28 mussels/m^2	Guttenberg, Iowa	2008	Settled in 2014 for $625,000
3	A company wanted to construct a barge loading facility on top of a 113-m^2 mussel bed with densities of ~16 mussels/m^2	Davenport, Iowa	2010	Active case
4	Derailment of a train containing ethanol	Balltown, Iowa	2015	Active case

The baseline scenario for HEA estimated the RH as 57 m^2 owed (Table 6). The highest bound, which was based on simultaneous changes to inputs, resulted in an RH estimate of 485 m^2—a 751% change from the baseline scenario. The inputs for this scenario included setting the years to natural recovery and the years to full-service flow after creation to the maximum value in their range (both 30 yr) and setting the relative productivity of created versus natural habitat and lifespan of created habitat to the minimum values in the assessed range (33% and 30 yr, respectively). Changing the inputs to the lowest bound resulted in an estimated RH of 15 m^2—a –74% change from the baseline scenario (Table 6). The inputs for this scenario included setting the years to natural recovery and the years to full-service flow after creation to the minimum value in their range (both 10 yr) and setting the relative productivity of created versus natural habitat and lifespan of the created habitat to the maximum values in the validated range (100% and 100 yr, respectively). Across all four UMR examples, the percent change in RH from baseline ranged from –73% in the low scenario to +759% in the high scenario (Table 6 and Appendix A).

MODEL LIMITATIONS AS APPLIED TO MUSSELS

In our opinion, the most serious limitation of the mussel HEA is that robust, peer-reviewed data are not available for accurate estimates of the input parameters. When peer-reviewed data are available, they are highly variable, and selecting an appropriate value is difficult without population models or more detailed empirical studies. These limitations can introduce considerable uncertainty in the amount of RH required to restore inured habitats. When empirical data were lacking, input values in the mussel HEA were estimated based on professional judgment. Experts often differ substantially in professional judgment, which can lead to uncertainty in input values. The uncertainty in professional judgment does not preclude its use in NRDAR, and several methods are available to produce consensus in a group of experts. The Delphi technique is an iterative structured elicitation process used to gather and evaluate professional opinions (Mukherjee et al. 2015). This technique was recently applied on the UMR to compare outputs from a mussel community assessment tool with professional judgment of resource managers (Dunn et al. 2020). The Delphi method provided a consistent evaluation

Table 5. Sensitivity analysis of input variables in a habitat equivalency analysis (HEA) for native mussels in the upper Mississippi River (UMR). The baseline scenario describes conditions where all input values were set to the median value based on data in the peer-reviewed literature. The alternative scenarios change one parameter at a time (bolded text) to the minimum or maximum value from the literature range (first four rows). The last five rows illustrate how the replacement habitat (RH in m^2) changed in four example HEAs that have been conducted in the UMR. The mean percent of baseline (the percent change in service losses) across the four examples was also calculated.

	Baseline scenario	Years to natural recovery		Relative productivity of created versus natural habitat		Years to full-service flow after creation		Lifespan of the created habitat	
		Min	Max	Min	Max	Min	Max	Min	Max
Years to natural recovery	20	**10**	**30**	20	20	20	20	20	20
Productivity of created versus natural habitat (%)	67	67	67	**33**	**100**	67	67	67	67
Years to full-service flow	20	20	20	20	20	**10**	**30**	20	20
Lifespan of created habitat (yr)	65	65	65	65	65	65	65	**100**	**30**
RH example 1	57	31	78	115	38	48	67	120	48
RH example 2	218	119	300	443	146	183	259	460	184
RH example 3	77	42	106	157	52	65	91	163	65
RH example 4	81	45	112	165	55	69	97	172	69
Mean change from baseline (%)	–	−45	38	103	−33	−16	19	112	−16

Table 6. An example habitat equivalency analysis for native mussels in the upper Mississippi River used to assess the cumulative effect of simultaneously changing multiple input variables. This sensitivity analysis compares estimates of replacement habitat (RH) from a baseline scenario (all variable inputs were set to the median values derived from the literature) to two bounded scenarios: the lowest possible RH (low scenario) and the highest possible RH (high scenario). This example corresponds to Example 1 in Table 4.

	Baseline scenario	Low scenario	High scenario
Constant inputs			
Injured area units (m^2)	353	353	353
Percent of services lost initially (%)	25	25	25
Real discount rate (%)	3	3	3
Variable inputs			
Years to natural recovery	20	10	30
Relative productivity of created versus natural habitat (%)	67	100	33
Years to full-service flow after creation	20	10	30
Lifespan of the created habitat (yr)	65	100	30
Performance measure			
RH (m^2)	57	15	485
Percent change from baseline (%)		−74	751

technique with uniform definitions that managers could use to evaluate mussel assemblages.

The mussel HEA was most sensitive to the relative productivity of the created versus natural habitat and lifespan of the created habitat; thus, users should carefully consider inputs for these variables. The cumulative effects of changing multiple input variables on the estimate of RH required was substantial. However, this level of difference is based on bounded examples that used only the minimum and maximum values for the input variables regardless of any relevant biological and local information. In the absence of empirical data, objective professional judgment will be essential for fair evaluations. One approach might be to start with median values and then adjust inputs up or down based on a priori information such as species composition, life history, density, and age structure. Peer-reviewed information might help assess how the injured bed compares to other beds. The mussel community assessment tool (Dunn et al. 2020) might provide useful context for evaluating the relative qualities of individual beds.

DATA NEEDED TO INFORM MUSSEL HEA MODELS

Although HEA shows promise as a tool to restore mussels after injury, substantial data gaps must be addressed. We identified four areas where additional research could benefit HEA: formal demographic modeling to predict years to natural recovery, the need to address habitat quality and quantity to inform lifespan of the created habitat, the identification of representative indicators for ecological services to inform relative productivity of created versus natural habitat, and the development of a relationship between services and species richness to produce more comprehensive measures of service losses and gains. Tools (e.g., population and production models) are lacking for using existing data to make robust estimates of the four inputs.

Both HEA and REA would benefit from development of demographic data on basic biological processes in mussels (i.e., rates of mortality, growth, and reproduction) across species, habitats, and ecosystems. For example, natural variation in vital rates of four species of mussels over a 4-yr period in the UMR varied considerably (survival varied six-fold, growth varied two-fold) and was related to life history, habitat quality, and hydrologic events (Newton et al. 2020). Similarly, recruitment rate and population growth rates of two species of mussels varied considerably in the Clinch River, Tennessee, and were strongly associated with stream discharge (Lane et al. 2021). Studies such as these, which quantify natural variation in population vital rates and the physical conditions that influence them, may reduce uncertainty in mussel HEA input values. Equivalency analyses also would benefit from development of Leslie matrix population models and associated life tables. Leslie matrix models are discrete, age-structured models of population growth often used in population ecology (e.g., Vindenes et al. 2021). This information can inform HEA and REA by documenting how many mussels are lost over time by age class based on survival and longevity. These models can help determine the restoration needed to replace what was lost to injury (e.g., Jones et al. 2012).

In HEA, managers seek to estimate the quantity of habitat restoration needed to compensate for ecological service losses over time. However, habitat quality may be as (or more) important than habitat quantity or configuration in enhancing species richness and persistence (Summerville and Crist 2004). Although habitat quantity can be measured directly, habitat quality remains elusive. Recently a few metrics have been proposed to assess habitat quality. For example, measures of substrate stability (as an indicator of habitat quality) might allow meaningful inference about the potential lifespan of a mussel bed at a particular location (Newton et al. 2020). Combined measures of substrate resistance (a measure of consolidation of surface sediments), redox potential (as a proxy for oxygen penetration), and substrate texture were strong indicators of mussel recruitment (Geist and Auerswald 2007). The amount of fine sediment in interstitial spaces largely explained the decline of *Margaritifera margaritifera* in German streams (Stoeckl et al. 2020). In a mark-recapture study in the UMR, survival of mussels was consistently higher in areas with stable substrate, relative to areas where the substrate was less stable (Newton et al. 2020). Importantly, habitat quality and quantity are not mutually exclusive and should be considered interactively. It is likely that there are locations where high-quality habitats (i.e., those where survival, growth, and reproduction are optimized) are present only in low quantity, or, conversely, locations where quantity is large but quality is uniformly low. Further complicating the

assessment of habitat quality is that it likely varies temporally. Research that identifies habitat attributes that optimize biological processes will provide valuable information for damage assessments.

Habitat equivalency analysis uses the percent of ecological services lost as part of the scaling process (see Table 2). HEA practitioners urgently need data on representative indicators for ecological services to inform the relative productivity of created versus natural habitat. Prior studies indicated that HEA results are sensitive to the choice of indicator used to assess ecological services lost (Strange et al. 2002; Vaissière et al. 2013). For example, the years to natural recovery in salt marsh ecosystems was highly dependent on which ecological indicator (i.e., primary production, soil development and biogeochemical cycling, invertebrate food supply, and secondary production) was used as a proxy for ecological services (Strange et al. 2002). It is not feasible to measure and quantify each of the ecological services provided by mussels and their habitats. The use of HEA to scale restoration is warranted only when the loss of ecological services can be quantified through a scientifically robust indicator that is representative of the damaged habitats and/or natural resource. In the mussel HEA, the pre-injury density of mussels (in mussels/m^2) was used as an indicator of secondary production (the ecological service), assuming that production is correlated with the magnitude of ecological services provided by mussels (e.g., McCay et al. 2003). However, estimates of secondary production in mussels in rivers are limited to a few studies (Strayer et al. 1994; Newton et al. 2011). Future mussel HEAs should consider other indicators such as abundance as a surrogate for population size, the number of live species as a surrogate for biodiversity, or stability of river substrates as a surrogate for habitat longevity. Regardless of the chosen indicator, sufficient data on the input values either need to exist or be cost-effective to obtain. Given the current state of research on quantifying ecological services provided by mussels and their habitats, this will be challenging.

The lack of an established relationship between services and species richness is a critical data gap in mussel HEAs. Although we know that the ecological services performed by mussels vary across species and environmental contexts (Spooner and Vaughn 2008), we do not know the degree to which restoration is dependent on recovering the original species richness. If reestablishing the original species assemblage is not possible or cost-effective, is restoration of species with similar functional traits sufficient? Also the relationship between services and species richness may depend on the mussel-provided ecological service of interest. For services such as biofiltration and nutrient cycling, those species that dominate the biomass typically provide most of the services (Vaughn 2018). However, there may be existence values for biodiversity (the value that people place on an item merely to know it exists, even if they do not use or ever intend to use that item; Strayer 2017) that would support restoration of all mussel species. Thus, although our assessment of the biological inputs to HEA was reasonable based on the literature or professional expertise, practitioners must recognize that conclusions about the amount of restoration needed depend on the data and assumptions that are used in the mussel HEA calculations.

FUTURE CONSIDERATIONS

As equivalency models continue to be applied to mussels, practitioners might consider the following points when trying to restore mussels, their habitats, and the ecological services they provide. Where practical, practitioners should ensure that conservation goals are inclusive of all life stages. Because the ecological services performed by mussels often scale with biomass, habitats that are restored with hatchery-reared juveniles may approach the same level of productivity as the original bed only when a size distribution similar to the original bed is achieved. Restoration efforts would benefit from re-creating a species composition similar to the original assemblage. This will be challenging because propagation methods are available for only a fraction of mussel species, and it may be difficult to propagate enough mussels to have a tangible effect on ecological services at large scales. If a similar species composition cannot be attained, practitioners should try to use species with similar life history strategies (i.e., equilibrium, opportunistic, periodic; Haag 2012). It also would be beneficial to ensure that appropriate hosts are available in the vicinity of the restored habitat. In conclusion, restoring mussels in large complex rivers like the UMR will be challenging and will not occur solely by stocking captively propagated individuals. Restoration of mussels will require a multifaceted approach that may include stocking captively propagated individuals, translocating mussels, protecting habitats that support both a high density and a high diversity of mussels, and aggressively re-creating habitats of sufficient quantity and quality to facilitate natural recolonization.

ACKNOWLEDGMENTS

We thank Jon Duyvejonck from the U.S. Fish and Wildlife Service for discussions that initiated this effort, Amy Horner Hanley (U.S. Department of the Interior, Office of the Solicitor), Steve McMurray (Missouri Department of Conservation), and Megan Bradley (U.S. Fish and Wildlife Service) for helpful comments on an earlier draft. The findings and conclusions in this article are those of the authors and do not necessarily represent the views of the U.S. Fish and Wildlife Service or the U.S. Department of Interior's Restoration Program, and no official endorsement should be inferred on Natural Resource Damage Assessment. Our work was funded by the U.S. Fish and Wildlife Service and the U.S. Geological Survey Ecosystems Mission Area Fisheries Program. Any use of trade, firm, or product names is for descriptive purposes only and does not imply endorsement by the U.S. Government. At the time of publication, these data have not been published by the Iowa

Department of Natural Resources or the U.S. Fish and Wildlife Service.

LITERATURE CITED

Ando, A., K. Madhu, A. Wildermuth, and S. Vig. 2004. Natural resource damage assessments: Methods and cases. Unpublished report RR-108, Illinois Waste Management and Research Center, Champaign, Illinois. Available at https://www.ideals.illinois.edu/bitstream/handle/2142/1979/RR-108.pdf?sequence=1 (accessed January 22, 2021).

Baker, M., A. Domanski, T. Hollweg, J. Murray, D. Lane, K. Skrabis, R. Taylor, T. Moore, and L. DiPinto. 2020. Restoration scaling approaches to addressing ecological injury: The habitat-based resource equivalency method. Environmental Management 65:161–177.

Barnthouse, L. W., and R. G. Stahl. 2002. Quantifying natural resource injuries and ecological service reductions: Challenges and opportunities. Environmental Management 30:1–12.

Bouska, K. L., A. Rosenberger, S. E. McMurray, G. A. Lindner, and K. N. Key. 2018. State-level freshwater mussel programs: Current status and a research framework to aid in mussel management and conservation. Fisheries 43:345–360.

Dunford, R. W., T. C. Ginn, and W. H. Desvousges. 2004. The use of habitat equivalency analysis in natural resource damage assessments. Ecological Economics 48:49–70.

Dunn, H., S. Zigler, and T. Newton. 2020. Validation of a mussel community assessment tool for the upper Mississippi River System. Freshwater Mollusk Biology and Conservation 23:109–123.

FMCS (Freshwater Mollusk Conservation Society). 2021. Scientific and common names of freshwater bivalves of the US and Canada. Available at https://molluskconservation.org/MServices_Names.html (accessed December 15, 2021).

Fonseca, M. S., B. E. Julius, and W. J. Kenworthy. 2000. Integrating biology and economics in seagrass restoration: How much is enough and why? Ecological Engineering 15:227–237.

Fridley, J. D. 2001. The influence of species diversity on ecosystem productivity: How, where, and why? Oikos 93:514–526.

Geist, J., and K. Auerswald. 2007. Physicochemical stream bed characteristics and recruitment of the freshwater pearl mussel (*Margaritifera margaritifera*). Freshwater Biology 52:2299–2316.

Haag, W. R. 2012. North American Freshwater Mussels: Natural History, Ecology, and Conservation. Cambridge University Press, New York. 505 pp.

Haag, W. R., and J. D. Williams. 2013. Biodiversity on the brink: An assessment of conservation strategies for North American freshwater mussels. Hydrobiologia 735:45–60.

Hanson, D. A., E. M. Britney, C. J. Earle, and T. G. Stewart. 2013. Adapting habitat equivalency analysis (HEA) to assess environmental loss and compensatory restoration following severe forest fires. Forest Ecology and Management 294:166–177.

Israel, B. 2019. State-by-state guide to NRD programs in all 50 states and Puerto Rico. Available at https://www.arnoldporter.com/-/media/files/perspectives/publications/2019/07/state-by-state-nrd-guide.pdf (accessed January 22, 2021).

Jirka, K. T., and R. J. Neves. 1992. Reproductive biology of four species of freshwater mussels (Mollusca: Unionidae) in the New River, Virginia, and West Virginia. Journal of Freshwater Ecology 7:35–44.

Johnston, M. W., S. J. Purkis, and R. E. Dodge. 2015. Measuring Bahamian lionfish impacts to marine ecological services using habitat equivalency analysis. Marine Biology 162:2501–2512.

Jones, J. W., R. J. Neves, and E. M. Hallerman. 2012. Population performance criteria to evaluate reintroduction and recovery of two endangered mussel species, *Epioblasma brevidens* and *Epioblasma capsaeformis* (Bivalvia: Unionidae). Walkerana 15:27–44.

Lane, T., J. Jones, B. Ostby, and R. Butler. 2021. Long-term monitoring of two endangered freshwater mussels (Bivalvia: Unionidae) reveals how demographic vital rates are influenced by species life history traits. PLoS ONE 16: e0256279.

McCay, D. P. F., C. H. Peterson, J. T. DeAlteris, and J. Catena. 2003. Restoration that targets function as opposed to structure: Replacing lost bivalve production and filtration. Marine Ecology Progressive Series 264:197–212.

Miller, A. C., and B. S. Payne 1998. Effects of disturbances on large-river mussel assemblages. Regulated Rivers: Research and Management 14:179–90.

Morales, Y., L. J. Weber, A. E. Mynett, and T. J. Newton. 2006. Effects of substrate and hydrodynamic conditions on the formation of mussel beds in a large river. Journal of the North American Benthological Society 25:664–676.

Mukherjee, N., J. Huge, W. J. Sutherland, J. McNeill, M. Van Opstal, F. Dahdouh-Guebas, and N. Koedam. 2015. The Delphi technique in ecology and biological conservation: Applications and guidelines. Methods in Ecology and Evolution 6:1097–1109.

Newton, T. J., D. A. Woolnough, and D. L. Strayer. 2008. Using landscape ecology to understand freshwater mussel populations. Journal of the North American Benthological Society 27:424–439.

Newton, T. J., S. J. Zigler, J. T. Rogala, B. R. Gray, and M. Davis. 2011. Population assessment and potential functional roles of native mussels in the upper Mississippi River. Aquatic Conservation: Marine and Freshwater Ecosystems 21:122–131.

Newton, T. J., S. J. Zigler, P. R. Schrank, M. Davis, and D. R. Smith. 2020. Estimation of vital rates to assess the relative health of mussel assemblages in the upper Mississippi River. Freshwater Biology 65:1726–1739.

NOAA (National Oceanic and Atmospheric Administration). 1997. Natural resource damage assessment guidance document: Scaling compensatory restoration actions (Oil Pollution Act of 1990). Available at http://losco.state.la.us/pdf_docs/NOAA_NRDA_Guidance_Scaling_1997.pdf (accessed January 22, 2021).

Payne, B. S., and A. C. Miller. 1989. Growth and survival of recent recruits to a population of *Fusconaia ebena* (Bivalvia: Unionidae) in the lower Ohio River. American Midland Naturalist 121:99–104.

Ries, P. R., N. R. De Jager, S. J. Zigler, and T. J. Newton. 2016. Spatial patterns of native freshwater mussels in the upper Mississippi River. Freshwater Science 35:934–947.

Roach, B., and W. Wade. 2006. Policy evaluation of natural resource injuries using habitat equivalency analysis. Ecological Economics 58:421–433.

Ruiz-Jaen, M. C., and T. M. Aide. 2005. Restoration success: How is it being measured? Restoration Ecology 13:569–577.

Sansom, B. J., S. J. Bennett, J. F. Atkinson, and C. C. Vaughn. 2018. Long-term persistence of freshwater mussel beds in labile river channels. Freshwater Biology 63:1469–1481.

Scemama, P., and H. Levrel. 2016. Using habitat equivalency analysis to assess the cost effectiveness of restoration outcomes in four institutional contexts. Environmental Management 57:109–122.

Southwick, R., and A. J. Loftus. 2017. Investigation and monetary values of fish and freshwater mussel kills. American Fisheries Society, Special Publication 35, Bethesda, Maryland.

Sperduto, M. B., S. P. Powers, and M. Donlan. 2003. Scaling restoration to achieve quantitative enhancement of loon, seaduck, and other seabird populations. Marine Ecology Progress Series 264:221–232.

Spooner, D. E., and C. C. Vaughn. 2008. A trait-based approach to species' roles in stream ecosystems: Climate change, community structure, and material cycling. Oecologia 158:307–317.

Spooner, D. E., and C. C. Vaughn. 2009. Species richness and temperature influence mussel biomass: A partitioning approach applied to natural communities. Ecology 90:781–790.

Stoeckl, K., M. Denic, and J. Geist. 2020. Conservation status of two

endangered freshwater mussel species in Bavaria, Germany: Habitat quality, threats, and implications for conservation management. Aquatic Conservation: Marine and Freshwater Ecosystems 30:647–661.

Strange, E., H. Galbraith, S. Bickel, D. Mills, D. Beltman, and J. Lipton. 2002. Determining ecological equivalence in service-to-service scaling of salt march restoration. Environmental Management 29:290–300.

Strayer, D. L. 2017. What are freshwater mussels worth? Freshwater Mollusk Biology and Conservation 20:103–113.

Strayer, D. L., D. C. Hunter, L. C. Smith, and C. K. Borg. 1994. Distribution, abundance, and roles of freshwater clams (Bivalvia, Unionidae) in the freshwater tidal Hudson River. Freshwater Biology 3:239–248.

Summerville, K. S., and T. O. Crist. 2004. Contrasting effects of habitat quantity and quality on moth communities in fragmented landscape. Ecography 27:3–12.

Tucker, J., and C. Thieling. 1999. Freshwater mussels. Pages 11.1–11.4 *in* K. Lubinski and C. Thieling, editors. Ecological status and trends of the Upper Mississippi system. U.S. Geological Survey, Report LTRMP 99-T001, La Crosse, WI. Available at https://www.umesc.usgs.gov/reports_publications/status_and_trends.html (accessed January 22, 2021).

UMRBA (Upper Mississippi River Basin Association). 2014. Upper Mississippi River spill response plan and resource manual. Available at www.umrba.org/hazspills/umrplan.pdf (accessed January 22, 2021).

Unsworth, R., and R. Bishop. 1994. Assessing natural resource damages using environmental annuities. Ecological Economics 11:35–41.

USACE (United States Army Corps of Engineers). 2012. Environmental Design Handbook. USACE, Washington, DC. 534 pp. Available at https://www.mvr.usace.army.mil/Portals/48/docs/Environmental/UMRR/HREP/EMP_Documents/2012%20UMRR%20EMP%20Environmental%20Design%20Handbook%20-%20FINAL.pdf (accessed September 16, 2021).

USFWS (United States Fish and Wildlife Service). 2006. Upper Mississippi River, National Wildlife and Fish Refuge, Comprehensive Conservation Plan. USFWS, Washington, DC. 242 pp. Available at https://www.fws.gov/midwest/planning/uppermiss/index.html (accessed January 22, 2021).

USFWS et al. (United States Fish and Wildlife Service, Nottawaseppi Huron Band of the Potawatomi Tribe, and the Match-E-Be-Nash-She-Wish Band of the Pottawatomi Indians). 2015. Final damage assessment and restoration plan/environmental assessment for the July 25–26, 2010 Enbridge Line 6B oil discharges near Marshall, MI. Available at https://www.fws.gov/midwest/es/ec/nrda/MichiganEnbridge/pdf/FinalDARP_EA_EnbridgeOct2015.pdf (accessed January 22, 2021).

Vaissière A. C., H. Levrel, C. Hily, and D. Le Guyader. 2013. Selecting ecological indicators to compare maintenance costs related to the compensation of damaged ecosystem services. Ecological Indicators 29:255–269.

Vaughn, C. C. 2018. Ecosystem services provided by freshwater mussels. Hydrobiologia 810:15–27.

Vaughn, C. C., and T. J. Hoellein. 2018. Bivalve impacts in freshwater and marine ecosystems. Annual Review of Ecology, Evolution, and Systematics 49:183–208.

Vindenes, Y., C. LeCoeur, and H. Caswell. 2021. Introduction to matrix population models. Pages 163–181 *in* R. Salguero-Gómez and M. Gamelon, editors. Demographic Methods across the Tree of Life. Oxford University Press, New York.

Watters, G. T., M. A. Hoggarth, and D. H. Stansberry. 2009. The Freshwater Mussels of Ohio. The Ohio State University Press, Columbus. 421 pp.

Zigler, S., T. Newton, J. Steuer, M. Bartsch, and J. Sauer. 2008. Importance of physical and hydraulic characteristics to unionid mussels: A retrospective analysis in a reach of large river. Hydrobiologia 598:343–360.

Appendix A. Three examples of the habitat equivalency analysis for native mussels in the upper Mississippi River used to assess the cumulative effect of simultaneously changing multiple input variables. This sensitivity analysis compares estimates of replacement habitat (RH) from a baseline scenario (all variable inputs were set to the median values derived from the literature) to two bounded scenarios: the lowest possible RH (low scenario) and highest possible RH (high scenario).

	Baseline scenario	Low scenario	High scenario
Example 2			
Constant inputs			
Injured area units (m^2)	301	301	301
Percent of services lost initially (%)	100	100	100
Real discount rate (%)	3	3	3
Variable inputs			
Years to natural recovery	20	10	30
Relative productivity of created versus natural habitat (%)	67	100	33
Years to full-service flow after creation	20	10	30
Lifespan of the created habitat (yr)	65	100	30
Performance measure			
RH (m^2)	218	58	1,863
Percentage change from baseline (%)		−73	755
Example 3			
Constant inputs			
Injured area units (m^2)	113	113	113
Percent of services lost initially (%)	100	100	100
Real discount rate (%)	3	3	3
Variable inputs			
Years to natural recovery	20	10	30
Relative productivity of created versus natural habitat (%)	67	100	33
Years to full-service flow after creation	20	10	30
Lifespan of the created habitat (yr)	65	100	30
Performance measure			
RH (m^2)	77	21	659
Percentage change from baseline (%)		−73	756
Example 4			
Constant inputs			
Injured area units (m^2)	7500	7500	7500
Percent of services lost initially (%)	1.5	1.5	1.5
Real discount rate (%)	3	3	3
Variable inputs			
Years to natural recovery	20	10	30
Relative productivity of created versus natural habitat (%)	67	100	33
Years to full-service flow after creation	20	10	30
Lifespan of the created habitat (yr)	65	100	30
Performance measure			
RH (m^2)	81	22	696
Percentage change from baseline (%)		-73	759

Freshwater Mollusk Biology and Conservation 25:27–36, 2022

DOI:10.31931/FMBC-D-21-00001

REGULAR ARTICLE

COMPARATIVE ASSESSMENT OF SHELL PROPERTIES IN EIGHT SPECIES OF COHABITING UNIONID BIVALVES

Robert S. Prezant[1]*, Gary H. Dickinson[2], Eric J. Chapman[3], Raymond Mugno[4], Miranda N. Rosen[2], and Maxx B. Cadmus[2]

[1] *Academic Affairs, Southern Connecticut State University, New Haven, CT 06515 USA*
[2] *Department of Biology, The College of New Jersey, Ewing, NJ 08628-0718 USA*
[3] *Western Pennsylvania Conservancy, Watershed Conservation Program, Indiana, PA 15701 USA*
[4] *Department of Mathematics, Southern Connecticut State University, New Haven, CT 06515 USA*

ABSTRACT

Freshwater unionid mussels produce a bilayered shell with the mineral proportion comprising an outer prismatic and an inner nacreous layer. The shell is the animals' primary structural means of protection from predators and environmental challenges; therefore, variations in shell strength and properties may lead to differences in survival. Few studies have systematically assessed shell properties in unionids. A major challenge in such work is separating effects of environment from those of evolutionary history, because ultimately, both can affect shell properties. We collected eight species of unionids within a small area of the Allegheny River, Pennsylvania, that was relatively homogeneous in substratum type and other environmental characteristics. For each species, we quantified shell thickness, including thickness of the prismatic and nacreous layers, and shell micromechanical properties (microhardness and crack propagation, a measure of fracture resistance) in three regions of the shell. Shell thickness varied dramatically among species and was about five times greater in the thickest-shelled species, *Pleurobema sintoxia*, than in the thinnest-shelled species, *Villosa iris*. Because all species experienced similar environmental conditions, variation in shell thickness can be attributed largely to evolutionary history. In contrast, microhardness and crack propagation showed little variation among species. Given that micromechanical properties are similar among species, shell strength may be largely a function of thickness. These results have conservation implications, as differences in shell thickness could reflect relative vulnerability to predators and physical conditions.

KEY WORDS: Unionidae, shell biomechanics, shell strength, nacre, prismatic

INTRODUCTION

Bivalve mollusks possess a multilayered shell, which serves to protect the animal from predators and hydrodynamic forces. In freshwater unionacean bivalves, the mineralized portion of the shell regularly consists of an outer prismatic layer and an inner nacreous layer (Checa and Rodriguez-Navarro 2001). This prismato-nacreous shell represents the most primitive of the extant bivalve shell structures (Giribet and Wheeler 2002; Graf and Cummings 2006; Marin et al. 2008). The role of the environment and local habitat in modifying the macro- and microstructure of shells has been well documented (e.g., Tan Tiu and Prezant 1987, 1989; Bailey and Green 1988; Prezant et al. 1988; Zieritz et al. 2010; Kishida and Sasaki 2018). In the field, however, environmental conditions often covary with local species composition, making it difficult to separate the effect of environment from that of evolutionary history in the development of shell properties.

Variations in shell properties can influence the strength of a shell and its resistance to fracture. The correlation between shell size, including shell thickness, and vulnerability to predation has been documented (Tyrrell and Hornbach 1998; Edelman et al. 2015). Shell strength is essentially resistance to breakage; shell fracture resistance is a measure of how easily a shell responds to an initial impact—that is, how easily a

*Corresponding Author: prezantr1@southernct.edu

fracture propagates through a shell. Variables that can affect shell strength include overall size, mass, shape, and sculpture; shell thickness and the thickness of composite layers; shell microstructural type and the nanometer and micrometer-scale mechanical properties of these microstructures; elemental content; and organic content, including intracrystalline organics (Fratzl et al. 2007; Meyers and Chen 2014; Kim et al. 2016). Shell microstructure and associated organic matrix are essential in resisting fractures from an incipient crack, for example, from a crayfish or other predator, by dissipating that initial fracture through organic interstices between calcified units without compromising the integrity of the entire mineralized shell (Zhang et al. 2019).

For unionids, studies that systematically assess structural and mechanical properties in multiple species from the same geographic location are rare. The opportunity to compare eight sympatric species of freshwater mussels availed itself through an initiative to translocate large numbers of unionids from beneath the Hunter Station Bridge (SR 62) over the Allegheny River in northwestern Pennsylvania during bridge replacement. We were able to obtain specimens from common species to assess shell properties. Our goal was to quantify shell size and thickness (including that of the nacreous vs. prismatic layers), microhardness (a measure of resistance to mechanical deformation that scales with shell strength) and fracture resistance across a variety of unionid taxa all from the same habitat, thus eliminating variation due to major differences in environment. From a conservation perspective, assessing variation in shell-layer thickness, shell strength, and fracture resistance can provide insight on survivability of unionids in the face of predatory pressures and changing environments.

MATERIALS AND METHODS

Collection Methodology

All mussels collected for this project were removed from the direct impact zone of the Hunter Station Bridge replacement, which occurred in summer 2016. The bridge is located on the Allegheny River in the town of Hunter, Pennsylvania, at 41°31′N 79°29′W. The river is relatively shallow (<3.0 m) in this area and flows are dependent upon releases from the Kinzua Dam on the Allegheny River and Tionesta Dam on Tionesta Creek.

Divers collected freshwater mussels in August 2016 using scuba, surface-supplied air, or snorkel gear depending upon river depth and current velocity. We mapped the entire survey reach of 4,884 m^2 and overlaid it with a grid for salvage purposes. We collected, enumerated, and bagged by species all mussels found within each of the salvage cells. This was not a survey study per se but a bulk translocation effort to better ensure survival of rare and endangered species of unionids. Thus, aside from anecdotal notes, specific details for quadrats or individual organisms collected are not available. We randomly selected individuals from among those recovered and held them in mesh bags in the Allegheny River until approximately 10 individuals per species were recovered. We analyzed eight species, including *Actinonaias ligamentina, Eurynia dilatata*, *Lampsilis ovata*, *Lampsilis fasciola*, *Pleurobema sintoxia*, *Ptychobranchus fasciolaris*, *Strophitus undulatus*, and *Villosa iris*.

The substratum was similar across the entire sampled reach of the river and was dominated by cobble (40%) and gravel (30%), with some sand (15%), silt (10%), and boulders (5%) present. The distribution of the eight species within this study was homogeneous across the sampled area. No obvious microhabitats were detected that might have created distribution bias for any one species. Most cells surveyed had some eelgrass (*Vallisenaria americana*) present; there are suggestions that survey cells with denser populations of eelgrass tended to have higher numbers of mussels but no differences in species diversity. The eight species assessed in this study were found in all survey cells, and their distribution (as opposed to the total numbers of unionids found) did not appear to vary with presence or absence of eelgrass or eelgrass density.

Sample Preparation

Mussels were preserved in 70% ethanol for shell analyses. While preservation in ethanol followed by drying can potentially influence shell mechanical properties (Leung and Sinha 2009; Brown et al. 2017), it is unlikely that these factors would differ among species or treatment groups. Since shells used in this study were uniformly preserved in 70% ethanol, and testing conditions were identical for all species, any alterations of the prismato-nacreous shell properties due to preservation and sample preparation should be uniform across species.

We used left shell valves for all assessments, with five valves randomly selected per species. Individual valves were removed from ethanol and any adhering soft tissue removed using a scalpel. Prior to cutting each sample, a line was drawn perpendicular to shell growth ridges, from the umbo to the growth edge of the shell (Fig. 1A). Samples were cut along this line using a water-cooled diamond band saw (model C-40, Gryphon Corporation, Sylmar, CA, USA). This produced two portions of the valve; the anterior portion was used for curved height measurements (see below), while the posterior portion was cut further and embedded for mechanical and thickness testing. Specifically, on the posterior portion of the shell, a second cut was made parallel to, and approximately 0.5–1.0 cm further posterior to, the first. The strip of shell produced from these cuts was then cut perpendicular to the original cuts into three equal-size segments, denoted as regions 1 (umbonal), 2 (midvalve), and 3 (periphery) (Fig. 1A). Shell segments were washed with distilled water after cutting, then dried at room temperature overnight, and finally dried at 45°C under 27 mm Hg in a vacuum oven for 24 h.

Shell segments were embedded in epoxy resin to enable polishing. We placed the dry shell segments individually into 31.75-mm mounting cups with the anterior side of the segment

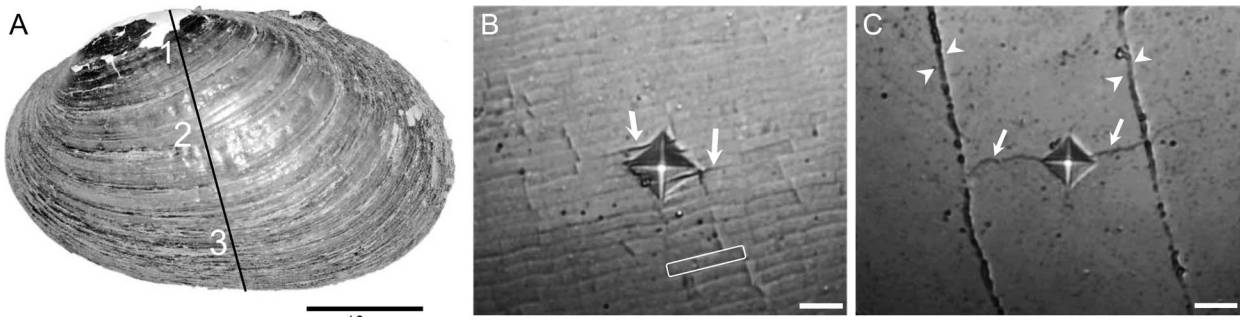

Figure 1. (A) *Actinonaias ligamentina*, left valve, showing regions of shell sampling for microhardness, crack propagation, and thickness measurements. Region 1 is umbonal, region 2 is midvalve, and region 3 is shell periphery. Light microscopy images of an indent (diamond shape) made within (B) the nacre and (C) the prismatic layer. An applied load of 30 g was used during indentation in both shell regions. Tailed arrows indicate cracks produced during indentation. (B) Individual nacre tablets are clearly designated as noted by the white rectangle. For the prismatic layer, the boundary between adjacent units is indicated by arrowheads. Scale bars: A = 10 mm; B and C = 5 μm.

oriented facing the bottom of the mounting cup. Samples that did not stand upright on their own were secured using plastic coil clips (Allied High Tech, Compton, CA, USA). Mounting cups were filled with epoxy (EpoxySet, Allied High Tech) and cured for approximately 24 h or until completely hardened.

Samples were polished using an automated grinder polisher machine (METPREP 3 PH-4, Allied High Tech). Each embedded sample was polished through a series of 320-grit, 600-grit, and 800-grit silicon carbide papers, then polished with a 1-μm polycrystalline diamond suspension and lastly a 0.04-μm colloidal silica suspension. Samples were cleaned between each polishing step with a solution of 2% microorganic soap. Once the polished surface was completely smooth and free of scratches, samples were dried at room temperature and then placed in a desiccator until testing.

Shell Curved-Height Measurements

The anterior portion of the shell valve produced after the initial cut (see above) was used for curved-height measurements. Images of the cut surface of each valve were scanned using a photo scanner to enable digital measurements. This was done by placing the cut surface of the valve directly onto the bed of the scanner so that the shell stood up on its own, and a high-resolution scan was acquired. Curved height, defined as the total distance from umbo to the ventral growth edge, was measured in ImageJ (Ver. 1.43, U.S. National Institutes of Health, Bethesda, Maryland, USA, https://imagej.nih.gov/ij/, accessed February 15, 2022) on the scans using a segmented line tool. To incorporate curvature of the valve, the line was drawn down the center of the cut surface of the valve from umbo to the shell edge.

Shell Thickness Measurements

We assembled panorama images of each embedded shell sample using Zen 2.3 software (Carl Zeiss Microscopy, White Plains, NY, USA). Individual images were taken under brightfield using an Axioscope A1 reflected-light microscope with an Axiocam 105 color camera (Carl Zeiss Microscopy). The number of individual images varied depending on the size of the sample and ranged from 3 to 36. We measured shell thickness at defined points along the breadth of each embedded shell segment. Measurement locations were determined by placing a grid over the image as described in Nardone et al. (2018). Thickness measurements were taken using the software's linear measurement tool for the prismatic and nacreous layers. Grid sizes varied depending on the size of the sample but were adjusted to enable 20–30 measurements per sample. In the samples that were from the region closest to the umbo (region 1), erosion produced a prismatic layer that was often not continuous, and in some cases, was missing completely, and therefore measurements were not recorded for this layer. In samples that contained the growth edge, measurements were recorded until the layers began to thin. Measurements from the nacreous and prismatic layers were added together to determine the total thickness. For regions containing a prismatic layer (regions 2 and 3), the ratio of prismatic to nacreous thickness was calculated as the prismatic layer thickness divided by the nacreous layer thickness.

Micromechanical Testing

Micromechanical testing was conducted on an HM-200 microhardness testing machine (Mitutoyo America Corporation, Aurora, IL, USA) on five individuals per species per shell region. Embedding and polishing of shell segments produced a cross-section of the shell, normal to the outer shell surface, as described in Dickinson et al. (2012). This procedure enabled separate tests to be made within both the prismatic and nacreous layers (Fig. 1B, C). In each sample, 10 indents were made in both the prismatic and nacreous layers. Values obtained from these repeated indentations were averaged for each shell layer prior to statistical analyses. Indents were spaced evenly along the breadth of the shell segment using the stage-positioning micrometers on the testing machine, with spacing between indents equivalent in the prismatic and

nacreous layers. Micromechanical indents were made at 30 g load and 5 s dwell time within both the prismatic and nacreous layers. For the first two replicates from each species, indents were measured directly on the hardness tester in two dimensions and Vickers hardness numbers (VHNs) were automatically calculated by the tester. For the other three replicates from each species, an image of each indent was taken using a Zeiss Axiocam 305 color microscope camera and the diagonals of the indent were measured on the digital image using Zen 2.3 software (Carl Zeiss Microscopy). We used the equation $1.854 \times F/d^2$ where F is force in kilograms and d^2 is the mean diagonal length in millimeters to calculate microhardness as a VHN (ASTM 2017). Variation between the two measurement techniques was minimal (on average, within 2.5% when the same indent was measured both ways). In samples from the region closest to the umbo (region 1 as shown in Fig. 1A), the prismatic layer was not continuous (due to umbonal erosion) and therefore microhardness could not be measured in the prismatic layer for these samples.

For all sample sets, crack propagation was assessed on digital microscope images taken on the hardness tester (Fig. 1B, C). Crack propagation was determined as the radius of a circle emanating from the center of the indent and encompassing all visible cracks (Anstis et al. 1981; Baldassarri et al. 2008).

Statistical Analyses

We explored differences in the response variables of measured hardness, crack propagation, curved height, and thickness among species. Since measured hardness, crack propagation, and thickness values were consistently and substantially different between the nacreous and prismatic layers (for example, by up to an order of magnitude for thickness metrics), these layers were analyzed separately. All response variables failed to satisfy the assumptions of analysis of variance, using either the Levene's test for homogeneity of variance or the Shapiro–Wilk test for normality, so we used nonparametric methods that compare median values (Ott and Longnecker 2010). The overall significance level was set at $P < 0.05$. Statistical tests were conducted in R (R Core Team 2013). We compared curved height among species using a Kruskal–Wallis test and Dunn's procedure for multiple comparisons with Holm's correction for P values (Pohlert 2014). We assessed the effect of species on shell microhardness and crack propagation using the Prentice test, which is a generalization of Friedman's test for use with replicates (Konietschke et al. 2015). Shell region was used as a blocking variable. Using Tukey's method, we made multiple comparisons between individual species. For thickness and the prismatic:nacreous-layer ratio, a Prentice test was also used, but multiple comparisons were made using pairwise Wilcoxon rank sum tests. This was due to missing values (shell samples where the nacre or prismatic layer was fractured and therefore thickness could not be measured) causing errors when using the Tukey's method (R Core Team 2013).

RESULTS

Visual examination of shell valves used from the eight species revealed an obvious difference in overall size of the shells, as well as variation in relative thickness of prismatic and nacreous layers; quantification of curved height and shell thickness support these observations. Curved height varied significantly among species (Kruskal–Wallis test: $H = 32.119$, $df = 7$, $P < 0.0001$; Fig. 2A). Curved height was nearly 2.5 times greater in the largest species tested, *L. ovata,* as compared to the smallest, *V. iris* (Dunn's multiple comparisons with Holm's correction: $P < 0.05$). Likewise, thickness of both the nacreous layer (Prentice test: $T = 90.305$, $df = 7$, $P < 0.0001$; Fig. 2B) and prismatic layer (Prentice test: $TS = 60.459$, $df = 7$, $P < 0.0001$; Fig. 2C) differed significantly among species. Nacre thickness was about eight times greater in the thickest species, *P. sintoxia,* as compared to the thinnest, *V. iris* (Wilcox rank sum tests: $P < 0.05$). *Lampsilis fasciola* had the thickest prismatic layer, with thickness about four times greater than *V. iris* (Wilcox rank sum tests: $P < 0.05$). For curved height and thickness metrics, numerous significant pairwise differences were observed between species, as detailed in Figure 2. Among all species and all shell regions, average nacreous layer thickness was about five times greater than that of the prismatic layer (note the difference in y-axis scale between Fig. 2B and C).

When comparing among regions of each shell valve (see Fig. 1), nacreous layer thickness for all species tended to be greatest closer to the umbo (region 1), reflecting the older age and longer mineral deposition times (Fig. 2B). The thinnest nacreous layer was typically found in region 3, nearest the valve edge, which is the youngest part of the shell with the shortest deposition time. Nacre was present in each region 3 measured, confirming that samples from these areas were always internal to the pallial line and not at the most distal shell margin.

As the outer layer of calcified shell, the prismatic layer is also most susceptible to external erosive conditions once the periostracum is either worn away or dissolved (not uncommon in unionids). As such, in the specimens collected, the umbonal area of prismatic shell (region 1) was consistently eroded and we were unable to take representative measurements of prismatic thickness. The shell periphery (region 3) in all taxa had the thickest prismatic layer (Fig. 2C).

The prismatic:nacreous-layer ratio varied significantly among species (Prentice test: $T = 52.684$, $df = 7$, $P < 0.0001$; Fig. 2D). Of note, this ratio was significantly lower in *P. sintoxia* compared to each of the other species assessed (Wilcox rank sum tests: $P < 0.05$); thus, nacre comprised a greater proportion of the total shell in this species (Table 1). The prismatic:nacreous-layer ratio did not differ significantly among any of the other species tested, except between *E. dilatata* and *L. ovata* (Wilcox rank sum tests: $P < 0.05$). Nacre comprised the bulk of total shell thickness in nearly all samples (with one exception, *L. fasciola*, region 3), as evidenced by prismatic:nacre ratios consistently well below 1.

Despite variations in nacreous thickness among species,

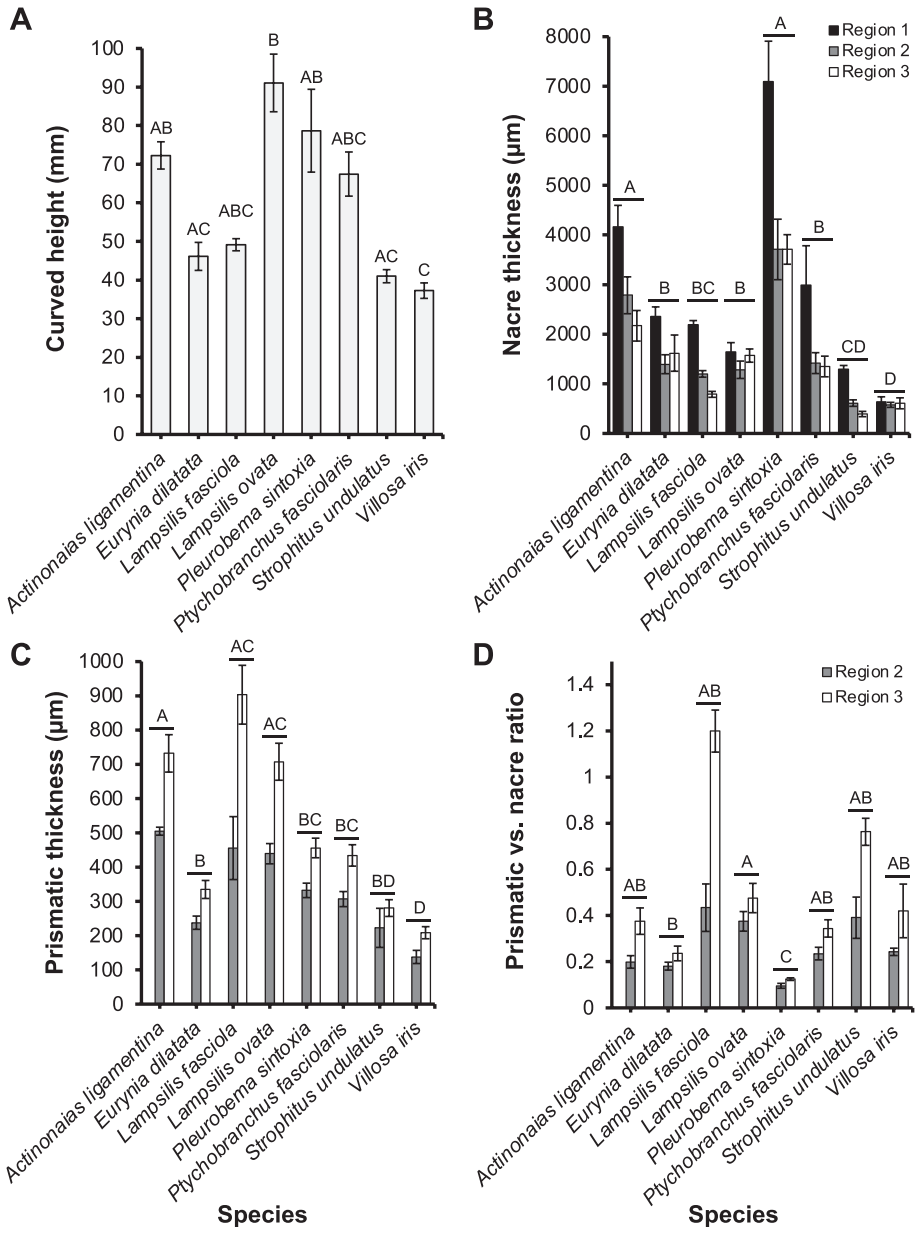

Figure 2. Curved height and thickness metrics (mean ± SE). (A) Curved height of left shell valves. (B) Nacre layer thickness. (C) Prismatic layer thickness. (D) Prismatic:nacrelayer thickness ratio. Within each panel, species marked with different letters are significantly different from one another, whereas those that share a letter do not differ. For curved height, pairwise comparisons were made using Dunn's multiple comparisons with Holm's correction ($P < 0.05$). For all other metrics, pairwise comparisons were made using Wilcoxon rank sum tests ($P < 0.05$), with region grouped within species. $n = 5$ replicates per species per shell region.

there was no effect of species on nacre microhardness (Prentice test: $T = 7.328$, df $= 7$, $P = 0.393$; Fig. 3A). Across all taxa and all shell regions measured, values ranged from 198 to 271 VHN. As with nacre, differences in microhardness in the prismatic layers among the species were minimal. Although the overall effect of species on microhardness was significant (Prentice test: $T = 18.21$, df $= 7$, $P = 0.011$; Fig. 3B), the only pairwise difference among the species assessed was between *L. ovata* and *E. dilatata* (Tukey's method: $P < 0.05$). Across all taxa and all shell regions measured, prismatic microhardness ranged from 258 to 419 VHN. For all species and all shell regions, the prismatic layer was consistently harder (on average, by 54%) than the nacre.

Higher crack propagation implies a lower resistance to the growth of fractures through a particular shell layer. There was relatively little difference across taxa in crack propagation resistance, nor was there much variation in resistance dependent upon shell location (Fig. 3C, D). There was a significant effect of species within the nacre (Prentice test: $T = 22.378$, df $= 7$, $P = 0.002$; Fig. 3A). However, significant

Table 1. Shell valve thickness metrics. Values are mean ± SE; $n = 5$ replicates per species per shell region. Region 2 = midvalve; region 3 = shell periphery.

	AL	ED	LF	LO	PS	PF	SU	VI
Region 2								
Total thickness (mm)	3.29 ± 0.38	1.62 ± 0.21	1.70 ± 0.11	1.72 ± 0.20	4.05 ± 0.63	1.73 ± 0.23	0.84 ± 0.08	0.71 ± 0.07
% thickness as prismatic	16.1 ± 1.8	15.1 ± 1.1	25.9 ± 4.5	26.2 ± 2.3	8.7 ± 0.9	18.4 ± 1.4	25.8 ± 4.5	19.2 ± 1.3
% thickness as nacre	83.9 ± 1.8	85.5 ± 1.4	71.2 ± 3.0	74.0 ± 2.1	91.1 ± 0.8	81.0 ± 1.9	72.7 ± 4.9	81.1 ± 1.2
Region 3								
Total thickness (mm)	2.90 ± 0.34	1.95 ± 0.39	1.70 ± 0.13	2.27 ± 0.13	4.17 ± 0.32	1.78 ± 0.23	0.67 ± 0.08	0.82 ± 0.12
% thickness as prismatic	26.1 ± 2.8	18.9 ± 2.1	53.0 ± 2.0	31.6 ± 3.2	11.0 ± 0.4	25.4 ± 2.2	42.4 ± 1.7	27.7 ± 4.7
% thickness as nacre	73.9 ± 2.8	81.1 ± 2.1	46.6 ± 2.2	68.6 ± 3.0	89.0 ± 0.4	74.5 ± 2.2	57.6 ± 1.7	71.9 ± 4.7

Abbreviations: AL = *Actinonaias ligamentina*; ED = *Eurynia dilatata*; LF = *Lampsilis fasciola*; LO = *Lampsilis ovata*; PS = *Pleurobema sintoxia*; PF = *Ptychobranchus fasciolaris*; SU = *Strophitus undulatus*; VI = *Villosa iris*.

pairwise differences were observed only between *P. sintoxia* and *L. ovata,* and between *P. sintoxia* and *V. iris* (Tukey's method: $P < 0.05$). Across all taxa and all shell regions measured, nacre crack propagation ranged from 8.6 μm to 18.7 μm. Variation in crack propagation within the prismatic layer among species was minimal in both regions (Fig. 3D). Overall, the effect of species was significant (Prentice test: $T = 19.760$, $df = 7$, $P = 0.006$), but individual pairwise differences between species were not significant (Tukey's method: $P > 0.05$ for all comparisons). Across all taxa and all shell regions measured, prismatic crack propagation ranged from 13.0 μm to 26.6 μm. In all species and all shell regions, crack propagation was consistently higher (on average, by 61%) in the prismatic layer as compared to the nacreous layer, suggesting that the former exhibits a lower resistance to fracture.

DISCUSSION

Shell formation in bivalve mollusks is a complex process affected by evolutionary history as well as environment (Tan Tiu and Prezant 1992; Kesler and Bailey 1993; Marin et al. 2007; Hornbach et al. 2010; Gilbert et al. 2017; Clark et al. 2020). Here, we assessed structural and mechanical properties of the shell in eight cohabiting species. Given that environmental conditions were relatively consistent among individuals—all were collected at the same location with no noticeable differences in substratum type—variation in shell properties between taxa can be attributed largely to evolutionary history. This conclusion has conservation implications, as shell structure and strength can influence population viability in the face of predation (including shell collection by humans), hydrodynamic forces, and shifts in water quality. We found that shell height and thickness varied dramatically among cohabiting species; in contrast, microscale mechanical properties were remarkably consistent among the species assessed.

At the whole-organism level, shell thickness is a good indicator of shell strength (Zuschin and Stanton 2001). Shell thickness can vary with latitude and hydrological conditions (Watson et al. 2012), as well as among species exposed to the same environment. Variation or changes in shell thickness, especially at the umbonal (oldest) areas for the latter, can leave the bivalve susceptible to shell fragmentation (Newell et al. 2007) and more vulnerable to shell-crushing predators. Unionid bivalves are preyed upon by birds, fish, a variety of mammals, crayfish, and turtles, and shell thickness and size affect predatory vulnerability (Haag 2012). In general, thinner-shelled unionids (by species or relative growth size) face greater predation threat (Leonard-Pingel and Jackson 2013). Nacre, considered the most fracture-resistant shell layer, can compose a substantive portion of total shell thickness in unionids. For the species we assessed, within the midshell region the nacreous layer comprised at least 71%, and as much as 91%, of the total shell thickness, consistent with previous assessments in *Unio elongatulus* (89% of the shell thickness, Checa 2000). Of the eight species we examined, total shell thickness in *P. sintoxia* and *A. ligamentina* (the thickest-shelled species examined) was four to six times greater than that of *S. undulatus* and *V. iris*, the species with the thinnest shells. Nacre also comprised a greater proportion of total shell thickness in *P. sintoxia*, as compared to all other species assessed. Such differences in shell thickness, and the proportion of the shell composed of fracture-resistant nacre, are likely to lead to variation in shell strength at the whole-shell level.

When considering shell thickness and relative thickness of shell layers, it must be kept in mind that nacre is usually deposited throughout the growing life of a bivalve (Marie et al. 2017). Despite the give-and-take of internal shell deposition and erosion, it is typical for nacre to thicken with age (Mann 2001). The Anodontini and Lampsilini (*Actinonais*, *Lampsilis*, *Ptychobranchus*) tend to be short-lived while the Amblimini (*Villosa*) and Pleurobemi (*Eurynia*, *Pleurobema*) are long-lived (Haag and Rypel 2011). Across the tribes examined here, one of the two species of Pleurobimini had the thickest shells in midregions, while *V. iris* (Amblemini) had the thinnest shells in middle and peripheral regions. Whether the shell thickness of *P. sintoxia* is representative of the longevity of the pleurobiminids will take additional study across more species within the group.

Despite observed differences in thickness at the micrometer scale, these bivalves, with one exception, did not show substantial variation in resistance to shell fracture or micro-

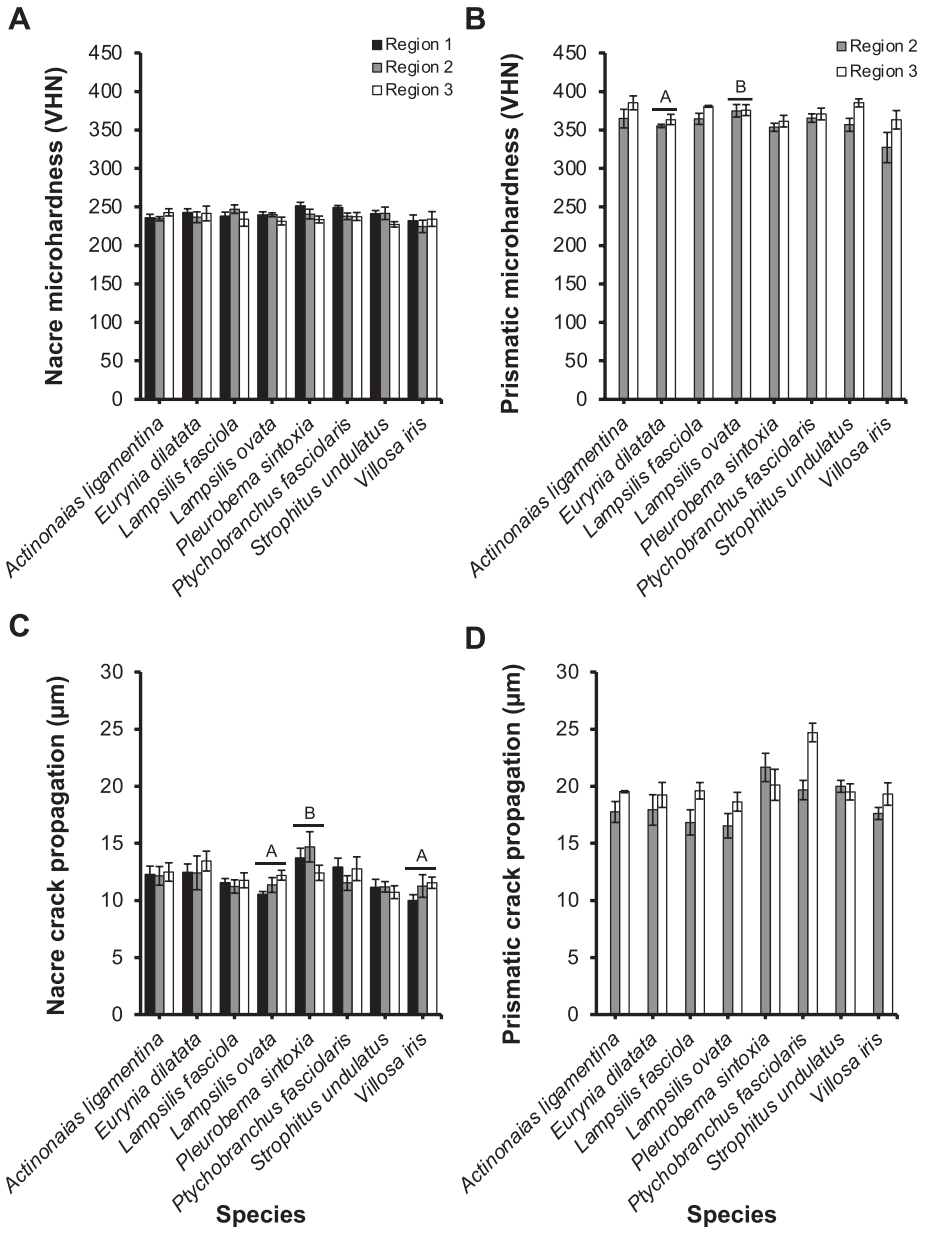

Figure 3. Micromechanical testing metrics (mean ± SE). Vickers microhardness, tested within the (A) nacre and (B) prismatic layers. Lengths of cracks propagating from indentations when tested in the (C) nacre and (D) prismatic layers. Within each panel, species marked with different letters are significantly different from one another using Tukey's method pairwise comparisons ($P < 0.05$). Species that lack a letter did not differ significantly from any of the other species assessed. $n = 5$ replicates per species per shell region.

hardness. Indeed, the thinnest-shelled unionids examined were no more vulnerable to fracture at the micrometer scale than any others we tested. The lack of correlation between nacreous layer thickness and relative fracture sensitivity is not surprising, as fractures take place at a microstructural level with fracture paths along intercrystalline junctures (Song et al. 2018). Under the load tested here, the length of cracks formed during mechanical testing (tens of micrometers) was an order of magnitude lower than nacreous layer thickness (hundreds of micrometers), even in the thinnest-shelled species (Currey 1977; Sun and Bhushan 2012). The exception noted above is *P. sintoxia,* which had the thickest nacre but showed higher crack propagation when compared to *V. iris*. The lower fracture resistance in *P. sintoxia* suggests that the nacre was tolerant of a lower fracture resistance (thus, a small crack would still have significant nacre to penetrate before the shell proper lost its structural stability). The statistical difference seen here also might be considered an outlier; overall, the difference demonstrated was small and does not impact the general trends revealed.

Molluscan shell strength reflects multiple factors, including shell thickness, shell microstructure, organic content ("con-

chiolin"), overall shape, and shell ornamentation (Zuschin and Stanton 2001). Multiple layers of different microstructures composing such shells evolved early in the lineage as demonstrated from Lower Cambrian fossils from China (Feng and Sun 2003). The multiple calcified layers offer some degree of structural plasticity because different layers differ in structural support. Nacre is resistant to fracture (Song et al. 2018), while prisms that align perpendicularly to the shell surface impart greater resistance to abrasion (Sun and Bhushan 2012). The organic interfaces that permeate the junctions between microstructures offer a path for fracture dissipation (Gim et al. 2019), while the dramatic change in structure from prismatic to nacreous structure offers a stoppage juncture. Fracture resistance in nacre reflects "constrained microcracking" (Song et al. 2018). Microcracks essentially form in advance of the primary crack deflection, releasing the local stress concentration, thus enhancing the crack extension resistance. Our data support the enhanced fracture resistance of nacre because the length of cracks produced by indentation was shorter in the nacreous layer than in the prismatic layer, implying greater fracture resistance. Microhardness showed the opposite trend, with substantially greater microhardness in the prismatic layer for all species. Similarly, the external shell layer of the large ranellid gastropod *Charonia lampas lampas* was harder than the inner layer, albeit the inner shell layer is crossed lamellar while the outer layer is prismatic (Boufala et al. 2019). It is not surprising that outer shell layers are harder than inner layers, and given the infaunal habitat of unionid mussels (and most bivalves), greater hardness of the outer (prismatic) layer enhances resistance to abrasion.

The eight unionid species assessed in this study are found typically in flowing waters, often with sand, gravel, and/or rock substratum (references noted here include information for all eight species: Burch 1975; Clarke 1981; Williams et al. 2008). The Hunter Station Bridge site is typical of their usual habitat (medium to large rivers with sand and gravel substratum). While some species of unionids are regularly found associated with specific microhabitats (Strayer 1981), there is no indication that the distribution of mussels in this study and at this site varied spatially. The consistency of habitat requirements across many unionid taxa and the uniformity of shell microhardness and fracture resistance in all mussels tested speaks to a successful and highly conservative evolutionary prismato-nacreous shell lineage. Our results suggest that shell microhardness and resistance to fracture are remarkably similar across these eight species of unionids. It also suggests that our focus, in terms of characteristics to monitor for vulnerability across unionid taxa, should not be on micrometer-scale shell strength or fracture resistance but on relative shell and shell layer (prismatic–nacreous) thicknesses.

While we uncovered a high level of conservativism in shell biomechanics within multiple species of unionids at a single location, our results suggest the need for broader study across a range of habitats to better discern environmentally induced differences in shell characters. We did not test phenotypic plasticity, but the high degree of biomechanical uniformity across these eight members of the Unionidae from two subfamilies (as per Lopes-Lima et al. 2017: Anodontinae, Ableminae) suggests that the prismato-nacreous shell of unionids has successfully supported the long-term survival of a group that dates to the Triassic (Skawina and Dzik 2011).

ACKNOWLEDGMENTS

We gratefully acknowledge the Pennsylvania Department of Transportation for allowing the retention of common mussels from the translocation project. Mussels were sacrificed by E.J.C under scientific collecting permit number 2016-01-0082 from the Pennsylvania Fish and Boat Commission. In addition, we greatly appreciate field assistance provided by Enviroscience, the United States Forest Service, and numerous Western Pennsylvania Conservancy staff members. We thank Natasha Chaudhari for collection of indentation images, and we are grateful to Rebecca Hedreen, Sciences and Distance Learning Librarian at Southern Connecticut State University, for important referencing assistance. This manuscript was improved through the contributions of the journal editors and anonymous reviewers. G.H.D and M.B.C. would like to acknowledge funding from The College of New Jersey's Mentored Undergraduate Summer Experience. M.N.R. was supported by a National Oceanic and Atmospheric Administration research grant to G.H.D. Funding to support this publication was supplied by Southern Connecticut State University.

LITERATURE CITED

Anstis, G. R., P. Chantikul, B. R. Lawn, and D. B. Marshall. 1981. A critical evaluation of indentation techniques for measuring fracture-toughness: 1, Direct crack measurements. Journal of the American Ceramic Society 64:533–538.

ASTM (American Society for Testing and Materials). 2017. ASTM Designation E384-17. Standard Test Method for Microhardness of Materials. American Society for Testing and Materials, West Conshohocken, Pennsylvania.

Bailey, R. C., and R. H. Green. 1988. Within-basin variation in the shell morphology and growth rate of a freshwater mussel. Canadian Journal of Zoology 66:1704–1708.

Baldassarri, M., H. C. Margolis, and E. Beniash. 2008. Compositional determinants of mechanical properties of enamel. Journal of Dental Research 87:645–649.

Boufala, K., S. Ouhenia, G. Louis, D. Betrancourt, D. Chicot, and I. Belabbas. 2019. Microstructure analysis and mechanical properties by instrumented indentation of *Charonia lampas lampas* shell. Journal of Mechanical Behavior of Biomedical Materials 89:114–121.

Brown, C. G., R. Fiorillo, R. Yi, S. Tangirala, and J. Ametepe. 2017. Drying, freezing, and ethanol preservation lower shell strength of two freshwater pulmonate gastropods. Georgia Journal of Science 75: 7. Available at http://digitalcommons.gaacademy.org/gjs/vol75/iss2/7 (accessed January 21, 2022).

Burch, J. B. 1975. Freshwater unionacean clams (Mollusca: Pelecypoda) of North America. Malacological Publications, Hamburg, Michigan.

Checa, A. 2000. A new model for periostracum and shell formation in Unionidae (Bivalvia, Mollusca). Tissue and Cell 32:405–416.

Checa, A.G., and A. Rodriguez-Navarro. 2001. Geometrical and crystallo-

graphic constraints determine the self-organization of shell microstructures in Unionidae (Bivalvia: Mollusca). Proceedings of the Royal Society, London 268:771–778.

Clark, M. S., L. S. Peck, J. Arivalagan, T. Backeljau, S. Berland, J. C. Cardoso, C. Caurcel, G. Chapelle, M. De Noia, S. Dupont, K. Gharbi, J. I. Hoffman, K. S. Last, A. Marie, F. Melzner, K. Michalek, J. Morris, D. M. Power, K. Ramesh, T. Sanders, K. Sillanpää, V. A. Sleight, P. J. Stewart-Sinclair, K. Sundell, L. Telesca, D. L. J. Vendrami, A. Ventura, T. A. Wilding, T. Yarra, and E. M. Harper. 2020. Deciphering mollusc shell production: the roles of genetic mechanisms through to ecology, aquaculture and biomimetics. Biological Reviews 95:1812–1837.

Clarke, A. H. 1981. The Freshwater Molluscs of Canada. National Museum of Natural Sciences, National Museums of Canada, Ottawa.

Currey, J. D. 1977. Mechanical properties of mother of pearl in tension. Proceedings of the Royal Society of London. Series B. Biological Sciences 196:443–463.

Dickinson, G. H., A. V. Ivanina, O. B. Matoo, H. O. Portner, G. Lannig, C. Bock, E. Beniash, and I. M. Sokolova. 2012. Interactive effects of salinity and elevated CO_2 levels on juvenile eastern oysters, *Crassostrea virginica*. Journal of Experimental Biology 215:29–43.

Edelman, A. J., J. Moran, T. J. Garrabrant, and K. C. Vorreiter. 2015. Muskrat predation of native freshwater mussels in Shoal Creek, Alabama. Southeastern Naturalist 14: 473–483.

Feng, W., and W. Sun. 2003. Phosphate replicated and replaced microstructure of molluscan shells from the earliest Cambrian of China. Acta Palaeontologica Polonica 48:21–30.

Fratzl, P., H. S. Gupta, F. D. Fischer, and O. Kolednik. 2007. Hindered crack propagation in materials with periodically varying Young's modulus—Lessons from biological materials. Advanced Materials 19:2657–2661.

Gilbert, P. U. P. A., K. D. Bergmann, C. E. Myers, M. A. Marcus, R. T. Devol, C.-Y. Sun, A. Z. Blonsky, E. Tamre, J. Zhao, E. A. Karan, N. Tamura, S. Lerner, A. J. Giuffre, G. Giribet, J. M. Eiler, and A. H. Knoll. 2017. Nacre tablet thickness records formation temperature in modern and fossil shells. Earth and Planetary Science Letters 460:281–292.

Gim, J., N. Schnitzer, L. M. Otter, Y. Cui, S. Motreuil, F. Marin, S. E. Wolf, D. E. Jacob, A. Misra, and R. Hovden. 2019. Nanoscale deformation mechanics reveal resilience in nacre of *Pinna nobilis* shell. Nature Communications 10:1–8.

Giribet, G., and W. Wheeler. 2002. On bivalve phylogeny: A high-level analysis of the Bivalvia (Mollusca) based on combined morphology and DNA sequence data. Invertebrate Biology 121:271–324.

Graf, D. L., and K. S. Cummings. 2006. Palaeoheterodont diversity (Mollusca: Trigonoida + Unionoida): What we know and what we wish we knew about freshwater mussel evolution. Zoological Journal of the Linnean Society 148:343–394.

Haag, W. R. 2012. North American Freshwater Mussels. Cambridge University Press, New York.

Haag, W. R., and A. L. Rypel. 2011. Growth and longevity in freshwater mussels: Evolutionary and conservation implications. Biological Reviews 86:225–247.

Hornbach, D. J., V. J. Kurth, and M. C. Hove. 2010. Variation in freshwater mussel shell sculpture and shape along a river gradient. American Midland Naturalist 164:22–36.

Kesler, D. H., and R. C. Bailey. 1993. Density and ecomorphology of a freshwater mussel (*Elliptio complanata*, Bivalvia: Unionidae) in a Rhode Island Lake. Journal of the North American Benthological Association 12:259–264.

Kim, Y.-Y., J. D. Carloni, B. Demarchi, D. Sparks, D. G. Reid, M. E. Kunitake, C. C. Tang, M. J. Duer, C. L. Freeman, and B. Pokroy. 2016. Tuning hardness in calcite by incorporation of amino acids. Nature Materials 15:903.

Kishida, K., and T. Sasaki. 2018. Geographical and seasonal variations of the shell microstructures in the bivalve *Scapharca broughtonii*. Pages 177–186 *in* K. Endo, T. Kogure, and H. Nagasawa, editors. Biomineralization: From Molecular and Non-Structural Analyses to Environmental Science. Springer, Singapore.

Konietschke, F., M. Placzek, F. Schaarschmidt, and L. A. Hothorn. 2015. nparcomp: An R software package for nonparametric multiple comparisons and simultaneous confidence intervals. Journal of Statistical Software 64:1–17.

Leonard-Pingel, J. S., and J. B. C. Jackson. 2013. Drilling intensity among Neogene tropical Bivalvia in relation to shell forms and life habit. Bulletin of Marine Science 89:905–919.

Leung, H. M., and S. K. Sinha. 2009. Scratch and indentation tests on seashells. Tribology International 42:40–49.

Lopes-Lima, M., E. Froufe, V. T. Do, M. Ghamizi, K. E. Mock, U. Kebapci, O. Klishko, S. Kovitvadhi, U. Kovitvadhi, O. S. Paul, J. M. Pfeiffer 3rd, M. Raley, N. Riccardi, H. Sereflisan, R. Sousa, A. Teixeira, S. Varandas, X. P. Wu, D. T. Zanatta, A. Zieritz, and A. E. Bogan. 2017. Phylogeny of the most species-rich freshwater bivalve family (Bivalvia: Unionida: Unionidae): Defining modern subfamilies and tribes. Molecular Phylogeny and Evolution 106:174–191.

Mann, S. 2001. Biomineralization: Principles and Concepts in Bioinorganic Materials Chemistry. Oxford University Press, New York.

Marie, B., J. Arivalagna, L. Marthéron, G. Bolbach, S. Berland, A. Marie, and F. Marin. 2017. Deep conservation of bivalve nacre proteins highlighted by shell matrix proteomics of the Unionoida *Elliptio complanata* and *Villosa lienosa*. Journal of the Royal Society Interface 14:20160846.

Marin, F., G. Luquet, B. Marie, and D. Medakovic. 2008. Molluscan shell proteins: primary structure, origin, and evolution. Current Topics in Developmental Biology 80: 209–276.

Meyers, M. A., and P. Chen. 2014. Biological Materials Science: Biological Materials, Bioinspired Materials, and Biomaterials. Cambridge University Press, Cambridge. United Kingdom.

Nardone, J. A., S. Patel, K. R. Siegel, D. Tedesco, C. G. McNicholl, J. O'Malley, J. Herrick, R. A. Metzler, B. Orihuela, D. Rittschof, and G. H. Dickinson. 2018. Assessing the impacts of ocean acidification on adhesion and shell formation in the barnacle *Amphibalanus amphitrite*. Frontiers in Marine Science 5:369.

Newell, A. J., D. J. Gower, M. J. Benton, and V. P. Tverdokhlebov. 2007. Bedload abrasion and the *in-situ* fragmentation of bivalve shells. Sedimentology 54:835–845.

Ott, L. O., and M. Longnecker. 2010. An Introduction to Statistical Methods and Data Analysis. Brooks/Cole, Cengage Learning, Belmont, California.

Pohlert, T. 2014. The Pairwise multiple comparison of mean ranks package (PMCMR). R package. Available at http://CRAN.R-project.org/package=PMCMR (accessed January 21, 2022).

Prezant, R. S., A. Tan Tiu, and K. Chalermwat. 1988. Shell microstructure and color changes in stressed *Corbicula fluminea* (Bivalvia: Corbiculidae). The Veliger 31:236–243.

R Core Team. 2013. R: A language and environment for statistical computing. R Foundation for Statistical Computing, Vienna, Austria. Available at http://www.R-project.org/ (accessed January 21, 2022).

Skawina, A., and J. Dzik. 2011. Umbonal musculature and relationships of the Late Triassic filibranch unionid bivalves. Zoological Journal of the Linnaean Society 163:863–883.

Song, J., Fan, C., H. Ma, L. Liang, and Y. Wei. 2018. Crack deflection occurs by constrained microcracking in nacre. Acta Mechanica Sinica 34:143–150.

Strayer, D. 1981. Notes on the microhabitats of Unionid mussels in some Michigan streams. American Midland Naturalist 106:411–415.

Sun, J., and B. Bhushan. 2012. Hierarchical structure and mechanical properties of nacre: A review. RSC Advances 2:7617–7632.

Tan Tiu, A., and R. S. Prezant. 1987. Shell microstructural responses of *Geukensia demissa granosissima* (Mollusca, Bivalvia) to continual submergence. American Malacological Bulletin 5:173–176.

Tan Tiu, A., and R. S. Prezant. 1989. Temporal variation in microstructure of the inner shell surface of *Corbicula fluminea* (Bivalvia: Heterodonta). American Malacological Bulletin 7:65–71.

Tan Tiu, A., and R. S. Prezant. 1992. The role of environment in shell growth dynamics of the Asian clam *Corbicula fluminea* (Mollusca: Bivalvia). Malacological Review 25:109–117.

Tyrrell, M., and D. J. Hornbach. 1998. Selective predation by muskrats on freshwater mussels in 2 Minnesota rivers. Journal of the North American Benthological Society 17:301–310.

Watson, S. A., L. S. Peck, P. A. Tyler, P. C. Southgate, K. S. Tan, R. W. Day, and S. A. Morley. 2012. Marine invertebrate skeleton size varies with latitude, temperature and carbonate saturation: implications for global change and ocean acidification. Global Change Biology 18:3026–3038.

Williams, J. D., A. E. Bogan, and J. T. Garner. 2008. Freshwater mussels of Alabama and the Mobile Basin in Georgia, Mississippi and Tennessee. University of Alabama Press, Tuscaloosa.

Zhang, Z., J. Zhu, Y. Chu, Z. Chen, S. Guo, and J. Xu. 2019. Correlation between microstructure and failure mechanism of *Hyriopsis cumingii* shell structure. Journal of Bionic Engineering 16:869–881.

Zieritz, A., J. I. Hoffman, W. Amos, and D. C. Aldridge. 2010. Phenotypic plasticity and genetic isolation-by-distance in the freshwater mussel *Unio pictorum* (Mollusca: Unionoida). Evolutionary Ecology 24:923–938.

Zuschin, M., and R. J. Stanton. 2001. Experimental measurement of shell strength and its taphonomic interpretation. Palaios 16:161–170.

Freshwater Mollusk Biology and Conservation 25:37–53, 2022

DOI:10.31931/fmbc-d-21-00007

REGULAR ARTICLE

UTILITY OF SHELL-VALVE OUTLINES FOR DISTINGUISHING AMONG FOUR LAMPSILINE MUSSEL SPECIES (BIVALVIA: UNIONIDAE) IN THE GREAT LAKES REGION

Madison R. Layer[1], Russell L. Minton[2], Todd J. Morris[3], and David T. Zanatta[1,4]*

[1] *Department of Biology, Central Michigan University, Mount Pleasant, MI 48859 USA*
[2] *Department of Biology, Gannon University, Erie, PA 16541 USA*
[3] *Fisheries and Oceans Canada, Great Lakes Laboratory for Fisheries and Aquatic Sciences, Burlington, ON L7S 1A1 Canada*
[4] *Institute for Great Lakes Research, Central Michigan University, Mount Pleasant, MI 48859 USA*

ABSTRACT

Four freshwater mussel species from the tribe Lampsilini found in the Laurentian Great Lakes region—*Lampsilis fasciola* (Wavy-rayed Lampmussel), *Lampsilis cardium* (Plain Pocketbook), *Ortmanniana ligamentina* (Mucket), and *Lampsilis siliquoidea* (Fatmucket)—have similar and variable shell morphologies that make some specimens difficult to identify in the field. Identification is further confounded by sexual dimorphism in three of the four species. We used landmark-based morphometric analyses of shell shape in conjunction with DNA barcoding to quantify shell-shape differences between the species. We collected specimens ($N = 388$) from Great Lakes tributaries in Michigan, USA, and Ontario, Canada. We photographed each specimen and made an initial identification in the field. We then took a tissue biopsy or swab from 248 of the specimens, sequenced a fragment of the mitochondrial cytochrome c oxidase subunit 1 (COI) gene, and confirmed identifications by comparing our sequences with sequences for all four species accessioned in GenBank. On the photographs, we digitized 21 two-dimensional landmarks along the shell margin and used multivariate methods to evaluate the correspondence of shell shape to our COI-confirmed species identifications and sex determinations. Principal-components analysis and linear-discriminant analysis of shell shape correctly identified only 77.8% of specimens to species and 72.2% to species and sex. Sex determination was particularly confounded by the similar shapes of female *L. fasciola* and female *L. cardium* specimens. This study demonstrates the limitations of using only two-dimensional valve shape in differentiating among some mussel species.

KEY WORDS: geometric morphometrics, DNA barcoding, species at risk

INTRODUCTION

Early classifications of freshwater mussel species in North America were often based almost solely on descriptions of shell morphology (Haag 2012). Even today, species are usually identified by shell characteristics. However, these identifications can be inaccurate due to wide intraspecific variation in shell characters. Genetic and morphometric techniques can improve the ability to differentiate among mussel species with similar and overlapping shell characteristics (Beauchamp et al. 2020; Beyett et al. 2020; Willsie et al. 2020).

In the Laurentian Great Lakes region, four lampsiline mussel species can be difficult to differentiate based on external shell features: *Lampsilis fasciola* (Rafinesque 1820), Wavy-rayed Lampmussel; *Lampsilis cardium* (Rafinesque 1820), Plain Pocketbook; *Ortmanniana ligamentina* (Lamarck

*Corresponding Author: zanat1d@cmich.edu

Table 1. Site locations of *Lampsilis fasciola*, *Lampsilis cardium*, *Ortmanniana ligamentina*, and *Lampsilis siliquoidea* and the number of field-identified and cytochrome c oxidase subunit 1 (COI)–confirmed specimens. Numbers represent the total number collected from the site, and, in parentheses, the number of specimens that had COI sequences generated.

			L. fasciola		*L. cardium*		*O. ligamentina*	*L. siliquoidea*	
Site (River)	Latitude	Longitude	Female	Male	Female	Male	—	Female	Male
Maitland River, Ontario	43.7719	−81.3092	—*	—*	22 (22)	—*	—*	37 (35)	—*
Belle River, Michigan	42.7745	−82.5510	—*	—*	—*	—*	—*	2 (2)	4 (4)
EBWF St. Joseph River, Michigan	41.7814	−84.6507	—*	—*	1 (0)	—*	—*	1 (1)	4 (4)
Salt River, Michigan	43.7053	−84.4878	—	—	3 (3)	—*	2 (2)	1 (1)	1 (1)
River Raisin, Michigan	42.1767	−84.0922	19 (19)	22 (22)	27 (20)	55 (20)	—*	—*	—*
Grand River, Michigan	42.9855	−84.9455	—	—	26 (18)	14 (13)	6 (6)	—*	—*
Chippewa River, Michigan	43.6045	−84.2906	—	—	—*	—*	80 (20)	—*	—*
Maple River at Elsie, Michigan	43.0902	−84.4053	—	—	1 (0)	5 (0)	1 (0)	13 (13)	40 (20)
Maple River at Maple Rapids, Michigan	43.1089	−84.6940	—	—	—*	—*	—*	2 (2)	—*

*Present in the river, but not found or collected at the sites.

1819) (= *Actinonaias ligamentina*), Mucket; and *Lampsilis siliquoidea* (Barnes 1823), Fatmucket. At sites where these species co-occur, identification can be challenging even for experts (Cummings and Mayer 1992). In the three *Lampsilis* species, identification is further confounded by sexual dimorphism (Watters et al. 2009; Mulcrone and Rathbun 2018). Sex determination based on shell characters also can have a high degree of error (Hess et al. 2018).

Accurate species and sex determination is important for many reasons. For example, *Lampsilis fasciola* is a species of special concern in Canada (COSEWIC 2010) and is threatened in Ontario and Michigan (OMNRF 2021; MNFI 2020). Confusion between *L. fasciola* and more common lampsiline species could result in an inaccurate assessment of its status. If the more common *L. cardium*, *O. ligamentina*, and *L. siliquoidea* are misidentified as *L. fasciola*, the latter species' distribution and abundance may be overestimated, resulting in a potential loss of protection needed to ensure its persistence. Lampsiline species are often used for laboratory studies including studies on the impacts of invasive species and toxicological studies (e.g., Wang et al. 2011; Gilroy et al. 2014; Larson et al. 2016; Waller and Bartsch 2018; Gillis et al. 2021). Improper identification of test organisms may lead to misinterpretations of laboratory results and can lead to improper management recommendations (Shea et al. 2011).

DNA barcoding (Hebert et al. 2003) has become an important tool for species identification. Partial mitochondrial cytochrome c oxidase subunit 1 (COI) gene sequences are frequently used as diagnostic barcode markers for many unionid species (e.g., Inoue et al. 2013, 2014; Beauchamp et al. 2020; Beyett et al. 2020; Willsie et al. 2020). The large and growing number of unionid COI sequences accessioned in GenBank serve as references to improve identifications.

Geometric morphometric analysis also can be a useful tool for species identification. Landmark-based analyses allow for quantification of mollusk shell shape while removing the effects of size, position, and rotation. The resulting shape data can be analyzed using traditional multivariate statistics to detect differences among individuals or a priori groups (Webster and Sheets 2010). Recent studies combining DNA barcoding and geometric morphometric analysis have been used to distinguish between morphologically similar species (Beauchamp et al. 2020; Beyett et al. 2020; Willsie et al. 2020).

We tested the utility of geometric morphometric analyses of shell shape in conjunction with DNA barcoding to differentiate between *L. fasciola*, *L. cardium*, *O. ligamentina*, and *L. siliqouidea*. Our specific objectives were (1) to assess whether two-dimensional geometric morphometric techniques can differentiate accurately among species and sexes, and, if so, (2) to establish diagnostic and quantifiable morphological characters for distinguishing among species and sexes.

METHODS

Field Collections

We collected 388 specimens of the four target species from eight rivers in Ontario and Michigan (Table 1). As we were seeking only to differentiate among species and sexes, we did not investigate intraspecific variation within and among source populations (i.e., environmental influences of shape variation), although this could be an interesting avenue for further study. We attempted to collect a minimum of 20 individuals of each species and sex (for dimorphic species) at each site, but this was not always possible. Field identifications and sex determinations were made by the field team upon collection. Mussel identification experience of field team members ranged from novice (<1 yr of experience), to intermediate (2 to 10 yr), to advanced (>10 yr). Species identifications in the field were made based on shell morphology, beak structure, and shell coloration using a consensus approach. Sex determination was made based on the degree of shell inflation and expansion of the posterior portion of the shell; more inflated or expanded shells are characteristic of females. We photographed the left valve of

each specimen. Photographs were later reviewed by the authors with advanced identification experience, and some field identifications or sex determinations were revised based on those reviews prior to analyses. We took mantle tissue biopsies (Berg et al. 1995) from a subset of individuals for each species except for *L. fasciola*; because of its protected status, we took less invasive swab samples from the foot and visceral mass (Henley et al. 2006). We obtained usable COI sequences from a total of 248 specimens. We preserved tissue biopsies in 95% ethanol and swabs were preserved in a lysis buffer (Sambrook et al. 1989). We measured shell length, width, height, and hinge length of every specimen using Vernier calipers (Appendix 1). After processing, all specimens were returned to the river alive.

DNA Barcoding

A Qiagen Blood and Tissue kit (Qiagen, Inc., Germantown, MD, USA) was used to extract DNA from the tissue and swab samples collected in the field. Extraction success and relative quality of genomic data were assessed by electrophoresing 2-μL amplicons of the extracted DNA on a 1.5% agarose gel. Polymerase chain reaction was used to amplify a 600-bp COI fragment using primers and amplification conditions described in Campbell et al. (2008). Amplification success and relative quality were assessed by electrophoresing 2 μL of amplicons (stained with SYBR green) on a 1.5% agarose gel. Amplicons were purified using exonuclease I and shrimp alkaline phosphates (EXOSAP). The EXOSAP solution was made using 78 μL double distilled H_2O, 2 μL exonuclease I, and 20 μL shrimp alkaline phosphates. To denature any remaining primers and enzymes, 1.5 μL of EXOSAP solution was added to each sample, which were then incubated at 37°C for 40 min and 80°C for 20 min. Once purified, amplicons were shipped to Eton Biosciences (San Diego, CA, USA) for Sanger sequencing. Generated sequences were compared to COI sequences for all four species in the GenBank database using BLAST (http://blast.ncbi.nlm.nih.gov/Blast.cgi; accessed November 20, 2020). The BLAST result with the highest percentage of identity was chosen as the most likely species and used as the confirmed identification for the sample.

Geometric Morphometrics

We digitized shell photographs of all 388 individuals using the MakeFan application in IMP8 (Sheets 2014). We placed homologous (Type I) anchor landmarks at the peak of the umbo and the posterior edge of the hinge ligament. We established a 40-ray fan anchored at the midpoint between landmarks 1 and 2; 19 additional (Type II) landmarks were located at equidistant points where fan rays intersected the shell margin (Fig. 1). Photographs of the left valves are available on MorphoBank (https://morphobank.org, Project Code 3918, accession nos. M738948–M739052).

Data Analysis

We obtained shape variables from our landmark configurations of COI-confirmed individuals using a generalized Procrustes analysis (Rohlf and Slice 1990). We performed two Procrustes analyses of variance (ANOVAs) (Goodall 1991) in the R package *geomorph* 4.0 (Adams et al. 2021): one to test for significant shape differences between the four species and the second to test for significant shape differences using species identity, sex, and the interaction between species and sex. Our sum-of-squared Procrustes distances were used as the measure of sum-of-squares (SS), with the observed SS evaluated through residual randomization permutation (Collyer and Adams 2018, 2021). Additionally, *geomorph* uses *z*-score centering and log-transformation to ensure that statistics are normally distributed. We determined significance at $\alpha = 0.05$.

We performed a principal components analysis (PCA) on the Procrustes-transformed landmark dataset. A broken-stick model was used to determine the number of dimensions to retain for further analyses (Jackson 1993). We subsequently used PCA–linear discriminant analysis (LDA) and Bayesian clustering to test the utility of shell shape in identifying specimens to species and sex. In a PCA-LDA, the dimensionality of the data is reduced through an initial PCA to preserve variance, remove collinearity, and reduce overfitting in the subsequent LDA of the components (Quinn and Keough 2002). We used PAST 4 (Hammer et al. 2001) to generate principal components from our Procrustes shape variables. We then performed an LDA in PAST on the components using the COI-confirmed species identities and used the jackknifed confusion matrix to compare COI identifications with those predicted by shape. We repeated the LDA using the COI identities by sex as groups and used the jackknifed confusion matrix to assess successful discrimination.

For Bayesian model-based clustering independent of a priori classification, we used the R package mclust 5.4.5 (Scrucca et al. 2016). We generated Bayesian information criteria (BIC) values for competing clustering models and chose the model with the highest BIC score (mclust reports BIC multiplied by −1). We created a model with four clusters (representing the four species) and a model with seven clusters (species and sex where applicable). We assessed the method by calculating classification errors as the percentage of incorrect group assignment relative to the COI species identification. We also calculated incorrect group assignment relative to the COI identities by sex.

RESULTS AND DISCUSSION

BLAST analysis identified 41 *L. fasciola*, 96 *L. cardium*, 28 *O. ligamentina*, and 83 *L. siliquoidea* (Appendix 1). We recovered 16 unique haplotypes from the 248 COI sequences generated: two *L. fasciola* (GenBank accession nos. MW753043–MW753044), eight *L. cardium* (GenBank accession nos. MW752863–MW752870, one *O. ligamentina* (GenBank accession no. MW752989), and five *L. siliquoidea*

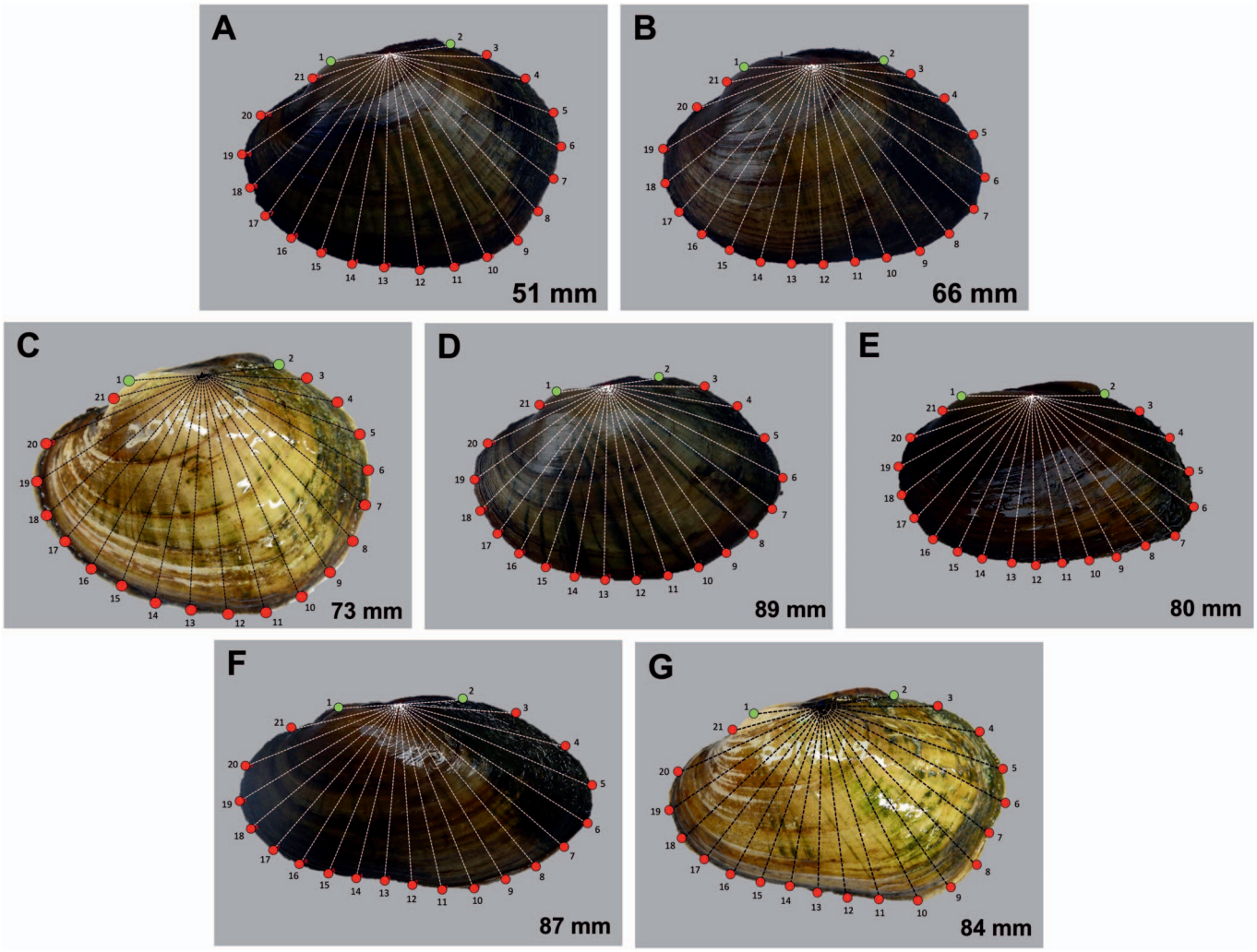

Figure 1. Examples of a fan and 21 landmarks superimposed on the left valve using the MakeFan application in IMP8 software. Type I landmarks are represented by the green points. Type II landmarks along the edge of the shell are represented by the red points. Shell specimens are (A) female and (B) male *Lampsilis fasciola*, (C) female and (D) male *Lampsilis cardium*, (E) *Ortmanniana ligamentina*, and (F) male and (G) female *Lampsilis siliquoidea*.

(GenBank accession nos. MW752895–MW752899). Overall, field identifications were 92.3% accurate when compared to the COI identifications. The most frequently misidentified specimens in the field were *L. cardium* and *L. siliquoidea* from the Maitland River, Ontario, with 73.6% correct identification; six *L. cardium* were mistaken for *L. siliquoidea* and nine *L. siliquoidea* were mistaken for *L. cardium*. A possible reason for the misidentification of these two species in the Maitland River is that there were instances when the shape of the shell or mantle lure morphology indicated one species (i.e., inflation and truncation of the shell and lure type typical of *L. cardium*), but the beak sculpture indicated another (i.e., 6–12 bars typical of *L. siliquoidea*, as opposed to 4–5 elevated ridges for *L. cardium*; Mulcrone and Rathbun 2018).

Procrustes ANOVA based on the transformed shape variables revealed significant differences in shape among the COI-confirmed species ($F = 8.569$, $P < 0.001$). ANOVA using both COI-confirmed species and field- and photo-assigned sex also showed significant differences between species and sexes ($F_{1,2} = 1.824$, $P = 0.027$). Pairwise post-hoc residual randomization permutation procedures (RRPP; 1,000 permutations) tests revealed significant differences between these six (of 42) pairs: male *L. cardium* and male *L. siliquoidea* ($P = 0.037$), male *L. cardium* and male *L. fasciola* ($P = 0.016$), male *L. cardium* and male *L. siliquoidea* ($P = 0.001$), male *L. fasciola* and male *L. siliquoidea* ($P = 0.001$), female and male *L. siliquoidea* ($P = 0.001$), and male *L. siliquoidea* and *O. ligamentina* ($P = 0.034$).

The first two principal components explained 90.5% of the total variation in valve shape (Fig. 2). However, there was considerable overlap among females of all *Lampsilis* species and between male *L. cardium* and male *L. fasciola*. Male *L. siliquoidea* and *O. ligamentina* had limited overlap, corresponding to the results of the ANOVA.

The PCA-LDA had 77.8% mean accuracy (73.1% to 83.1%) in assigning specimens to the correct species (Table 2)

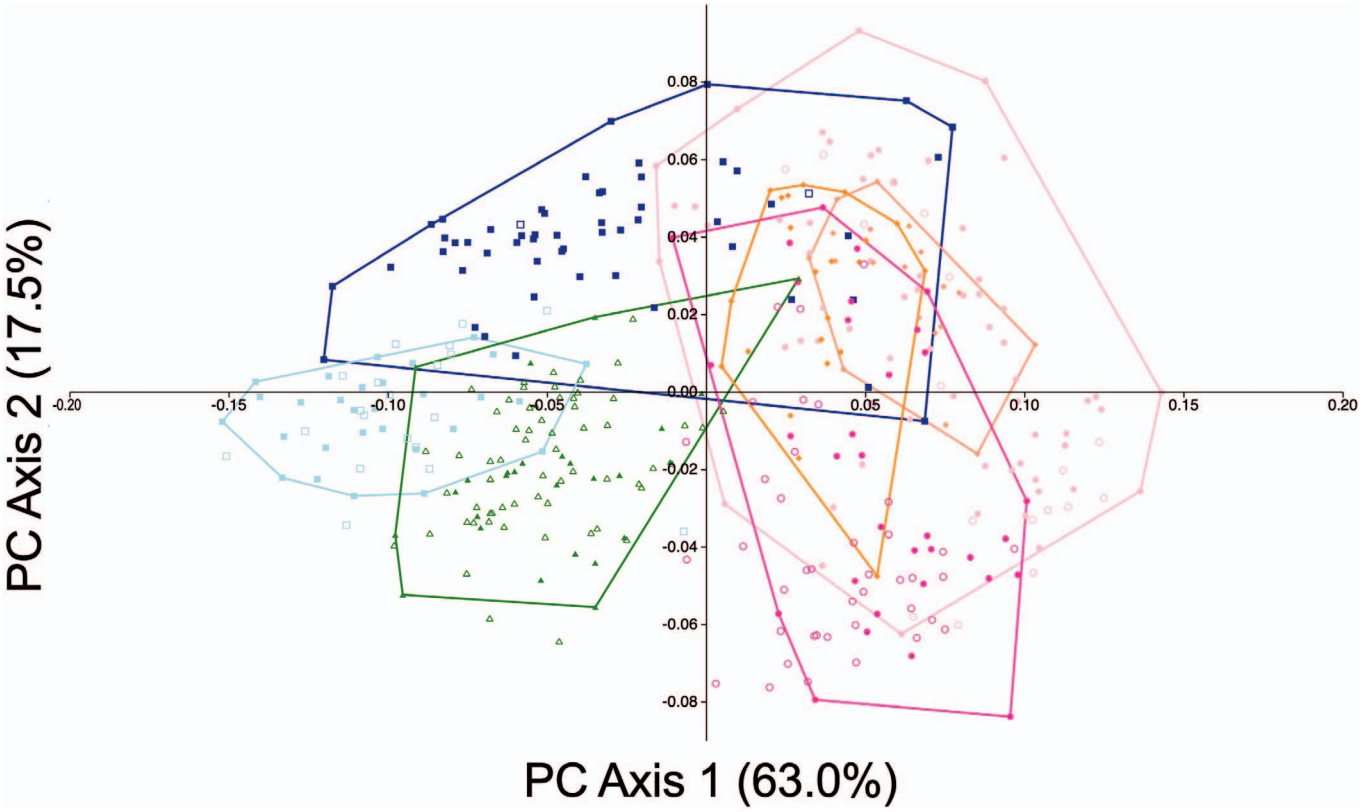

Figure 2. Principal component analysis (PCA) of 21 Procrustes-transformed landmark points from female (squares) and male (circles) *Lampsilis fasciola* (orange/salmon), *Lampsilis cardium* (pink shades), *Lampsilis siliquoidea* (blue shades), and *Ortmanniana ligamentina* (green). Filled symbols represent specimens with cytochrome c oxidase subunit 1–confirmed identifications. Open symbols represent specimens that only have morphological data and were assigned to a group using the PCA–linear discriminant analysis model. Numbers in parentheses on each axis indicate the percentage of variation explained.

and 72.1% (57.1% to 93.1%) mean accuracy in assigning specimens to the correct species and sex (Table 3). The species with the highest accuracy in the PCA-LDA model was *L. siliquoidea* (83.1%), but all four species were generally similar. Groups with the highest accuracy in the PCA-LDA model were male *L. siliquoidea* (93.1%) and *O. ligamentina* (82.1%) (Table 3). Groups with the lowest accuracy were female *L. cardium* (57.1%) and female *L. fasciola* (68.4%), each of which was usually misidentified as the other species. Female *L. cardium* were misidentified as female *L. fasciola* 19.0% of the time, and female *L. fasciola* were misidentified as female *L. cardium* 21.0% of the time. Similar to the field identifications, the Maitland River samples had the highest error rates for the LDA model: 20 out of 57 (35.1%) Maitland specimens of *L. cardium* and *L. siliquoidea* were misidentified by shell morphometrics. Thirteen out of these 20 specimens were a result of misidentifying *L. cardium* as *L. siliquoidea*. Of the remaining 122 genetically confirmed *L. cardium* and *L. siliquoidea* specimens (from all rivers), only three *L. siliquoidea* and 14 *L. cardium* (13.9%) were misidentified in

Table 2. Jackknifed confusion matrix of the four lampsiline species to the assignments based on results of the linear discriminant analysis of the principal components of 21 Procrustes-transformed landmark points. Darkened cells represent specimens that were correctly assigned by the linear discriminant analysis (LDA).

	LDA Assignment					
Genetic Assignment	***L. cardium***	***L. siliquoidea***	***O. ligamentina***	***L. fasciola***	**Total**	**% Correct**
L. cardium	73	5	4	14	96	76.0
L. siliquoidea	9	69	3	2	83	83.1
O. ligamentina	1	2	21	4	28	75.0
L. fasciola	10	0	1	30	41	73.1
Total	93	76	29	50	248	

Table 3. Jackknifed confusion matrix of the four lampsiline species and sexes to the assignments based on results of the linear discriminant analysis of the principal components of 21 Procrustes-transformed landmark points. Darkened cells represent specimens that were correctly assigned by the linear discriminant analysis (LDA).

	LDA Assignment								
	L. fasciola		*L. cardium*		*O. ligamentina*	*L. siliquoidea*			
Genetic Assignment	**Female**	**Male**	**Female**	**Male**	**–**	**Male**	**Female**	**Total**	**% Correct**
L. fasciola Female	13	2	4	0	0	0	0	19	68.4
L. fasciola Male	3	17	0	2	0	0	0	22	77.3
L. cardium Female	12	2	36	6	2	0	5	63	57.1
L. cardium Male	3	4	2	24	0	0	0	33	72.7
O. ligamentina	0	2	0	2	23	1	0	28	82.1
L. siliquoidea Male	0	0	0	0	2	27	0	29	93.1
L. siliquoidea Female	1	0	10	0	1	3	39	54	72.2
Total	34	27	34	34	28	31	44	248	

the morphometric model. Most of these misidentifications were *L. cardium* being mistaken for *L. fasciola* (10 of 17). A possible reason for lower accuracy in the LDA model compared to field identification accuracy is that the model only accounts for the two-dimensional shape of the specimen. Other characters, such as color, ray pattern, beak sculpture, overall size and three-dimensional attributes (e.g., shell inflation), are important characters that are also taken into consideration when making field identifications (Mulcrone and Rathbun 2018).

For the three species with distinct sexual dimorphism, males of each species were more accurately assigned by LDA to the correct species and sex than females (Table 3). Overall, 81.0% of males were assigned correctly in the LDA model compared to only 64.7% of females. The greater similarity of females across species could result from convergence of female shape necessary to accommodate the greatly swollen

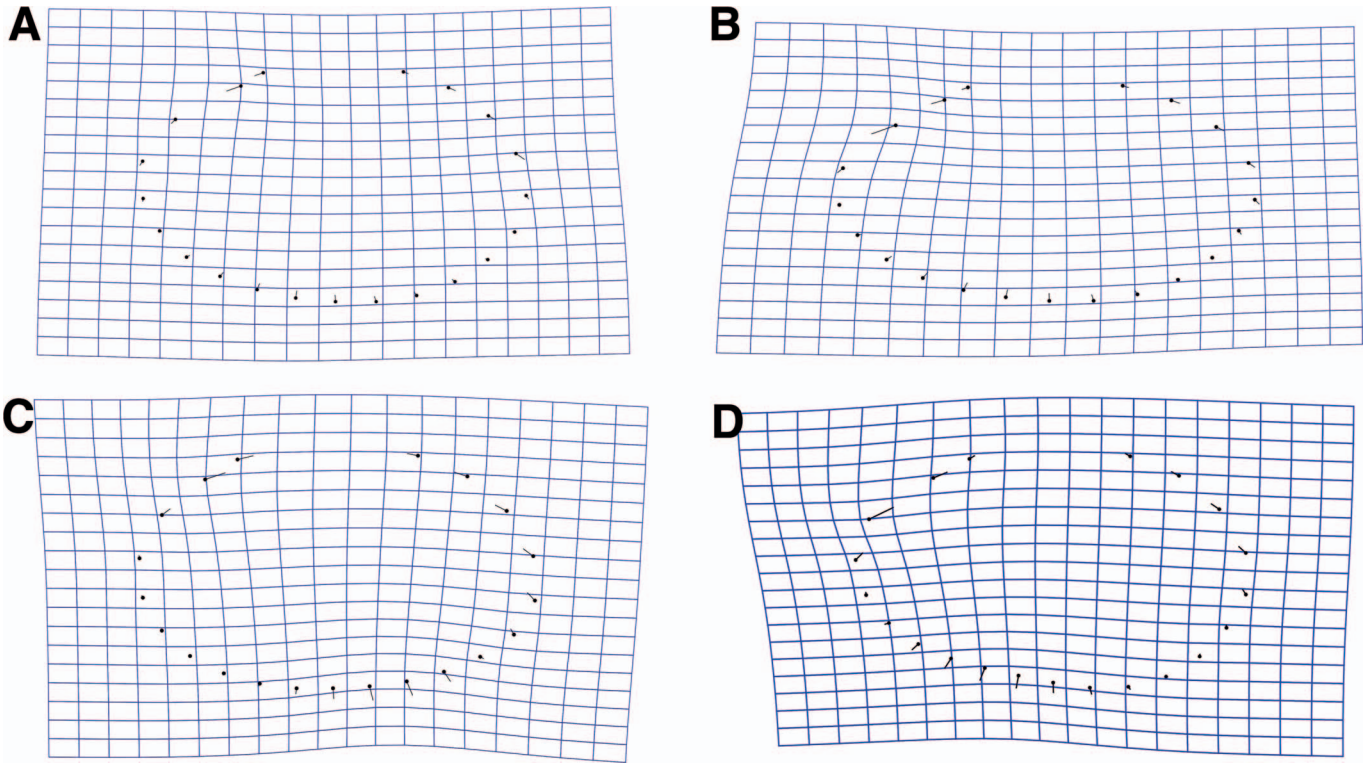

Figure 3. Deformation grids of two-dimensional shell shape showing difference between the combined mean shape of all specimens and the mean shape of: (A) *Lampsilis fasciola*, (B) *Lampsilis cardium*, (C) *Ortmanniana ligamentina*, and (D) *Lampsilis siliquoidea*.

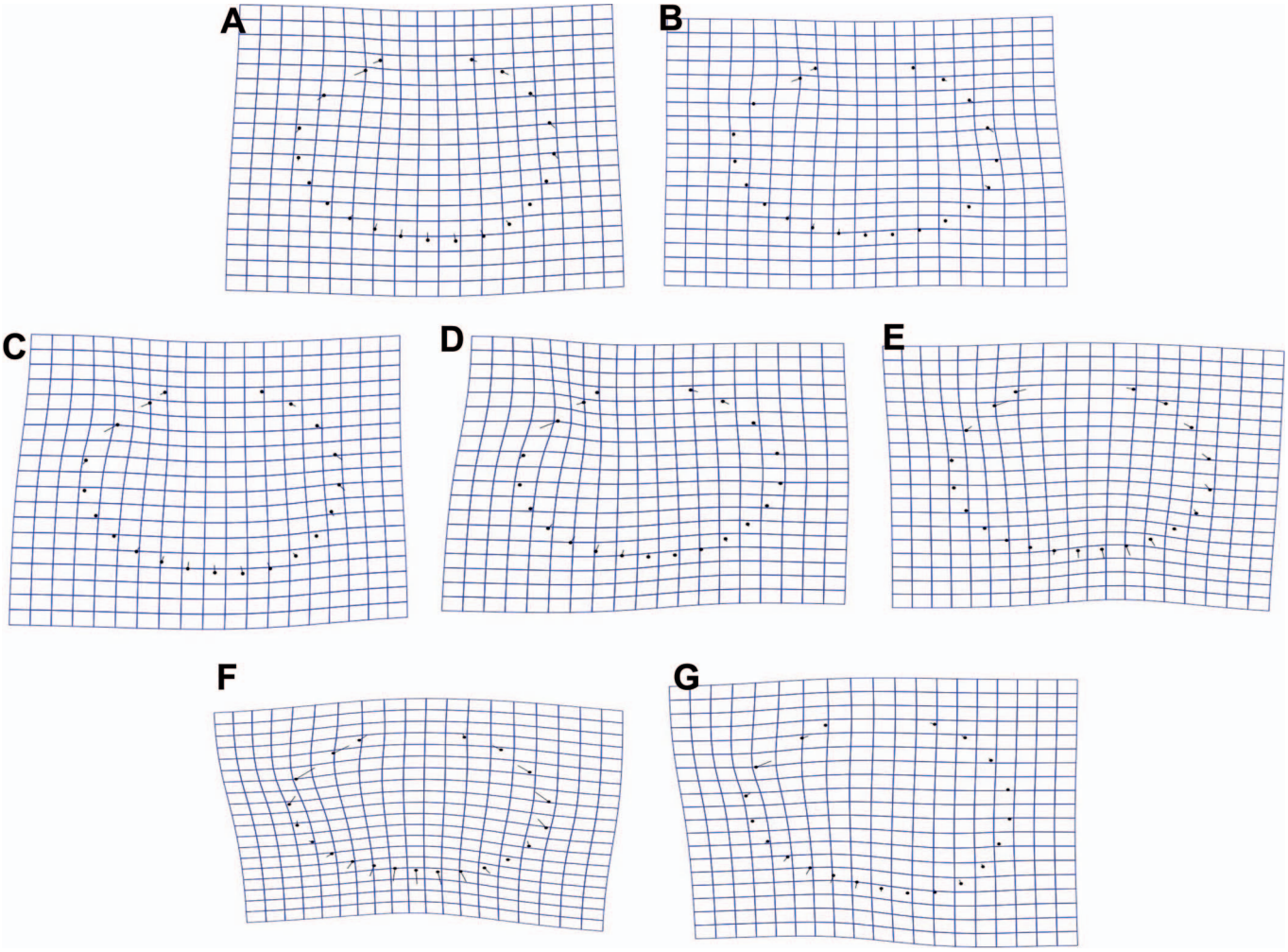

Figure 4. Deformation grids of two-dimensional shell shape showing difference between the combined mean shape of all specimens and the mean shape of: (A) female and (B) male *Lampsilis fasciola*, (C) female and (D) male *Lampsilis cardium*, (E) *Ortmanniana ligamentina*, and (F) male and (G) female *Lampsilis siliquoidea*.

gills of gravid females (Haag 2012, Zieritz and Aldridge 2011, Hewitt et al. 2021).

Using Bayesian clustering, a four-cluster model (model = VEI, BIC = 2,807.75, log-likelihood = 1,461.72) and a seven-cluster model (model = EII, BIC = 2,785.30, log-likelihood = 1,469.78) were created and assessed to determine how they performed in assigning specimens to groups based on their Procrustes valve shapes. The arbitrary groups created by Bayesian clustering were agnostic to the four COI-confirmed species groups and seven COI-confirmed species + sex groups, but performed similarly (79.0% for four groups, 77.8% for seven groups) to the PCA-LDA assignments. The agnostic Bayesian groupings performed similarly to the confirmed groupings, suggesting that patterns of intra- and interspecific variation in the four lampsilines are not necessarily as diagnostic as previously thought and thus require additional characters for species diagnosis (e.g., Mulcrone and Rathbun 2018 and other field identification guides).

The thin-plate splines show that the generalized mean shape across sexes of *L. fasciola* and *L. cardium* is more rounded, whereas the mean shape of *L. siliquoidea* and *O. ligamentina* is more elongate (Fig. 3). Thin-plate splines also show the truncated and rounded posterior end characteristic of females of the three species with distinct sexual dimorphism (Fig. 4A, C, and G). These shape characteristics match descriptions of the species found in field guides (e.g., Mulcrone and Rathbun 2018).

In contrast to other studies that showed the utility of landmark-based morphometric analysis for species identification (Inoue et al. 2014; Beauchamp et al. 2020; Beyett et al. 2020; Willsie et al. 2020), our results show that this method is of limited utility for these four lampsiline species. Landmark-based morphometric analysis could help improve field identifications of *O. ligamentina* and *L. siliquoidea* because it was somewhat useful for differentiating these two species from the other two species we studied. However, the high degree of overlap in shell shape among other species, particularly female *L. siliquoidea* and female *L. cardium*,

limits the utility of morphometric traits for identification. Improvements to the model could be made by incorporating an assessment of shell variation among different watersheds. Local variation in water chemistry, hydrology, and other factors can influence shell shape, and two distinct shell morphologies of *L. fasciola* have been described (Watters et al. 2009).

Using two-dimensional landmarks to assess variation in valve shape to differentiate among four species of lampsiline mussels examined in this study has limited utility. Differentiating among more than two species and species with sexual dimorphism was problematic and had error rates between 20% and 30%. In addition to two-dimensional valve shape, we recommend exploring methods for including three-dimensional landmarks that reflect shell inflation. A DNA barcoding–calibrated morphometric key also could be used to examine differences among the closely related species *L. cardium*, *Lampsilis ovata* (Say 1817), *Lampsilis cariosa* (Say 1817), and *Lampsilis ornata* (Conrad 1835), including potential hybrids of *L. cardium* and *L. ovata* (Hewitt et al. 2019) and *L. siliquoidea* and *Lampsilis radiata* (Rafinesque 1820) (supposedly restricted to the Lake Ontario, St. Lawrence, and Atlantic Coast drainages; Krebs et al. 2013, Porto-Hannes et al. 2021). Improving the ability to correctly differentiate among species using nongenetic techniques remains important for field biologists. Misidentifications could result in inaccurate population estimates and biases in field surveys, which could in turn mislead conservation and management strategies (Shea et al. 2011).

ACKNOWLEDGMENTS

Funding for this project came from Fisheries and Oceans Canada and the Central Michigan University (CMU) Office of Research and Graduate Studies Summer Scholars Program. Specimens from Michigan were collected using scientific collection and threatened and endangered species permits issued by the Michigan Department of Natural Resources. Ontario specimens were collected under Canadian Species at Risk permit 19-PCAA-0036. We thank everyone who assisted in field collections and laboratory work including Nichelle VanTassel, Shay Keretz, Dylan Powell, Emmett Smrcka, and Julia Willsie (CMU Biology Department) as well as Dr. Patty Gillis and staff from Environment and Climate Change Canada and Fisheries and Oceans Canada. The paper is contribution 164 of the CMU Institute for Great Lakes Research.

LITERATURE CITED

Adams, D. C., M. L. Collyer, A. Kaliontzopoulou, and E. K. Balken. 2021. *Geomorph*: Software for geometric morphometric analyses. R package version 4.0. Available at https://cran.r-project.org/packages/geomorph (accessed October 12, 2021).

Beauchamp, K. A., T. W. Beyett, M. W. Scott, and D. T. Zanatta. 2020. Detection of hybrid *Pyganodon grandis* and *P. lacustris* (Bivalvia: Unionidae) using F- and M-lineage mtDNA sequences and geometric morphometrics. Journal of Molluscan Studies 86:233–239.

Berg, D. J., W. R. Haag, S. I. Guttman, and J. B. Sickel. 1995. Mantle biopsy: A technique for nondestructive tissue-sampling of freshwater mussels. Journal of the North American Benthological Society 14:577–581.

Beyett, T. W., K. McNichols-O'Rourke, T. J. Morris, and D. T. Zanatta. 2020. Use of morphometric analyses and DNA barcoding to distinguish *Truncilla donaciformis* and *Truncilla trucata* (Bivalvia: Unionidae). Freshwater Mollusk Biology and Conservation 23:99–108.

Campbell, D. C., P. D. Johnson, J. D. Williams, A. K. Rindsberg, J. M. Serb, K. K. Small, and C. Lydeard. 2008. Identification of 'extinct' freshwater mussel species using DNA barcoding. Molecular Ecology Resources 8:711–724.

Collyer, M. L., and D. C. Adams. 2018. RRPP: An R package for fitting linear models to high-dimensional data using residual randomization. Methods in Ecology and Evolution 9:1772–1779.

Collyer, M. L., and D. C. Adams. 2021. RRPP: Linear model evaluation with randomized residuals in a permutation procedure. Available at https://cran.r-project.org/web/packages/RRPP (accessed October 12, 2021).

COSEWIC (Committee on the Status of Endangered Wildlife in Canada). 2010. COSEWIC assessment and status update report on the Wavy-rayed Lampmussel *Lampsilis fasciola* in Canada. Committee on the Status of Endangered Wildlife in Canada. Ottawa. Xi + 60 pp. Available at https://wildlife-species.canada.ca/species-risk-registry/virtual_sara/files/cosewic/sr_Wavy-rayed%20Lampmussel_0810_e.pdf (accessed February 11, 2022).

Cummings, K. S., and C. A. Mayer. 1992. Field Guide to Freshwater Mussels of the Midwest. Illinois Natural History Survey Manual 5, Champaign. 194 pp.

Gillis, P. L., J. Salerno, V. L. McKay, C. J. Bennett, K. L. K. Lemon, Q. J. Rochfort, and R. S. Prosser. 2021. Salt-laden winter runoff and freshwater mussels; Assessing the effect on early life stages in the laboratory and wild mussel populations in receiving waters. Archives of Environmental Contamination and Toxicology 82:239–254.

Gilroy, E. A. M., J. S. Klinck, S. D. Campbell, R. McInnis, P. L. Gillis, and S. R. de Solla. 2014. Toxicity and bioconcentration of the pharmaceuticals moxifloxacin, rosuvastatin, and drospirenone to the unionid mussel *Lampsilis siliquoidea*. Science of the Total Environment 487:537–544.

Goodall, C. 1991. Procrustes methods in the statistical analysis of shape. Journal of the Royal Statistical Society B 53:285–339.

Haag, W. R. 2012. North American freshwater mussels: Natural history, ecology, and conservation. Cambridge University Press, New York. 505 pp.

Hammer, Ø., D. A. T. Harper, and P. D. Ryan. 2001. PAST: Paleontological statistics software package for education and data analysis. Palaeontologia Electronica 4:9. Software available at https://www.nhm.uio.no/english/research/infrastructure/past/ (accessed February 11, 2022).

Hebert, P. D. N., A. Cywinska, S. L. Ball, and J. R. Dewaard. 2003. Biological identifications through DNA barcodes. Proceedings of the Royal Society of London Series B: Biological Sciences 270:313–321.

Henley, W. F., P. J. Grobler, and R. J. Neves. 2006. Non-invasive method to obtain DNA from freshwater mussels (Bivalvia: Unionidae). Journal of Shellfish Research 25:975–977.

Hess, M. C., K. Inoue, E. T. Tsakiris, M. Hart, J. Morton, J. Dudding, C. R. Robertson, and C. R. Randklev. 2018. Misidentification of sex for *Lampsilis teres*, Yellow Sandshell, and its implications for mussel conservation and wildlife management. PloS ONE 13:e0197107.

Hewitt, T. L., A. E. Haponski, D. Ó Foighil. 2021. Evolution of diverse host infection mechanisms delineates an adaptive radiation of lampsiline freshwater mussels centered on their larval ecology. PeerJ 9:e12287.

Hewitt, T. L., D. A. Woolnough, and D. T. Zanatta. 2019. Population genetic analyses of *Lampsilis cardium* (Bivalvia: Unionidae) reveal multiple post-glacial colonization routes into the Great Lakes drainage. American Malacological Bulletin 37:21–34.

Inoue, K., D. M. Hayes, J. L. Harris, and A. D. Christian. 2013. Phylogenetic and morphometric analyses reveal ecophenotypic plasticity in freshwater

mussels *Obovaria jackoniana* and *Villosa arkansasensis* (Bivalvia: Unionidae). Ecology and Evolution 3:2670–2683.

Inoue, K., A. L. McQueen, J. L. Harris, and D. J. Berg. 2014. Molecular phylogenetics and morphological variation reveal recent speciation in freshwater mussels of the genera *Arcidens* and *Arkansia* (Bivalvia: Unionidae). Biological Journal of the Linnean Society 112:535–545.

Jackson, D. A. 1993. Stopping rules in principal components analysis: a comparison of heuristical and statistical approaches. Ecology 74:2204–2214.

Krebs, R. A., W. C. Borden, N. M. Evans, and F. P. Doerder. 2013. Differences in population structure estimated within maternally- and paternally-inherited forms of mitochondria in *Lampsilis siliquoidea* (Bivalvia: Unionidae). Biological Journal of the Linnean Society 109:229–240.

Larson, J. H., W. B. Richardson, R. J. Kennedy, J. C. Nelson, M. A. Evans, and J. S. Schaeffer. 2016. Spatial variation in biofouling of a unionid mussel (*Lampsilis siliquoidea*) across the western basin of Lake Erie. American Midland Naturalist 176:119–129.

MNFI (Michigan Natural Features Inventory). 2020. Michigan's rare animals. Available at https://mnfi.anr.msu.edu/species/animals (accessed February 11, 2022).

Mulcrone, R. S., and J. E. Rathbun. 2018. Field Guide to the Freshwater Mussels of Michigan. Michigan Department of Natural Resources, Lansing. 59 pp.

OMNRF (Ontario Ministry of Natural Resources and Forestry). 2021. Species at risk in Ontario. Available at https://www.ontario.ca/page/species-risk-ontario (accessed February 11, 2022).

Porto-Hannes, I., L. E. Burlakova, D. T. Zanatta, and H. R. Lasker. 2021. Boundaries and hybridization in a secondary contact zone between freshwater mussel species (Family: Unionidae). Heredity 126:955–973.

Quinn, G. P., and M. J. Keough. 2002. Experimental Design and Data Analysis for Biologists. Cambridge University Press, New York. 557 pp.

Rohlf, J. F., and D. Slice. 1990. Extensions of the Procrustes method for the optimal superimposition of landmarks. Systematic Biology 39:40–59.

Sambrook, J., E. F. Fritsch, and T. Maniatis. 1989. Molecular Cloning: A Laboratory Manual. Cold Spring Harbor Laboratory Press, Cold Spring Harbor, New York.

Scrucca, l., M. Fop, T. B. Murphy, and A. E. Raftery. 2016. Mclust 5: Clustering, classification and density estimation using Gaussian finite mixture models. The R Journal 8:289–317.

Shea, C. P., J. T. Peterson, J. M. Wisniewski, and N. A. Johnson. 2011. Misidentification of freshwater mussel species (Bivalvia:Unionidae): Contributing factors, management implications, and potential solutions. Journal of the North American Benthological Society 30:446–458.

Sheets, H. D. 2014. Integrated Morphometrics Package (IMP) v. 8. Canisius College, New York. Available at: https://www.animal-behaviour.de/imp/ (accessed November 12, 2020).

Waller, D. L., and M. R. Bartsch. 2018. Use of carbon dioxide in zebra mussel (*Dreissena polymorpha*) control and safety to a native freshwater mussel (Fatmucket, *Lampsilis siliquoidea*). Management of Biological Invasions 9:439–450.

Wang, N., R. A. Consbrock, C. G. Ingersoll, and M. C. Barnhart. 2011. Evaluation of influence of sediment on the sensitivity of a unionid mussel (*Lampsilis siliquoidea*) to ammonia in 28-day water exposures. Environmental Toxicology and Chemistry 30:2270–2276.

Watters, G. T., M. A. Hoggarth, and D. H. Stansbery. 2009. The Freshwater Mussels of Ohio. The Ohio State University, Columbus. 400 pp.

Webster, M., and H. D. Sheets. 2010. A practical introduction to landmark-based geometric morphometrics. Pages 163–188 *in* J. Alroy and G. Hunt, editors. Quantitative Methods in Paleontology. Vol. 16. Yale University Press, New Haven, Connecticut.

Willsie, J. A., T. J. Morris, and D. T. Zanatta. 2020. Morphometric analyses distinguish Wabash Pigtoe (*Fusconaia flava*) and Round Pigtoe (*Pleurobema sintoxia*) mussels. Diversity 12:337.

Zieritz, A., and D. C. Aldridge. 2011. Sexual, habitat-constrained and parasite-induced dimorphism in the shell of a freshwater mussel (*Anodonta anatina*, Unionidae). Journal of Morphology 272:1365–1375.

Appendix 1. Length, height, width, and hinge-length measurements and field, cytochrome c oxidase subunit 1, and (jackknifed) morphometric identifications for all specimens collected.

Sample code	L (mm)	H (mm)	W (mm)	HL (mm)	Field species ID	Field sex ID	COI ID	PCA-LDA assignment: species	PCA-LDA assignment: species + sex
MLR-01	75.0	52.7	37.3	—	*Lampsilis siliquoidea*	Female	*Lampsilis cardium*	*Lampsilis fasciola*	*L. fasciola* female
MLR-02	72.5	57.5	35.5	—	*L. cardium*	Female	*L. cardium*	*Ortmanniana ligamentina*	*L. cardium* female
MLR-03	98.4	68.3	46.1	—	*L. siliquoidea*	Female	*L. siliquoidea*	*L. siliquoidea*	*L. siliquoidea* female
MLR-04	98.1	62.7	42.0	—	unknown	Female	*L. siliquoidea*	*L. siliquoidea*	*L. siliquoidea* female
MLR-05	90.0	61.1	41.1	—	*L. siliquoidea*	Female	*L. siliquoidea*	*L. siliquoidea*	*L. siliquoidea* female
MLR-06	91.0	62.5	42.8	—	*L. siliquoidea*	Female	*L. siliquoidea*	*L. siliquoidea*	*L. cardium* female
MLR-07	88.8	58.9	41.2	—	*L. siliquoidea*	Female	*L. cardium*	*L. cardium*	*L. fasciola* female
MLR-08	90.2	61.0	38.7	—	*L. siliquoidea*	Female	*L. siliquoidea*	*L. siliquoidea*	*L. siliquoidea* female
MLR-09	82.2	51.3	32.2	—	*L. siliquoidea*	Female	*L. siliquoidea*	*L. cardium*	*L. siliquoidea* female
MLR-10	80.4	56.0	34.0	—	*L. siliquoidea*	Female	*L. siliquoidea*	*L. cardium*	*L. siliquoidea* female
MLR-11	87.6	60.8	37.7	—	*L. siliquoidea*	Female	*L. cardium*	*L. siliquoidea*	*L. siliquoidea* female
MLR-12	85.0	52.0	31.4	—	*L. siliquoidea*	Female	*L. siliquoidea*	*L. siliquoidea*	*L. siliquoidea* female
MLR-13	86.0	55.3	31.5	—	*L. siliquoidea*	Female	*L. siliquoidea*	*L. siliquoidea*	*L. siliquoidea* female
MLR-14	78.7	50.1	31.3	—	*L. siliquoidea*	Female	*L. siliquoidea*	*L. siliquoidea*	*L. siliquoidea* female
MLR-15	82.3	53.3	32.2	—	*L. siliquoidea*	Female	*L. siliquoidea*	*L. siliquoidea*	*L. siliquoidea* female
MLR-16	83.0	54.7	33.6	—	*L. siliquoidea*	Female	*L. cardium*	*L. siliquoidea*	*L. siliquoidea* female
MLR-17	89.2	59.4	38.4	—	*L. siliquoidea*	Female	*L. siliquoidea*	*L. fasciola*	*L. siliquoidea* female
MLR-18	85.7	58.3	35.1	—	*L. siliquoidea*	Female	*L. cardium*	*L. siliquoidea*	*L. siliquoidea* female
MLR-19	83.6	52.5	34.1	—	*L. siliquoidea*	Female	*L. siliquoidea*	*L. siliquoidea*	*L. siliquoidea* female
MLR-20	76.4	49.6	26.0	—	*L. siliquoidea*	Female	*L. siliquoidea*	*L. siliquoidea*	*L. siliquoidea* female
MLR-21	88.8	53.1	30.3	—	*L. siliquoidea*	Female	*L. siliquoidea*	*L. siliquoidea*	*L. siliquoidea* female
MLR-22	80.5	49.8	29.6	—	*L. siliquoidea*	Female	*L. siliquoidea*	*L. siliquoidea*	*L. siliquoidea* female
MLR-23	80.6	34.4	54.4	—	*L. siliquoidea*	Female	*L. siliquoidea*	*L. siliquoidea*	*L. siliquoidea* female
MLR-24	76.1	32.0	49.0	—	*L. siliquoidea*	Female	*L. siliquoidea*	*L. siliquoidea*	*L. siliquoidea* female
MLR-25	75.5	26.6	49.9	—	*L. siliquoidea*	Female	*L. siliquoidea*	*L. siliquoidea*	*L. siliquoidea* female
MLR-26	85.5	34.1	52.7	—	*L. siliquoidea*	Female	*L. siliquoidea*	*L. siliquoidea*	*L. siliquoidea* female
MLR-27	106.6	78.8	51.1	—	*L. cardium*	Female	*L. cardium*	*O. ligamentina*	*L. cardium* female
MLR-28	82.5	57.6	35.5	—	*L. cardium*	Female	*L. cardium*	*L. cardium*	*L. cardium* female
MLR-29	81.7	57.7	35.7	—	*L. cardium*	Female	*L. siliquoidea*	*L. siliquoidea*	*L. fasciola* female
MLR-30	92.1	65.5	47.4	—	*L. cardium*	Female	*L. cardium*	*O. ligamentina*	*L. cardium* female
MLR-31	75.6	55.5	39.3	—	*L. cardium*	Female	*L. cardium*	*L. cardium*	*L. cardium* female
MLR-32	89.9	60.8	41.6	—	*L. cardium*	Female	*L. cardium*	*L. siliquoidea*	*L. cardium* female
MLR-33	81.0	57.1	34.7	—	*L. cardium*	Female	*L. siliquoidea*	*L. cardium*	*L. cardium* female
MLR-34	83.6	53.6	36.4	—	*L. cardium*	Female	*L. cardium*	*L. siliquoidea*	*L. siliquoidea* female
MLR-35	90.1	57.8	44.9	—	*L. cardium*	Female	*L. siliquoidea*	*L. cardium*	*L. cardium* female
MLR-36	76.1	45.8	33.6	—	shape-FM, lure-PB	Female	*L. siliquoidea*	*L. siliquoidea*	*L. siliquoidea* female
MLR-37	83.3	59.2	38.9	—	*L. cardium*	Female	*L. cardium*	*O. ligamentina*	*L. cardium* female
MLR-38	98.1	66.0	46.9	—	*L. cardium*	Female	*L. cardium*	*L. cardium*	*L. cardium* female
MLR-39	99.2	65.0	50.0	—	*L. cardium*	Female	*L. cardium*	*O. ligamentina*	*L. cardium* female
MLR-40	98.0	61.4	48.1	—	*L. cardium*	Female	*L. siliquoidea*	*L. cardium*	*L. cardium* female
MLR-41	89.4	56.3	43.4	—	*L. cardium*	Female	*L. siliquoidea*	*L. siliquoidea*	*L. cardium* female
MLR-42	92.1	65.8	44.7	—	*L. cardium*	Female	*L. cardium*	*L. cardium*	*L. fasciola* female
MLR-43	74.4	49.6	28.6	—	*L. cardium*	Female	*L. cardium*	*L. cardium*	*L. cardium* female
MLR-44	79.0	53.3	31.2	—	*L. cardium*	Female	*L. cardium*	*O. ligamentina*	*L. cardium* female
MLR-45	98.6	66.8	50.6	—	*L. cardium*	Female	*L. siliquoidea*	*L. cardium*	*L. cardium* female
MLR-46	92.7	62.9	45.1	—	*L. cardium*	Female	*L. siliquoidea*	*L. cardium*	*L. cardium* female

Appendix 1, continued.

Sample code	L (mm)	H (mm)	W (mm)	HL (mm)	Field species ID	Field sex ID	COI ID	PCA-LDA assignment: species	PCA-LDA assignment: species + sex
MLR-47	97.6	66.1	44.6	—	*L. cardium*	Female	*L. siliquoidea*	*L. cardium*	*L. cardium* female
MLR-48	92.5	62.3	37.7	—	*L. cardium*	Female	*L. siliquoidea*	*L. cardium*	*L. cardium* female
MLR-49	85.9	57.7	36.9	—	*L. cardium*	Female	*L. cardium*	*L. cardium*	*L. cardium* female
MLR-50	77.9	53.9	36.0	—	*L. cardium*	Female	*L. cardium*	*O. ligamentina*	*L. cardium* female
MLR-51	79.4	44.7	25.8	—	*L. siliquoidea*	Female	*L. siliquoidea*	*L. siliquoidea*	*L. siliquoidea* female
MLR-52	103.8	59.1	40.9	—	*L. siliquoidea*	Female	*L. siliquoidea*	*L. cardium*	*L. siliquoidea* female
MLR-53	85.8	54.6	32.3	—	*L. siliquoidea*	Female	*L. siliquoidea*	*L. fasciola*	*L. cardium* female
MLR-54	87.2	58.3	37.5	—	*L. siliquoidea*	Female	*L. cardium*	*O. ligamentina*	*L. fasciola* female
MLR-55	77.3	47.7	32.3	—	*L. siliquoidea*	Female	—	*L. siliquoidea*	*L. siliquoidea* female
MLR-56	84.9	52.6	37.2	—	*L. siliquoidea*	Female	*L. siliquoidea*	*L. siliquoidea*	*L. siliquoidea* female
MLR-57	82.3	51.3	33.5	—	*L. siliquoidea*	Female	*L. cardium*	*O. ligamentina*	*L. fasciola* female
MLR-58	77.2	48.5	32.5	—	*L. siliquoidea*	Female	—	*L. siliquoidea*	*L. siliquoidea* female
MLR-59	78.8	46.4	29.2	—	*L. siliquoidea*	Female	*L. siliquoidea*	*L. fasciola*	*L. siliquoidea* female
BRFM-01	—	—	—	—	*L. siliquoidea*	Female	*L. siliquoidea*	*L. siliquoidea*	*L. siliquoidea* female
BRFM-02	—	—	—	—	*L. siliquoidea*	Male	*L. siliquoidea*	*L. siliquoidea*	*L. siliquoidea* male
BRFM-03	—	—	—	—	*L. siliquoidea*	Female	*L. siliquoidea*	*L. siliquoidea*	*L. siliquoidea* female
BRFM-04	—	—	—	—	*L. siliquoidea*	Female	*L. siliquoidea*	*L. siliquoidea*	*L. siliquoidea* male
BRFM-05	—	—	—	—	*L. siliquoidea*	Male	*L. siliquoidea*	*L. fasciola*	*O. ligamentina*
BRFM-06	—	—	—	—	*L. siliquoidea*	Male	*L. siliquoidea*	*L. siliquoidea*	*L. siliquoidea* male
MAPLE-01	—	—	—	—	*L. siliquoidea*	Female	*L. siliquoidea*	*L. cardium*	*L. siliquoidea* female
MAPLE-02	—	—	—	—	*L. siliquoidea*	Female	*L. siliquoidea*	*L. siliquoidea*	*L. siliquoidea* female
EBWF-01	—	—	—	—	*L. siliquoidea*	Male	*L. siliquoidea*	*L. siliquoidea*	*L. siliquoidea* male
EBWF-02	—	—	—	—	*L. siliquoidea*	Male	*L. siliquoidea*	*L. siliquoidea*	*L. siliquoidea* male
EBWF-03	—	—	—	—	*L. siliquoidea*	Male	*L. siliquoidea*	*L. fasciola*	*L. siliquoidea* male
EBWF-04	—	—	—	—	*L. siliquoidea*	Male	*L. siliquoidea*	*L. cardium*	*L. siliquoidea* male
EBWF-05	—	—	—	—	*L. siliquoidea*	Female	*L. siliquoidea*	*L. siliquoidea*	*O. ligamentina*
EBWF-06	—	—	—	—	*L. cardium*	Female	—	*L. cardium*	*L. cardium* female
SALT-01	85	45	29	30	*L. siliquoidea*	Male	*L. siliquoidea*	*L. fasciola*	*O. ligamentina*
SALT-02	54	29	20	18	*L. siliquoidea*	Female	*L. siliquoidea*	*L. siliquoidea*	*L. siliquoidea* female
SALT-03	94	53	31	44	*O. ligamentina*	—	*O. ligamentina*	*L. siliquoidea*	*O. ligamentina*
SALT-04	93	59	41	40	*L. cardium*	Female	*L. cardium*	*O. ligamentina*	*L. fasciola male*
SALT-05	101	66	43	46	*L. cardium*	Female	*L. cardium*	*O. ligamentina*	*O. ligamentina*
SALT-06	114	66	48	56	*L. cardium*	Male	*O. ligamentina*	*L. siliquoidea*	*O. ligamentina*
SALT-07	103	72	51	49	*L. cardium*	Female	*L. cardium*	*O. ligamentina*	*L. cardium* female
RR-01	51	33	21	26	*L. fasciola*	Female	*L. fasciola*	*L. cardium*	*L. fasciola* female
RR-02	47	33	22	28	*L. fasciola*	Female	*L. fasciola*	*O. ligamentina*	*L. fasciola* female
RR-03	49	32	22	27	*L. fasciola*	Female	*L. fasciola*	*L. cardium*	*L. fasciola* female
RR-04	45	35	20	24	*L. fasciola*	Female	*L. fasciola*	*L. cardium*	*L. fasciola* female
RR-05	56	42	31	34	*L. fasciola*	Female	*L. fasciola*	*L. fasciola*	*L. cardium* female
RR-06	39	25	16	21	*L. fasciola*	Female	*L. fasciola*	*L. siliquoidea*	*L. fasciola* female
RR-07	48	33	23	26	*L. fasciola*	Female	*L. fasciola*	*L. fasciola*	*L. fasciola* female
RR-08	40	28	17	18	*L. fasciola*	Female	*L. fasciola*	*L. fasciola*	*L. fasciola* female
RR-09	83	59	39	50	*L. fasciola*	Female	*L. fasciola*	*L. cardium*	*L. fasciola* female
RR-10	45	29	19	24	*L. fasciola*	Female	*L. fasciola*	*L. cardium*	*L. cardium* female
RR-11	66	43	29	31	*L. fasciola*	Female	*L. fasciola*	*L. cardium*	*L. fasciola* female
RR-12	38	24	25	17	*L. fasciola*	Female	*L. fasciola*	*L. fasciola*	*L. fasciola* male
RR-13	46	31	21	22	*L. fasciola*	Female	*L. fasciola*	*L. cardium*	*L. fasciola* female
RR-14	54	39	27	30	*L. fasciola*	Female	*L. fasciola*	*L. cardium*	*L. cardium* female
RR-15	47	25	20	25	*L. fasciola*	Female	*L. fasciola*	*L. fasciola*	*L. fasciola* female
RR-16	40	26	16	19	*L. fasciola*	Female	*L. fasciola*	*L. fasciola*	*L. fasciola* female

Appendix 1, continued.

Sample code	L (mm)	H (mm)	W (mm)	HL (mm)	Field species ID	Field sex ID	COI ID	PCA-LDA assignment: species	PCA-LDA assignment: species + sex
RR-17	47	31	19	23	*L. fasciola*	Female	*L. fasciola*	*L. cardium*	*L. cardium* female
RR-18	52	33	21	28	*L. fasciola*	Female	*L. fasciola*	*L. fasciola*	*L. fasciola* male
RR-19	61	37	29	27	*L. fasciola*	Male	*L. fasciola*	*O. ligamentina*	*L. fasciola* male
RR-20	47	31	19	22	*L. fasciola*	Male	*L. fasciola*	*L. fasciola*	*L. fasciola* male
RR-21	47	32	21	18	*L. fasciola*	Male	*L. fasciola*	*L. fasciola*	*L. fasciola* male
RR-22	46	30	19	19	*L. fasciola*	Male	*L. fasciola*	*L. fasciola*	*L. fasciola* male
RR-23	57	38	24	23	*L. fasciola*	Male	*L. fasciola*	*L. cardium*	*L. fasciola* male
RR-24	43	28	18	17	*L. fasciola*	Female	*L. fasciola*	*L. fasciola*	*L. fasciola* female
RR-25	73	47	34	33	*L. fasciola*	Male	*L. fasciola*	*L. cardium*	*L. fasciola* male
RR-26	66	45	27	31	*L. fasciola*	Male	*L. fasciola*	*L. fasciola*	*L. fasciola* male
RR-27	51	35	23	22	*L. fasciola*	Male	*L. fasciola*	*O. ligamentina*	*L. fasciola* male
RR-28	47	32	20	23	*L. fasciola*	Male	*L. fasciola*	*O. ligamentina*	*L. fasciola* male
RR-29	52	33	19	21	*L. fasciola*	Male	*L. fasciola*	*L. fasciola*	*L. fasciola* male
RR-30	59	41	26	22	*L. fasciola*	Male	*L. fasciola*	*O. ligamentina*	*L. fasciola* male
RR-31	50	30	21	19	*L. fasciola*	Male	*L. fasciola*	*L. fasciola*	*L. fasciola* male
RR-32	39	27	14	14	*L. fasciola*	Male	*L. fasciola*	*L. siliquoidea*	*L. fasciola* female
RR-33	43	29	18	17	*L. fasciola*	Male	*L. fasciola*	*O. ligamentina*	*L. fasciola* male
RR-34	39	27	17	14	*L. fasciola*	Male	*L. fasciola*	*O. ligamentina*	*L. fasciola* female
RR-35	53	32	21	23	*L. fasciola*	Male	*L. fasciola*	*L. fasciola*	*L. fasciola* male
RR-36	66	46	27	27	*L. fasciola*	Male	*L. fasciola*	*L. fasciola*	*L. fasciola* male
RR-37	60	40	24	24	*L. fasciola*	Male	*L. fasciola*	*L. fasciola*	*L. cardium* male
RR-38	54	36	22	21	*L. fasciola*	Male	*L. fasciola*	*L. fasciola*	*L. fasciola* male
RR-39	36	22	14	14	*L. fasciola*	Male	*L. fasciola*	*L. fasciola*	*L. fasciola* male
RR-40	40	26	17	16	*L. fasciola*	Male	*L. fasciola*	*L. fasciola*	*L. fasciola* male
RR-41	39	25	16	14	*L. fasciola*	Male	*L. fasciola*	*O. ligamentina*	*L. fasciola* female
RR-42	109	81	51	40	*L. cardium*	Female	*L. cardium*	*L. cardium*	*L. cardium* female
RR-43	98	67	39	28	*L. cardium*	Female	*L. cardium*	*L. cardium*	*L. cardium* male
RR-44	76	52	34	27	*L. cardium*	Female	*L. cardium*	*L. fasciola*	*L. cardium* female
RR-45	86	60	38	28	*L. cardium*	Female	*L. cardium*	*L. fasciola*	*L. fasciola* female
RR-46	99	69	45	33	*L. cardium*	Female	*L. cardium*	*L. fasciola*	*L. fasciola* female
RR-47	94	70	41	43	*L. cardium*	Female	*L. cardium*	*O. ligamentina*	*L. cardium* female
RR-48	114	80	50	46	*L. cardium*	Female	*L. cardium*	*L. cardium*	*L. cardium* female
RR-49	94	66	38	35	*L. cardium*	Female	*L. cardium*	*O. ligamentina*	*L. cardium* female
RR-50	114	77	46	41	*L. cardium*	Female	*L. cardium*	*L. cardium*	*L. cardium* female
RR-51	94	59	42	32	*L. cardium*	Female	*L. cardium*	*L. cardium*	*L. cardium* male
RR-52	119	82	56	47	*L. cardium*	Female	*L. cardium*	*L. cardium*	*L. cardium* male
RR-53	92	62	39	29	*L. cardium*	Female	*L. cardium*	*L. cardium*	*L. cardium* male
RR-54	108	71	44	38	*L. cardium*	Female	*L. cardium*	*O. ligamentina*	*L. cardium* female
RR-55	97	77	47	43	*L. cardium*	Female	*L. cardium*	*L. cardium*	*L. cardium* female
RR-56	87	56	38	31	*L. cardium*	Female	*L. cardium*	*L. cardium*	*L. cardium* female
RR-57	97	70	37	30	*L. cardium*	Female	*L. cardium*	*L. cardium*	*L. cardium* female
RR-58	94	68	40	29	*L. cardium*	Female	*L. cardium*	*L. cardium*	*L. cardium* female
RR-59	97	63	41	32	*L. cardium*	Female	*L. cardium*	*L. cardium*	*L. cardium* female
RR-60	109	71	47	35	*L. cardium*	Female	*L. cardium*	*L. cardium*	*L. cardium* male
RR-61	108	68	51	38	*L. cardium*	Female	*L. cardium*	*L. cardium*	*L. cardium* female
RR-62	136	95	60	54	*L. cardium*	Male	—	*L. cardium*	*L. cardium* male
RR-63	112	82	53	42	*L. cardium*	Female	—	*L. cardium*	*L. cardium* female
RR-64	100	67	42	30	*L. cardium*	Female	—	*L. cardium*	*L. cardium* female
RR-65	106	78	56	40	*L. cardium*	Female	—	*L. fasciola*	*L. cardium* female
RR-66	108	84	50	40	*L. cardium*	Female	—	*L. cardium*	*L. cardium* female

Appendix 1, continued.

Sample code	L (mm)	H (mm)	W (mm)	HL (mm)	Field species ID	Field sex ID	COI ID	PCA-LDA assignment: species	PCA-LDA assignment: species + sex
RR-67	127	86	52	47	*L. cardium*	Male	—	*L. cardium*	*L. cardium* male
RR-68	99	65	42	37	*L. cardium*	Female	—	*O. ligamentina*	*L. cardium* female
RR-69	121	76	50	44	*L. cardium*	Male	*L. cardium*	*L. siliquoidea*	*L. cardium* male
RR-70	116	72	52	39	*L. cardium*	Male	*L. cardium*	*L. cardium*	*L. cardium* male
RR-71	142	89	61	58	*L. cardium*	Male	*L. cardium*	*O. ligamentina*	*L. cardium* male
RR-72	112	72	44	33	*L. cardium*	Male	*L. cardium*	*L. fasciola*	*L. cardium* male
RR-73	145	90	55	57	*L. cardium*	Male	*L. cardium*	*L. cardium*	*L. cardium* male
RR-74	121	81	51	43	*L. cardium*	Male	*L. cardium*	*L. siliquoidea*	*L. cardium* male
RR-75	146	94	61	57	*L. cardium*	Male	*L. cardium*	*O. ligamentina*	*L. cardium* male
RR-76	89	59	34	28	*L. cardium*	Male	*L. cardium*	*L. cardium*	*L. cardium* male
RR-77	89	54	31	25	*L. cardium*	Male	*L. cardium*	*L. fasciola*	*L. cardium* male
RR-78	147	94	59	62	*L. cardium*	Male	*L. cardium*	*L. cardium*	*L. cardium* male
RR-79	123	75	50	44	*L. cardium*	Male	*L. cardium*	*L. cardium*	*L. cardium* male
RR-80	115	71	50	41	*L. cardium*	Male	*L. cardium*	*L. cardium*	*L. cardium* male
RR-81	135	82	58	49	*L. cardium*	Male	*L. cardium*	*L. cardium*	*L. cardium* male
RR-82	141	92	59	52	*L. cardium*	Male	*L. cardium*	*L. cardium*	*L. cardium* male
RR-83	114	77	48	39	*L. cardium*	Male	*L. cardium*	*L. fasciola*	*L. cardium* male
RR-84	112	69	43	34	*L. cardium*	Male	*L. cardium*	*L. cardium*	*L. cardium* male
RR-85	104	63	43	37	*L. cardium*	Male	*L. cardium*	*L. siliquoidea*	*L. cardium* male
RR-86	106	70	42	30	*L. cardium*	Male	*L. cardium*	*L. cardium*	*L. cardium* male
RR-87	118	76	52	39	*L. cardium*	Male	*L. cardium*	*O. ligamentina*	*L. cardium* male
RR-88	109	69	45	40	*L. cardium*	Male	*L. cardium*	*L. cardium*	*L. cardium* male
RR-89	128	82	53	46	*L. cardium*	Male	—	*L. cardium*	*L. cardium* male
RR-90	124	78	52	44	*L. cardium*	Male	—	*L. cardium*	*L. cardium* male
RR-91	135	83	53	52	*L. cardium*	Male	—	*L. cardium*	*L. cardium* male
RR-92	105	66	37	40	*L. cardium*	Male	—	*O. ligamentina*	*L. cardium* male
RR-93	135	84	59	53	*L. cardium*	Male	—	*L. cardium*	*L. cardium* male
RR-94	127	80	52	46	*L. cardium*	Male	—	*L. cardium*	*L. cardium* male
RR-95	112	72	44	36	*L. cardium*	Male	—	*L. fasciola*	*L. cardium* male
RR-96	132	91	51	49	*L. cardium*	Male	—	*L. cardium*	*L. cardium* male
RR-97	123	76	46	46	*L. cardium*	Male	—	*L. siliquoidea*	*L. cardium* male
RR-98	134	88	57	45	*L. cardium*	Male	—	*L. fasciola*	*L. cardium* male
RR-99	139	88	59	56	*L. cardium*	Male	—	*L. cardium*	*L. cardium* male
RR-100	124	74	48	49	*L. cardium*	Male	—	*L. cardium*	*L. cardium* male
RR-101	129	83	59	56	*L. cardium*	Male	—	*L. cardium*	*L. cardium* male
RR-102	139	90	47	47	*L. cardium*	Male	—	*L. fasciola*	*L. cardium* male
RR-103	129	83	57	48	*L. cardium*	Male	—	*L. cardium*	*L. cardium* male
RR-104	146	93	57	57	*L. cardium*	Male	—	*O. ligamentina*	*L. cardium* male
RR-105	137	85	49	54	*L. cardium*	Male	—	*L. siliquoidea*	*L. cardium* male
RR-106	130	80	54	52	*L. cardium*	Male	—	*L. cardium*	*L. cardium* male
RR-107	125	76	46	40	*L. cardium*	Male	—	*L. cardium*	*L. cardium* male
RR-108	133	82	50	50	*L. cardium*	Male	—	*L. cardium*	*L. cardium* male
RR-109	136	85	51	49	*L. cardium*	Male	—	*L. fasciola*	*L. cardium* male
RR-110	137	89	60	50	*L. cardium*	Male	—	*L. siliquoidea*	*L. cardium* male
RR-111	130	87	53	47	*L. cardium*	Male	—	*L. cardium*	*L. cardium* male
RR-112	127	82	52	51	*L. cardium*	Male	—	*L. fasciola*	*L. cardium* male
RR-113	135	86	59	48	*L. cardium*	Male	—	*L. cardium*	*L. cardium* male
RR-114	135	85	57	53	*L. cardium*	Male	—	*L. fasciola*	*L. cardium* male
RR-115	124	77	50	40	*L. cardium*	Male	—	*L. cardium*	*L. cardium* male
RR-116	119	74	50	37	*L. cardium*	Male	—	*L. cardium*	*L. cardium* male

Appendix 1, continued.

Sample code	L (mm)	H (mm)	W (mm)	HL (mm)	Field species ID	Field sex ID	COI ID	PCA-LDA assignment: species	PCA-LDA assignment: species + sex
RR-117	141	86	52	56	*L. cardium*	Male	—	*L. cardium*	*L. cardium* male
RR-118	76	49	32	20	*L. cardium*	Male	—	*L. fasciola*	*L. cardium* male
RR-119	133	82	56	53	*L. cardium*	Male	—	*O. ligamentina*	*L. cardium* male
RR-120	125	84	52	47	*L. cardium*	Male	—	*O. ligamentina*	*L. cardium* male
RR-121	101	64	38	31	*L. cardium*	Male	—	*O. ligamentina*	*L. cardium* male
RR-122	39	23	16	8	*L. cardium*	Male	—	*L. fasciola*	*L. cardium* male
RR-123	118	72	51	43	*L. cardium*	Male	—	*L. cardium*	*L. cardium* male
GR-01	67	43	27	19	*L. cardium*	Male	*L. cardium*	*L. fasciola*	*L. fasciola* male
GR-02	112	74	49	36	*L. cardium*	Male	*L. cardium*	*L. cardium*	*L. fasciola* female
GR-03	93	64	42	28	*L. cardium*	Male	*L. cardium*	*L. fasciola*	*L. cardium* male
GR-04	49	31	23	15	*L. cardium*	Male	*L. cardium*	*L. fasciola*	*L. fasciola* male
GR-05	104	68	43	42	*L. cardium*	Male	*L. cardium*	*L. siliquoidea*	*L. cardium* male
GR-06	118	76	47	41	*L. cardium*	Male	*L. cardium*	*L. cardium*	*L. cardium* male
GR-07	120	78	55	39	*L. cardium*	Male	*L. cardium*	*L. cardium*	*L. cardium* female
GR-08	68	45	28	20	*L. cardium*	Male	*L. cardium*	*L. fasciola*	*L. fasciola* female
GR-09	114	75	48	37	*L. cardium*	Male	*L. cardium*	*L. cardium*	*L. cardium* male
GR-11	102	67	43	35	*L. cardium*	Male	*L. cardium*	*L. cardium*	*L. cardium* female
GR-12	95	61	35	28	*L. cardium*	Male	*L. cardium*	*O. ligamentina*	*L. fasciola* male
GR-13	75	42	23	28	*L. cardium*	Male	*O. ligamentina*	*L. siliquoidea*	*O. ligamentina*
GR-14	119	78	52	42	*L. cardium*	Male	*L. cardium*	*L. cardium*	*L. cardium* male
GR-15	97	62	40	30	*L. cardium*	Male	*L. cardium*	*L. siliquoidea*	*L. fasciola* female
GR-16	34	21	12	9	*L. cardium*	Male	—	*L. fasciola*	*L. fasciola* female
GR-17	109	81	56	45	*L. cardium*	Female	*L. cardium*	*O. ligamentina*	*L. cardium* female
GR-18	84	60	41	23	*L. cardium*	Female	*L. cardium*	*O. ligamentina*	*L. cardium* male
GR-19	87	61	46	25	*L. cardium*	Female	*L. cardium*	*L. siliquoidea*	*L. siliquoidea* female
GR-21	90	63	42	27	*L. cardium*	Female	*L. cardium*	*L. cardium*	*L. cardium* female
GR-22	71	49	32	18	*L. cardium*	Female	*L. cardium*	*L. fasciola*	*L. fasciola* male
GR-23	75	52	37	21	*L. cardium*	Female	*L. cardium*	*O. ligamentina*	*O. ligamentina*
GR-24	91	63	41	30	*L. cardium*	Female	*L. cardium*	*L. cardium*	*L. cardium* female
GR-25	96	67	44	31	*L. cardium*	Female	*L. cardium*	*L. cardium*	*L. cardium* female
GR-26	82	55	39	29	*L. cardium*	Female	*L. cardium*	*L. cardium*	*L. cardium* female
GR-27	115	82	59	41	*L. cardium*	Female	*L. cardium*	*O. ligamentina*	*L. fasciola* female
GR-28	71	46	31	21	*L. cardium*	Female	*L. cardium*	*L. fasciola*	*L. cardium* female
GR-29	102	70	46	39	*L. cardium*	Female	*L. cardium*	*L. siliquoidea*	*L. cardium* female
GR-30	75	49	34	17	*L. cardium*	Female	*L. cardium*	*L. cardium*	*L. fasciola* female
GR-31	93	64	41	32	*L. cardium*	Female	*L. cardium*	*L. cardium*	*L. cardium* female
GR-32	104	70	50	34	*L. cardium*	Female	*L. cardium*	*L. cardium*	*L. cardium* female
GR-33	82	54	36	23	*L. cardium*	Female	*L. cardium*	*L. cardium*	*L. fasciola* female
GR-34	93	66	43	38	*L. cardium*	Female	*L. cardium*	*L. siliquoidea*	*L. fasciola* female
GR-35	91	62	37	24	*L. cardium*	Female	*L. cardium*	*L. fasciola*	*L. fasciola* female
GR-37	65	45	29	14	*L. cardium*	Female	—	*O. ligamentina*	*L. cardium* female
GR-38	69	47	33	18	*L. cardium*	Female	—	*L. cardium*	*L. cardium* female
GR-39	79	52	35	24	*L. cardium*	Female	—	*L. siliquoidea*	*L. siliquoidea* female
GR-40	72	47	33	18	*L. cardium*	Female	—	*L. fasciola*	*L. cardium* female
GR-41	84	57	38	27	*L. cardium*	Female	—	*L. cardium*	*L. cardium* female
GR-42	60	39	26	15	*L. cardium*	Female	—	*L. fasciola*	*L. cardium* female
GR-43	66	45	31	16	*L. cardium*	Female	—	*L. siliquoidea*	*L. fasciola* female
GR-44	132	79	56	52	*O. ligamentina*	—	*O. ligamentina*	*O. ligamentina*	*O. ligamentina*
GR-45	139	86	52	68	*O. ligamentina*	—	*O. ligamentina*	*O. ligamentina*	*O. ligamentina*
GR-46	149	88	55	72	*O. ligamentina*	—	*O. ligamentina*	*O. ligamentina*	*O. ligamentina*

Appendix 1, continued.

Sample code	L (mm)	H (mm)	W (mm)	HL (mm)	Field species ID	Field sex ID	COI ID	PCA-LDA assignment: species	PCA-LDA assignment: species + sex
GR-47	137	83	51	63	*O. ligamentina*	—	*O. ligamentina*	*O. ligamentina*	*O. ligamentina*
GR-48	74	44	26	20	*O. ligamentina*	—	*O. ligamentina*	*L. cardium*	*L. cardium male*
CR-01	100	60	34	49	*O. ligamentina*	—	*O. ligamentina*	*L. cardium*	*O. ligamentina*
CR-02	115	68	44	56	*O. ligamentina*	—	*O. ligamentina*	*L. siliquoidea*	*O. ligamentina*
CR-03	107	61	35	46	*O. ligamentina*	—	*O. ligamentina*	*O. ligamentina*	*O. ligamentina*
CR-04	101	60	37	50	*O. ligamentina*	—	*O. ligamentina*	*O. ligamentina*	*O. ligamentina*
CR-05	116	67	45	58	*O. ligamentina*	—	*O. ligamentina*	*O. ligamentina*	*O. ligamentina*
CR-06	83	50	31	34	*O. ligamentina*	—	*O. ligamentina*	*O. ligamentina*	*O. ligamentina*
CR-07	109	60	39	52	*O. ligamentina*	—	*O. ligamentina*	*L. siliquoidea*	*L. siliquoidea* male
CR-08	107	62	38	53	*O. ligamentina*	—	*O. ligamentina*	*L. fasciola*	*O. ligamentina*
CR-09	102	61	37	48	*O. ligamentina*	—	*O. ligamentina*	*O. ligamentina*	*O. ligamentina*
CR-10	104	64	39	50	*O. ligamentina*	—	*O. ligamentina*	*O. ligamentina*	*O. ligamentina*
CR-11	102	65	37	46	*O. ligamentina*	—	*O. ligamentina*	*O. ligamentina*	*O. ligamentina*
CR-12	125	73	42	60	*O. ligamentina*	—	*O. ligamentina*	*L. fasciola*	*O. ligamentina*
CR-13	100	59	37	42	*O. ligamentina*	—	*O. ligamentina*	*O. ligamentina*	*O. ligamentina*
CR-14	94	54	34	40	*O. ligamentina*	—	*O. ligamentina*	*O. ligamentina*	*O. ligamentina*
CR-15	108	68	43	49	*O. ligamentina*	—	*O. ligamentina*	*O. ligamentina*	*O. ligamentina*
CR-16	107	64	37	48	*O. ligamentina*	—	*O. ligamentina*	*L. fasciola*	*L. fasciola* male
CR-17	55	36	15	26	*O. ligamentina*	—	*O. ligamentina*	*L. fasciola*	*L. fasciola* male
CR-18	100	61	35	45	*O. ligamentina*	—	*O. ligamentina*	*L. cardium*	*L. cardium male*
CR-19	94	56	32	42	*O. ligamentina*	—	*O. ligamentina*	*O. ligamentina*	*O. ligamentina*
CR-20	103	62	36	50	*O. ligamentina*	—	*O. ligamentina*	*L. fasciola*	*O. ligamentina*
CR-21	44	26	13	15	*O. ligamentina*	—	—	*L. fasciola*	*O. ligamentina*
CR-22	104	61	37	46	*O. ligamentina*	—	—	*O. ligamentina*	*O. ligamentina*
CR-23	80	47	27	36	*O. ligamentina*	—	—	*L. fasciola*	*O. ligamentina*
CR-24	90	57	29	44	*O. ligamentina*	—	—	*O. ligamentina*	*O. ligamentina*
CR-25	89	53	29	37	*O. ligamentina*	—	—	*O. ligamentina*	*O. ligamentina*
CR-26	80	49	28	40	*O. ligamentina*	—	—	*O. ligamentina*	*O. ligamentina*
CR-27	114	65	38	49	*O. ligamentina*	—	—	*O. ligamentina*	*O. ligamentina*
CR-28	118	72	42	55	*O. ligamentina*	—	—	*L. siliquoidea*	*O. ligamentina*
CR-29	96	59	33	41	*O. ligamentina*	—	—	*O. ligamentina*	*O. ligamentina*
CR-30	97	61	37	44	*O. ligamentina*	—	—	*O. ligamentina*	*O. ligamentina*
CR-31	103	58	34	40	*O. ligamentina*	—	—	*L. cardium*	*O. ligamentina*
CR-32	106	63	36	46	*O. ligamentina*	—	—	*L. fasciola*	*O. ligamentina*
CR-33	97	57	30	45	*O. ligamentina*	—	—	*O. ligamentina*	*O. ligamentina*
CR-34	95	57	31	40	*O. ligamentina*	—	—	*O. ligamentina*	*O. ligamentina*
CR-35	100	59	35	45	*O. ligamentina*	—	—	*L. fasciola*	*O. ligamentina*
CR-36	105	67	34	54	*O. ligamentina*	—	—	*O. ligamentina*	*O. ligamentina*
CR-37	82	54	27	42	*O. ligamentina*	—	—	*O. ligamentina*	*O. ligamentina*
CR-38	125	69	41	59	*O. ligamentina*	—	—	*L. fasciola*	*O. ligamentina*
CR-39	114	66	44	50	*O. ligamentina*	—	—	*O. ligamentina*	*O. ligamentina*
CR-40	95	61	32	45	*O. ligamentina*	—	—	*O. ligamentina*	*O. ligamentina*
CR-41	89	55	34	37	*O. ligamentina*	—	—	*L. siliquoidea*	*O. ligamentina*
CR-42	93	56	32	40	*O. ligamentina*	—	—	*O. ligamentina*	*O. ligamentina*
CR-43	98	59	34	50	*O. ligamentina*	—	—	*L. cardium*	*O. ligamentina*
CR-44	102	62	37	44	*O. ligamentina*	—	—	*L. siliquoidea*	*O. ligamentina*
CR-45	113	63	45	50	*O. ligamentina*	—	—	*O. ligamentina*	*L. siliquoidea* male
CR-46	111	68	43	53	*O. ligamentina*	—	—	*O. ligamentina*	*O. ligamentina*
CR-47	111	63	43	38	*O. ligamentina*	—	—	*O. ligamentina*	*O. ligamentina*
CR-48	85	55	28	36	*O. ligamentina*	—	—	*O. ligamentina*	*O. ligamentina*

Appendix 1, continued.

Sample code	L (mm)	H (mm)	W (mm)	HL (mm)	Field species ID	Field sex ID	COI ID	PCA-LDA assignment: species	PCA-LDA assignment: species + sex
CR-49	99	59	35	47	*O. ligamentina*	—	—	*L. siliquoidea*	*O. ligamentina*
CR-50	87	57	30	42	*O. ligamentina*	—	—	*O. ligamentina*	*O. ligamentina*
CR-51	100	59	36	47	*O. ligamentina*	—	—	*L. cardium*	*O. ligamentina*
CR-52	91	54	32	42	*O. ligamentina*	—	—	*O. ligamentina*	*O. ligamentina*
CR-53	87	55	34	40	*O. ligamentina*	—	—	*O. ligamentina*	*O. ligamentina*
CR-54	89	56	28	41	*O. ligamentina*	—	—	*L. cardium*	*O. ligamentina*
CR-55	101	61	36	45	*O. ligamentina*	—	—	*O. ligamentina*	*O. ligamentina*
CR-56	127	79	48	59	*O. ligamentina*	—	—	*O. ligamentina*	*O. ligamentina*
CR-57	97	58	34	49	*O. ligamentina*	—	—	*O. ligamentina*	*O. ligamentina*
CR-58	98	59	34	47	*O. ligamentina*	—	—	*O. ligamentina*	*O. ligamentina*
CR-59	85	51	27	37	*O. ligamentina*	—	—	*L. fasciola*	*O. ligamentina*
CR-60	97	60	35	48	*O. ligamentina*	—	—	*O. ligamentina*	*O. ligamentina*
CR-61	105	65	35	41	*O. ligamentina*	—	—	*L. cardium*	*O. ligamentina*
CR-62	121	77	46	56	*O. ligamentina*	—	—	*O. ligamentina*	*O. ligamentina*
CR-63	94	61	32	45	*O. ligamentina*	—	—	*O. ligamentina*	*O. ligamentina*
CR-64	98	61	37	46	*O. ligamentina*	—	—	*O. ligamentina*	*O. ligamentina*
CR-65	93	61	34	49	*O. ligamentina*	—	—	*O. ligamentina*	*O. ligamentina*
CR-66	84	55	30	35	*O. ligamentina*	—	—	*O. ligamentina*	*O. ligamentina*
CR-67	97	57	32	41	*O. ligamentina*	—	—	*L. fasciola*	*O. ligamentina*
CR-68	94	55	31	42	*O. ligamentina*	—	—	*O. ligamentina*	*O. ligamentina*
CR-69	86	55	30	44	*O. ligamentina*	—	—	*L. cardium*	*O. ligamentina*
CR-70	79	50	27	32	*O. ligamentina*	—	—	*O. ligamentina*	*O. ligamentina*
CR-71	85	55	30	37	*O. ligamentina*	—	—	*O. ligamentina*	*O. ligamentina*
CR-72	90	52	30	42	*O. ligamentina*	—	—	*L. siliquoidea*	*L. siliquoidea* male
CR-73	104	68	37	51	*O. ligamentina*	—	—	*O. ligamentina*	*O. ligamentina*
CR-74	90	52	30	42	*O. ligamentina*	—	—	*O. ligamentina*	*O. ligamentina*
CR-75	113	68	41	62	*O. ligamentina*	—	—	*O. ligamentina*	*O. ligamentina*
CR-76	136	77	51	62	*O. ligamentina*	—	—	*L. cardium*	*O. ligamentina*
CR-77	114	69	39	59	*O. ligamentina*	—	—	*O. ligamentina*	*O. ligamentina*
CR-78	111	66	38	50	*O. ligamentina*	—	—	*O. ligamentina*	*O. ligamentina*
CR-79	100	64	35	46	*O. ligamentina*	—	—	*O. ligamentina*	*O. ligamentina*
CR-80	98	57	34	52	*O. ligamentina*	—	—	*O. ligamentina*	*O. ligamentina*
MAP-01	104	55	31	39	*L. siliquoidea*	Male	*L. siliquoidea*	*L. siliquoidea*	*L. siliquoidea* male
MAP-02	102	49	33	36	*L. siliquoidea*	Male	*L. siliquoidea*	*L. siliquoidea*	*L. siliquoidea* male
MAP-03	105	50	33	36	*L. siliquoidea*	Male	*L. siliquoidea*	*L. siliquoidea*	*L. siliquoidea* male
MAP-04	109	56	39	38	*L. siliquoidea*	Male	*L. siliquoidea*	*L. cardium*	*L. siliquoidea* male
MAP-05	86	43	27	30	*L. siliquoidea*	Male	*L. siliquoidea*	*L. siliquoidea*	*L. siliquoidea* male
MAP-06	130	61	46	52	*L. siliquoidea*	Male	*L. siliquoidea*	*L. siliquoidea*	*L. siliquoidea* male
MAP-07	87	43	26	25	*L. siliquoidea*	Male	*L. siliquoidea*	*L. cardium*	*L. siliquoidea* male
MAP-08	95	48	30	27	*L. siliquoidea*	Male	*L. siliquoidea*	*L. siliquoidea*	*L. siliquoidea* male
MAP-09	102	55	35	37	*L. siliquoidea*	Male	*L. siliquoidea*	*L. siliquoidea*	*L. siliquoidea* male
MAP-10	99	51	34	38	*L. siliquoidea*	Male	*L. siliquoidea*	*L. siliquoidea*	*L. siliquoidea* male
MAP-11	112	55	37	38	*L. siliquoidea*	Male	*L. siliquoidea*	*L. siliquoidea*	*L. siliquoidea* male
MAP-12	113	58	39	41	*L. siliquoidea*	Male	*L. siliquoidea*	*O. ligamentina*	*L. siliquoidea* male
MAP-13	122	61	43	55	*L. siliquoidea*	Male	*L. siliquoidea*	*O. ligamentina*	*L. siliquoidea* male
MAP-14	91	47	31	30	*L. siliquoidea*	Male	*L. siliquoidea*	*L. siliquoidea*	*L. siliquoidea* male
MAP-15	95	45	30	33	*L. siliquoidea*	Male	*L. siliquoidea*	*L. siliquoidea*	*L. siliquoidea* male
MAP-16	121	61	47	44	*L. siliquoidea*	Male	*L. siliquoidea*	*L. siliquoidea*	*L. siliquoidea* male
MAP-17	107	56	37	35	*L. siliquoidea*	Male	*L. siliquoidea*	*L. siliquoidea*	*L. siliquoidea* male
MAP-18	93	45	31	34	*L. siliquoidea*	Male	*L. siliquoidea*	*L. siliquoidea*	*L. siliquoidea* male

Appendix 1, continued.

Sample code	L (mm)	H (mm)	W (mm)	HL (mm)	Field species ID	Field sex ID	COI ID	PCA-LDA assignment: species	PCA-LDA assignment: species + sex
MAP-19	127	66	46	59	*L. siliquoidea*	Male	*L. siliquoidea*	*L. siliquoidea*	*L. siliquoidea* male
MAP-20	100	52	30	33	*L. siliquoidea*	Male	*L. siliquoidea*	*L. siliquoidea*	*L. siliquoidea* male
MAP-21	92	49	31	35	*L. siliquoidea*	Female	*L. siliquoidea*	*L. cardium*	*L. siliquoidea* female
MAP-22	77	41	31	24	*L. siliquoidea*	Female	*L. siliquoidea*	*L. siliquoidea*	*L. siliquoidea* female
MAP-23	99	56	40	34	*L. siliquoidea*	Female	*L. siliquoidea*	*L. siliquoidea*	*L. siliquoidea* male
MAP-24	88	49	34	30	*L. siliquoidea*	Female	*L. siliquoidea*	*L. siliquoidea*	*L. siliquoidea* female
MAP-25	97	51	31	38	*L. siliquoidea*	Female	*L. siliquoidea*	*L. siliquoidea*	*L. siliquoidea* female
MAP-26	73	42	27	25	*L. siliquoidea*	Female	*L. siliquoidea*	*L. cardium*	*L. siliquoidea* female
MAP-27	85	41	30	30	*L. siliquoidea*	Female	*L. siliquoidea*	*L. siliquoidea*	*L. siliquoidea* male
MAP-28	114	62	50	42	*L. siliquoidea*	Female	*L. siliquoidea*	*L. cardium*	*L. siliquoidea* female
MAP-29	87	47	32	29	*L. siliquoidea*	Female	*L. siliquoidea*	*L. siliquoidea*	*L. siliquoidea* male
MAP-30	117	57	42	40	*L. siliquoidea*	Female	*L. siliquoidea*	*L. siliquoidea*	*L. siliquoidea* female
MAP-31	75	42	27	21	*L. siliquoidea*	Female	*L. siliquoidea*	*L. siliquoidea*	*L. siliquoidea* female
MAP-32	107	61	45	49	*L. siliquoidea*	Female	*L. siliquoidea*	*L. siliquoidea*	*L. siliquoidea* female
MAP-33	97	51	42	40	*L. siliquoidea*	Female	*L. siliquoidea*	*L. siliquoidea*	*L. siliquoidea* female
MAP-34	90	45	31	30	*L. siliquoidea*	Male	—	*L. siliquoidea*	*L. siliquoidea* male
MAP-35	110	60	40	35	*L. siliquoidea*	Male	—	*L. cardium*	*L. siliquoidea* male
MAP-36	114	57	44	39	*L. siliquoidea*	Male	—	*L. siliquoidea*	*L. siliquoidea* male
MAP-37	67	36	22	18	*L. siliquoidea*	Male	—	*L. fasciola*	*L. siliquoidea* male
MAP-38	125	62	46	48	*L. siliquoidea*	Male	—	*L. siliquoidea*	*L. siliquoidea* male
MAP-39	88	48	29	27	*L. siliquoidea*	Male	—	*L. siliquoidea*	*L. siliquoidea* male
MAP-40	95	52	35	33	*L. siliquoidea*	Male	—	*L. siliquoidea*	*L. siliquoidea* male
MAP-41	77	39	26	24	*L. siliquoidea*	Male	—	*L. siliquoidea*	*L. siliquoidea* male
MAP-42	103	55	36	36	*L. siliquoidea*	Male	—	*L. siliquoidea*	*L. siliquoidea* male
MAP-43	87	44	29	28	*L. siliquoidea*	Male	—	*L. siliquoidea*	*L. siliquoidea* male
MAP-44	98	50	34	33	*L. siliquoidea*	Male	—	*L. cardium*	*L. siliquoidea* male
MAP-45	79	39	27	23	*L. siliquoidea*	Male	—	*L. siliquoidea*	*L. siliquoidea* male
MAP-46	55	30	19	14	*L. siliquoidea*	Male	—	*L. siliquoidea*	*L. siliquoidea* male
MAP-47	83	47	28	25	*L. siliquoidea*	Male	—	*L. siliquoidea*	*L. siliquoidea* male
MAP-48	92	47	32	30	*L. siliquoidea*	Male	—	*L. siliquoidea*	*L. siliquoidea* male
MAP-49	95	50	35	35	*L. siliquoidea*	Male	—	*O. ligamentina*	*L. siliquoidea* male
MAP-50	103	48	32	39	*L. siliquoidea*	Male	—	*L. siliquoidea*	*L. siliquoidea* male
MAP-51	92	47	31	29	*L. siliquoidea*	Male	—	*L. siliquoidea*	*L. siliquoidea* male
MAP-52	89	50	35	27	*L. siliquoidea*	Male	—	*L. fasciola*	*L. siliquoidea* male
MAP-53	87	48	32	32	*L. siliquoidea*	Male	—	*L. siliquoidea*	*L. siliquoidea* male
MAP-55	160	103	72	81	*O. ligamentina*	—	—	*O. ligamentina*	*O. ligamentina*
MAP-56	158	103	73	79	*L. cardium*	Male	—	*O. ligamentina*	*L. cardium* male
MAP-57	155	100	75	70	*L. cardium*	Male	—	*O. ligamentina*	*L. cardium* male
MAP-58	129	84	54	61	*L. cardium*	Male	—	*O. ligamentina*	*L. cardium* male
MAP-59	131	91	64	59	*L. cardium*	Male	—	*L. cardium*	*L. cardium* female
MAP-60	122	83	49	51	*L. cardium*	Male	—	*O. ligamentina*	*L. cardium* male
MAP-61	133	84	61	65	*L. cardium*	Male	—	*O. ligamentina*	*O. ligamentina*

L = length, W, width, H = height, COI = cytochrome c oxidase subunit 1, PCA-LDA = principal component analysis–linear discriminant analysis.

Freshwater Mollusk Biology and Conservation

ISSN 2472-2944